Measuring distal airspace dimensions with nanoparticles. Initial development of a diagnostic method.

Aaltonen, H Laura

2019

Document Version:
Publisher's PDF, also known as Version of record

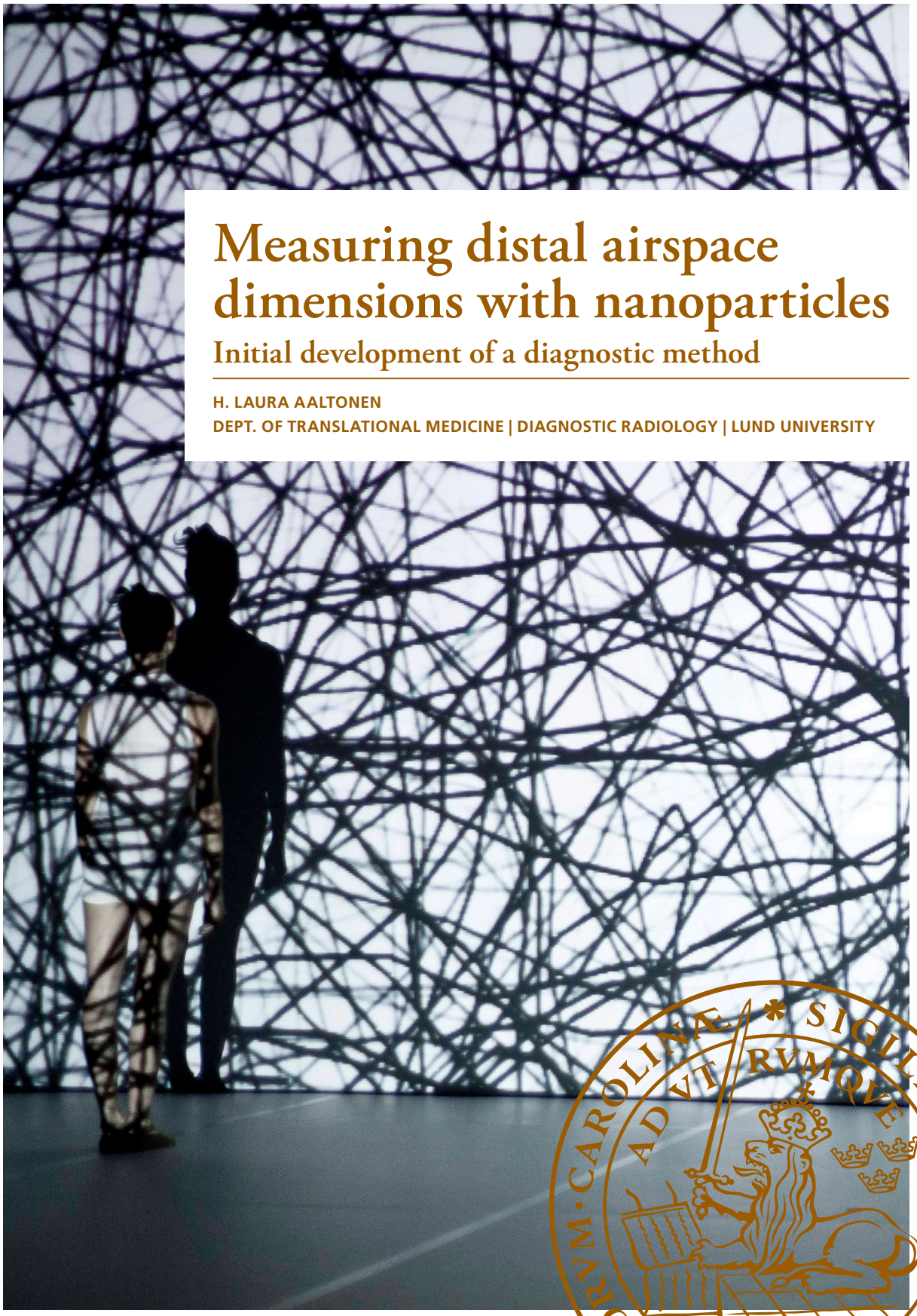

Measuring distal airspace dimensions with nanoparticles

Initial development of a diagnostic method

H. LAURA AALTONEN
DEPT. OF TRANSLATIONAL MEDICINE | DIAGNOSTIC RADIOLOGY | LUND UNIVERSITY

Measuring distal airspace dimensions with nanoparticles

Measuring distal airspace dimensions with nanoparticles

Initial development of a diagnostic method

H. Laura Aaltonen

LUND
UNIVERSITY

DOCTORAL DISSERTATION
by due permission of the Faculty of Medicine, Lund University, Sweden.
To be defended at Skåne University Hospital, Malmö,
Department of Medical Imaging and Physiology
May 15, 2019 at 9:00 am.

Faculty opponent
Prof Johny Verschakelen, MD, PhD
KU Leuven, Belgium

Organization LUND UNIVERSITY	Document name DOCTORAL DISSERTATION
	Date of issue May 15th 2019
Author H Laura Aaltonen	Sponsoring organization

Title and subtitle
Measuring distal airspace dimensions with nanoparticles
-Initial development of a diagnostic method

Abstract

Chronic obstructive pulmonary disease (COPD) consists of emphysema and bronchial disease. The pulmonary function tests currently used to diagnose COPD have poor sensitivity for early disease. This may delay diagnosis and lead to a poorer prognosis compared to establishing the diagnosis at an earlier stage.

The aim of this thesis was to investigate a new nanoparticle-based method, termed Airspace Dimension Assessment (AiDA), to chart distal airspace morphology, and to examine the technique as a possible diagnostic biomarker for emphysema. In AiDA, inhaled nanoparticles' deposition behavior is utilized to characterize distal airspace properties. Nanoparticles, as opposed to larger particles, are able to penetrate into the distal lung, where they deposit almost exclusively by diffusion. The particles' likelihood to deposit is dependent on the diffusion distance. The thesis is based on the hypothesis that in persons with enlarged, emphysematous airspaces, fewer particles will deposit, as opposed to healthy persons with narrower airspaces.

In paper I, significant nanoparticle deposition differences between 19 COPD-patients with mainly moderate-to-advanced emphysema and 19 healthy controls were found. The deposition correlated to disease severity as measured by computed tomography (CT) densitometry and diffusion capacity for carbon monoxide ($D_{L,CO}$). In paper II, nanoparticle deposition was used to calculate distal airspace radius in 19 healthy volunteers. The radius correlated to lung density as measured by magnetic resonance imaging (MRI). In paper III, the average radius in 403 individuals without previous pulmonary disease or respiratory symptoms was found to be 293 ± 36 µm. The radius and its variation in population was found to be approximately comparative to other methods. It was noted that the radius was on average 13 µm larger in male ever-smokers compared to never-smokers, which may reflect early smoking-related changes. In paper IV, we concluded that in a population sample of 618 individuals, the persons with computed tomography evidence of emphysema (N = 47) had significantly larger distal airspace radii compared to persons without emphysema. We also showed that comorbidities did not significantly affect the results.

In conclusion, we suggest the AiDA radius is a promising biomarker candidate for emphysema. Further validating studies, including a diagnostic study in a population seeking health care attention with symptoms and history indicative of COPD, are warranted.

Key words: nanoparticles, distal airspaces, small airways, Airspace Dimension Assessment with nanoparticles, AiDA, respiratory diagnostics

Classification system and/or index terms (if any)

Supplementary bibliographical information		Language English
ISSN and key title 1652-8220		ISBN 978-91-7619-778-3
Recipient's notes	Number of pages 77	Price
	Security classification	

Signature  Date 2019-04-05

Measuring distal airspace dimensions with nanoparticles

Initial development of a diagnostic method

H. Laura Aaltonen, M.D.

LUND
UNIVERSITY

Cover photo and the photo on p 7 © by Pablo Palacio

Faculty of Medicine
Department of Translational Medicine, Diagnostic Radiology
Lund University, Lund, Sweden, 2019

ISBN 978-91-7619-778-3
ISSN 1652-8820

Printed in Sweden by Media-Tryck, Lund University
Lund 2019

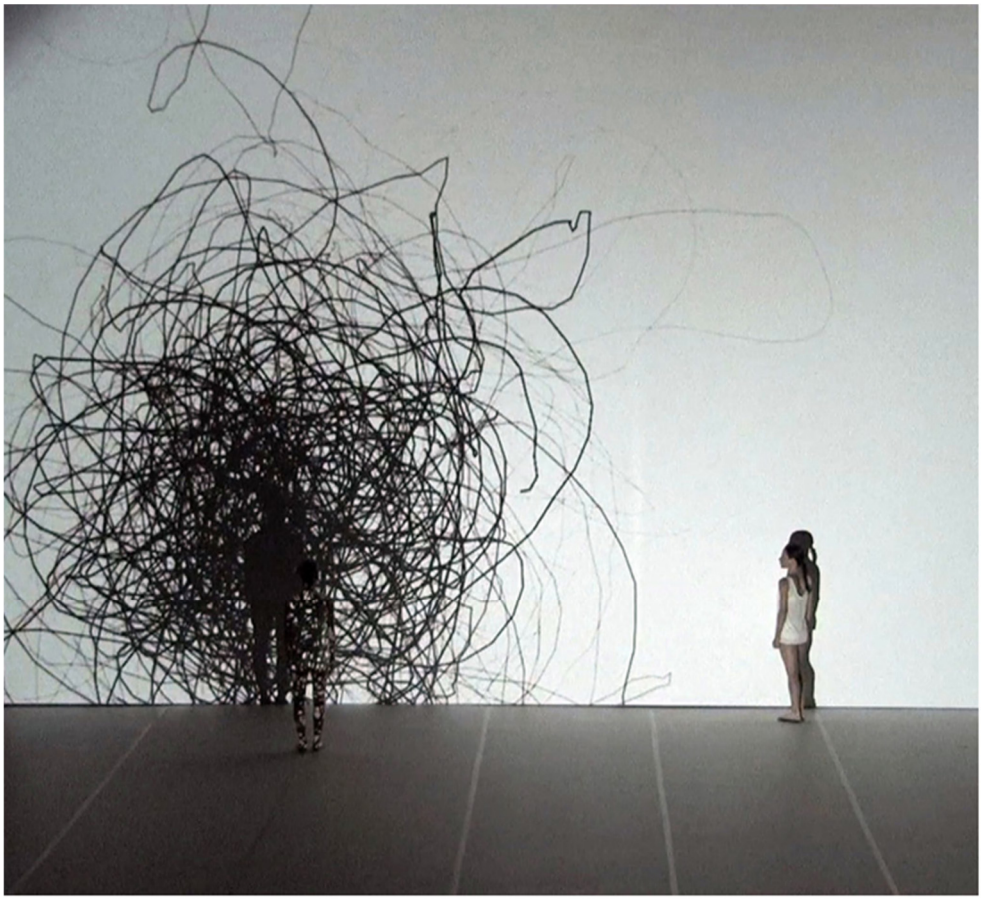

Nanoparticles are so small they behave like gases. According to the kinetic theory of gases, airborne nanoparticles are in a constant motion, colliding with each other and their surrounding structures. This movement is termed Brownian motion, and it involves particles dispersing in space in a haphazard, stochastic manner.

The cover image, and the image on this page, are reprinted with kind permission from the Instituto Stocos group, whose goal is to connect art and science. Stocos is a trans-disciplinary project, combining stochastic processes and artificial intelligence-based simulations in order to create behavioural dependencies and aesthetic relationships between dancers, simulated entities, music, visuals and light.

Table of Contents

List of original papers

This thesis is based on the following papers, referenced to in the text by their Roman numerals.

Paper I:

Deposition of inhaled nanoparticles is reduced in subjects with COPD and correlates with the extent of emphysema: proof of concept for a novel diagnostic technique
Aaltonen HL, Jakobsson JK, Diaz S, Zackrisson S, Piitulainen E, Löndahl J, Wollmer P. *Clinical Physiology and Functional Imaging* 2018, 38, 1008-1014.

Paper II:

Airspace Dimension Assessment with nanoparticles reflects lung density as quantified by MRI
Aaltonen HL, Kindvall SS, Jakobsson JK, Löndahl J, Olsson E, Diaz S, Zackrisson S, Wollmer P. *International Journal of Nanomedicine* 2018, 13, 2989-2995

Paper III:

Distal airspace dimensions as measured by nanoparticles in a population without respiratory symptoms.
Aaltonen HL, Jakobsson JKF, Diaz S, Nicklasson H, Zackrisson S, Engström G, Petersson Sjögren M, Ideböhn V, Löndahl J, Wollmer P. (Unpublished manuscript, submitted)

Paper IV:

In vivo morphometry of distal airspaces with nanoparticles as a potential biomarker for emphysema.
Aaltonen HL, Petersson Sjögren M, Jakobsson JKF, Ideböhn V, Diaz S, Sánchez Montiel F, Nicklasson H, Zackrisson S, Engström G, Löndahl J, Wollmer P. (Unpublished manuscript, submitted)

Abstract

Chronic obstructive pulmonary disease (COPD) consists of emphysema and bronchial disease. The pulmonary function tests currently used to diagnose COPD have poor sensitivity for early disease. This may delay diagnosis and lead to a poorer prognosis compared to establishing the diagnosis at an earlier stage.

The aim of this thesis was to investigate a new nanoparticle-based method, termed Airspace Dimension Assessment (AiDA), to chart distal airspace morphology, and to examine the technique as a possible diagnostic biomarker for emphysema. In AiDA, inhaled nanoparticles' deposition behavior is utilized to characterize distal airspace properties. Nanoparticles, as opposed to larger particles, are able to penetrate into the distal lung, where they deposit almost exclusively by diffusion. The particles' likelihood to deposit is dependent on the diffusion distance. The thesis is based on the hypothesis that in persons with emphysematous, enlarged airspaces, fewer particles will deposit, as opposed to healthy persons with narrower airspaces.

In **Paper I**, significant nanoparticle deposition differences between 19 COPD-patients with mainly moderate-to-advanced emphysema, and 19 healthy controls were found. The deposition correlated to disease severity as measured by computed tomography (CT) densitometry and diffusion capacity for carbon monoxide ($D_{L,CO}$).

In **Paper II**, nanoparticle deposition was used to calculate distal airspace radius in 19 healthy volunteers. The radius correlated to lung density as measured by magnetic resonance imaging (MRI).

In **Paper III**, the average radius in 403 individuals without previous pulmonary disease or respiratory symptoms was found to be 293 ± 36 μm. The radius and its variation in the population were found to be approximately comparative to other methods. It was noted that the radius was on average 13 μm larger in male ever-smokers compared to never-smokers, which may reflect early smoking-related changes.

In **Paper IV**, we concluded that in a population sample of 618 individuals, the persons with computed tomography evidence of emphysema, (N = 47) had significantly larger distal airspace radii compared to persons without emphysema. We also showed that comorbidities did not significantly affect the results.

In conclusion, we suggest the radius is a promising biomarker candidate for emphysema. Further validating studies, including a diagnostic study in a population seeking health care attention with symptoms and history indicative of COPD, are warranted.

Populärvetenskaplig sammanfattning (in Swedish)

Kroniskt obstruktiv lungsjukdom (KOL) är ett samlingsbegrepp för två sjukdomar som ofta förekommer tillsammans och ger delvis liknande besvär. KOL består delvis av oåterkallelig nedbrytning av lungblåsor, även kallat emfysem, och delvis av stadigvarande inflammation och ärrbildning i luftvägar. När man får KOL kan lungblåsorna bli större än vanligt, medan luftrören kan bli trängre än vanligt. Båda dessa förändringar leder till att man kan ha svårt att få i sig syrgas. I början märker patienten oftast inget själv, vilket är olyckligt då det är just då som man har bästa möjligheter att påverka förloppet. Senare kan man få långvarig hosta, infektioner och andnöd. Sjukdomen går för närvarande inte att bota med mindre än lungtransplantation.

De tidigaste förändringarna utgörs av skada i de allra minsta luftvägarna, som i sin tur orsakas av inandade skadliga ämnen, vanligtvis tobaksrök. KOL drabbar områden i kroppen som är svårtillgängliga för analys. Det är svårt att ta sig in i lungans minsta beståndsdelar och ta vävnadsprov, och diagnostiken måste därför ske genom indirekta vägar. Trots att KOL är en vanligt förekommande folksjukdom är det förhållandevis svårt att ställa diagnosen i tidigt skede. Vanligt är att man söker sjukvård och får gjort ett lungfunktionstest, s.k. spirometri, vilket visar tecken på svårigheter att pressa luft ut ur lungorna. Dock har sjukdomen i många fall löpt långt innan den gör sig tillkänna genom vanliga lungfunktionstester.

I denna avhandling undersöks en metod som vi tror kan utvecklas till att påvisa KOL baserat på hur väl nanopartiklar fastnar i de minsta luftvägarna. Med nanopartiklar avses partiklar som är mindre än 100 miljarddelsmeter stora. Dessa partiklar kan transporteras med inandad luft in i lungans minsta beståndsdelar där en del av partiklarna träffar en yta, medan en del kommer tillbaka till rumsluft med utandningen. Väl framme djupt i lungan är sannolikheten för att en nanopartikel fastnar där mindre, desto större lungblåsor man har.

I denna avhandling undersöks en ny metod som vi tror kan utvecklas till att påvisa KOL baserat på hur luftburna nanopartiklar fastnar i de minsta luftvägarna. Avhandlingens grundläggande teori är att personer med emfysem, d.v.s. stora lungblåsor, kommer att ha större antal nanopartiklar kvar vid utandningen jämfört med friska personer. Utifrån detta kan man sedan enligt matematisk modell beräkna medelavståndet för de minsta luftrummen i lungan. Detta kan användas som ett mått på luftvägarnas radie. Metoden, och tillhörande apparaten som byggts för att testa teorin, heter AiDA, (Airspace Dimension Assessment).

I delarbete I finner vi att personer med KOL har större antal nanopartiklar kvar vid utandningsluften jämfört med friska personer, samt att ju mer emfysem man har, desto färre partiklar är det som fastnar.

I delarbete II mäter vi de minsta luftvägarnas radie, och finner att den är relaterad till lungans täthet hos friska.

I delarbete III mäter vi radien hos en grupp individer från den allmän befolkning 50-64 år gamla utan lungsjukdomar och symptom, och finner att radien överensstämmer med andra liknande sätt som beskrivits i litteraturen. Vi finner också att det finns skillnader mellan rökande och icke-rökande män, vilket kan tala för att metoden hittar tidiga tecken på skada som rökning medför.

I delarbete IV finner vi att personer i allmänna befolkningen mellan 50 och 64 år med tecken på emfysem i skiktröntgenbilder har större radie än personer utan emfysem. Vi finner också att andra sjukdomar som personerna har inte påverkar radien.

Metoden är än så länge i tidigt utvecklingsstadium. Resultaten är lovande, men metoden kan i dagsläget inte användas på en läkarmottagning. Man måste göra fler validerande studier. För att bevisa att metoden kan användas till diagnostik måste man göra en så kallad diagnostisk studie.

Kansantajuinen tiivistelmä (in Finnish)

Keuhkoahtaumatauti on yleiskäsite kahdenlaiselle sairaudelle, joilla on yhteinen syntymämekanismi, ja jotka aiheuttavat samanlaisia oireita. Keuhkoahtaumatautiin kuuluu sekä keuhkorakkuloiden pysyvä tuhoutuminen ja laajeneminen, jota myös emfyseemaksi kutsutaan, että ilmateiden tulehtuminen ja arpeutuminen. Keuhkoahtaumataudissa voivat näin ollen keuhkorakkulat tulla tavallista suuremmiksi ja ilmatiet tavallista kapemmiksi. Yhdessä ja erikseen, nämä muutokset vaikeuttavat hapensaantia. Sairauden alkuvaiheessa potilas voi olla hyvinkin oireeton. Tämä on sikäli harmillista, että juuri alkuvaiheessa olisi parhaat mahdollisuudet vaikuttaa sairauden kulkuun. Myöhemmin oireina ovat pitkäkestoinen yskä, keuhkoputkentulehdukset ja hengenahdistus. Tällä hetkellä keuhkoahtaumatautiin ei - keuhkonsiirtoa lukuunottamatta - ole parantavaa hoitoa.

Sairaus aiheutuu sisään hengitetyistä, myrkyllisistä aineista, useimmiten tupakansavusta. Myrkyt kirvoittavat tulehdusvasteen, joka vaurioittaa erityisesti pienimpiä (< 2 mm) ilmatiehyeitä. Pienet ilmatiet sijaitsevat syvällä keuhkojen pienimmissä haarakkeissa, juuri ennen kuin ne aukeavat keuhkorakkuloihin, ja niihin on kokeellisesti vaikea päästä käsiksi. Vaikka keuhkoahtaumatauti on merkittävä kuolleisuutta ja sairastavuutta aiheuttava kansantauti, on taudin todentaminen varhaisessa vaiheessa juuri muutosten hankalan sijainnin vuoksi haastavaa. Tavallisesti tutkittava hakeutuu vastaanotolle hengitysoireiden vuoksi, jolloin tehdään keuhkojen toiminnallinen tutkimus, spirometria. Tässä ilmenee vaikeus puhaltaa uloshengitysilma pois keuhkoista. Sairaus on kuitenkin usein edennyt pitkälle, ennen kuin muutokset ovat spirometrian keinoin havaittavissa.

Tässä väitöskirjassa esitetään uusi, nanohiukkasiin perustuva menetelmä emfyseeman toteamiseksi. Termi nanohiukkanen tarkoittaa alle sadan miljardisosametrin kokoista hiukkasta. Pienenpienet nanohiukkaset voivat, toisin kuin suuremmat hiukkaset, kulkeutua sisäänhengityksen mukana aivan kaikista pienimpiin ilmateihin, joissa ne poukkoilevat sattumanvaraisesti kaasumolekyylien tavoin. Osa hiukkasista asettuu kudoksen pinnalle, ja osa kulkeutuu uloshengityksen mukana pois. Perillä pienissä ilmateissä ja keuhkorakkuloissa hiukkasen todennäköisyys jäädä kudoksen pinnalle on sitä pienempi, mitä väljemmät henkilön pienet ilmatiet ja keuhkorakkulat ovat. Väitöskirja perustuu teoriaan siitä, että emfyseemapotilaalla, jolla keuhkorakkulat ovat laajentuneet, suurempi osa hiukkasista palautuu uloshengityksen mukana terveisiin henkilöihin nähden. Mittaamalla hiukkasten määrä sisään- ja uloshengityksessä selviää, kuinka moni hiukkanen jäi kudokseen. Näistä tuloksista voidaan matemaattisella mallintamisella laskea keskimääräinen etäisyys lähimpään kudoksen pintaan, nk. keskidiffuusioetäisyys. Tämä etäisyys kuvaa pienten ilma-alueiden sädettä.

Teorian tutkimiseksi on kehitetty laite nimeltä AiDA (Airspace Dimension Assessment), jossa tutkittava hengittää sisään hyvin pienen määrän nanohiukkasia.

Väitöskirjan ensimmäisessä osatyössä havaittiin, että keuhkoahtaumatautipotilailla on enemmän nanohiukkasia uloshengityksessä terveisiin verrokkeihin nähden. Lisäksi havaittiin, että mitä pidemmälle edennyt emfyseema oli, sitä enemmän hiukkasia palautui uloshengityksen mukana.

Toisessa osatyössä tutkittiin eri ikäisiä, terveitä henkilöitä. Ilmatiehyeiden keskidiffuusioetäisyys, siis säde, määriteltiin kokeellisesti. Ilmeni myös, että säde on suhteessa keuhkon tiheyteen.

Kolmannessa osatyössä mitattiin pienten ilmatiehyiden säde terveillä 50-64 –vuotiailla henkilöillä. Todettiin, että nanohiukkasmenetelmällä mitattu säde on muutaman sadan mikrometrin luokkaa. Tämä vastaa kutakuinkin muiden kokeellisten menetelmien kautta havaittujen pienten ilma-alueiden sädettä. Samalla havaittiin eroja tupakoitsevien ja tupakoimattomien miesten välillä. Esitetään, että nanohiukkastesti voisi mahdollisesti havaita varhaisia, tupakoinnin aiheuttamia kudosvaurioita.

Neljäs osatyö oli poikkimittaustutkimus 50-64-vuotiaassa väestössä. Tuloksena oli, että henkilöillä joilla on eri menetelmin havaittavissa oleva emfyseema, on suurempi pienten ilma-alueiden säde verrattuna niihin joilla ei ole emfyseemaa. Tässä työssä esitetään, että nanohiukkasmenetelmää voisi mahdollisesti käyttää emfyseemaa kuvaavana biomerkkiaineena.

Menetelmä on toistaiseksi varhaisessa kehitysvaiheessa. Vaikkakin väitöskirjassa esitetyt tulokset ovat lupaavia, ei nanohiukkastestia tässä vaiheessa voi käyttää taudin diagnosointiin. Menetelmä on vielä todennettava lisätutkimuksissa, mm. on on suoritettava ns. diagnostinen tutkimus, jossa testi tehdään nille henkilöille, joiden epäillään sairastavan keuhkoahtaumatautia.

Abbreviations and terms

^{3}He	Hyperpolarized helium
ADAM	Aerosol derived airway morphometry
ADC	Apparent diffusion coefficient
AiDA	Airspace dimension assessment with nanoparticles
AUC	Area under graph
BMI	Body mass index
COPD	Chronic obstructive pulmonary disease
CPC	Condensation particle counter
CT	Computed tomography
$D_{L,CO}$	Diffusing capacity for carbon monoxide
DMA	Differential mobility analyzer
FEV_1	Forced expiratory flow in one second
FVC	Forced vital capacity
GOLD	Global Initiative on Obstructive Disease
HRCT	High resolution computed tomography
HU	Hounsfield unit
ln	Natural logarithm
MLD	Mean lung density
MRI	Magnetic resonance imaging
OR	Odds ratio
PD	Proton density
PD(TLC)	Proton density normalized to total lung capacity
PD15	The 15^{th} percentile of CT attenuation histogram, measured in g/L
PFT	Pulmonary function test
R(0)	Particle recovery at an imaginary breath-hold time of zero seconds
RA 7.5	Relative area under 7.5% PD
r_{AiDA}	Airspace radius estimated by the AiDA-method
ROC	Receiver operator curve
ROI	Region of interest
RV	Residual volume
RV-950	Percentage of voxels with a Hounsfield unit value below -950.
SD	Standard deviation
SPECT	Single photon emission computed tomography
STARD	Standard for reporting of diagnostic accuracy
TLC	Total lung capacity
TLC (CTV)	Total lung capacity measured by a volumetric CT scan
UTE	Ultra short echo-time
VC	Vital capacity
V_{MRI}	Lung volume at the MRI acquisition
WHO	World Health Organization

Distal airspaces	Airspaces distal to the conducting airways
Small airways	Airways < 2 mm in diameter
Volumetric lung depth	A predetermined volume of exhaled air

1 Introduction

> In many ways, emphysema is to the pulmonologist of the last half of the twentieth century what tuberculosis was to the pulmonologist of the first half of the twentieth century."
>
> – Gordon I. Snider M.D. 1992, (1)

The midpoint of the twentieth century can be seen as a turning point in pulmonary medicine, where disease caused mainly by anthropogenic pathogens surpassed those of natural or microbiological origin. Human efforts had successfully conquered Mycobacterium tuberculosis, while other human activities created increasing global exposure to noxious inhalants, resulting in increasing incidence of emphysema. Chronic obstructive pulmonary disease (COPD), which includes emphysema and bronchial disease, is caused by the body's reaction to noxious inhalants. Cigarette smoking, pollution and biomass exhaustion are the main sources of exposure. (2)

For the pulmonologist of the first half of the twenty-first century, the above quote still holds true, as COPD/emphysema incidence and prevalence have further increased. According to WHO, COPD is currently the third global leading cause of death, with a high disease burden in middle and low income countries. (3, 4)

Emphysema is defined as a condition of the lung characterized by abnormal, permanent enlargement of airspaces distal to the terminal bronchioli, accompanied by destruction of their walls without obvious fibrosis. (5, 6) The definition is derived from pathological specimens, and establishing the diagnosis this way would require invasive biopsy. In current clinical praxis, in vivo diagnosis is established using a proxy, most often by quantification of airflow obstruction using pulmonary function tests (PFTs). This method, however, does not differentiate between emphysema and the bronchial component of COPD. The presence of emphysema can also be investigated by measuring the diffusing capacity for carbon monoxide ($D_{L,CO}$), or by obtaining a computed tomography (CT) scan. Numerous publications have, however, stated what pulmonologists and primary care practitioners worldwide experience in their day-to-day practice – these methods are not sensitive to early changes, which may lead to a delay in diagnosis. (7) The diagnosis may also be delayed by the gradual onset of the symptoms. The patients may experience dyspnoea, wheezing and coughing for years, but fail to recognize the findings as signs of disease, interpreting their symptoms as normal smoking, aging or

deconditioning-related findings. (8) Later in the course of the disease, the patients experience shortness of breath, wheezing, increased phlegm and infections. The symptoms may be alleviated by bronchodilators, steroids and physiotherapy. Periodic exacerbations are treated with antibiotics and steroids. In advanced disease, ambulatory oxygen treatment may become necessary. Currently, besides lung transplantation, there is no definitive cure for COPD. Smoking cessation remains the single most important therapy to prevent the disease, and to slow down its course. (9)

There is a need for a simple, cost-effective and easily available method to identify the disease early, preferably in primary care settings, including countries with scarcer healthcare resources. (10) Early diagnosis may help patients understand the importance of lifestyle changes. Also, making earlier diagnosis available may stimulate research for potential cures. Being able to phenotype a COPD patient into predominantly emphysematous or predominantly bronchial group could be beneficial in future treatment trials.

2 Background

2.1 The respiratory system

The respiratory system provides the body with oxygen and removes excess carbon dioxide. It also humidifies the inhaled air, clears deposited airborne particulates and contributes to the body's immune response. The respiratory system may be divided into extrathoracic airways, intrathoracic airways and the acinar airways. (11) The extrathoracic airways refers to the nose, mouth, pharynx and larynx. The intrathoracic airways consist of a series of branching tubes leading the inhaled air through the trachea to the acinar airways, where the gaseous exchange takes place. (Figure 1.)

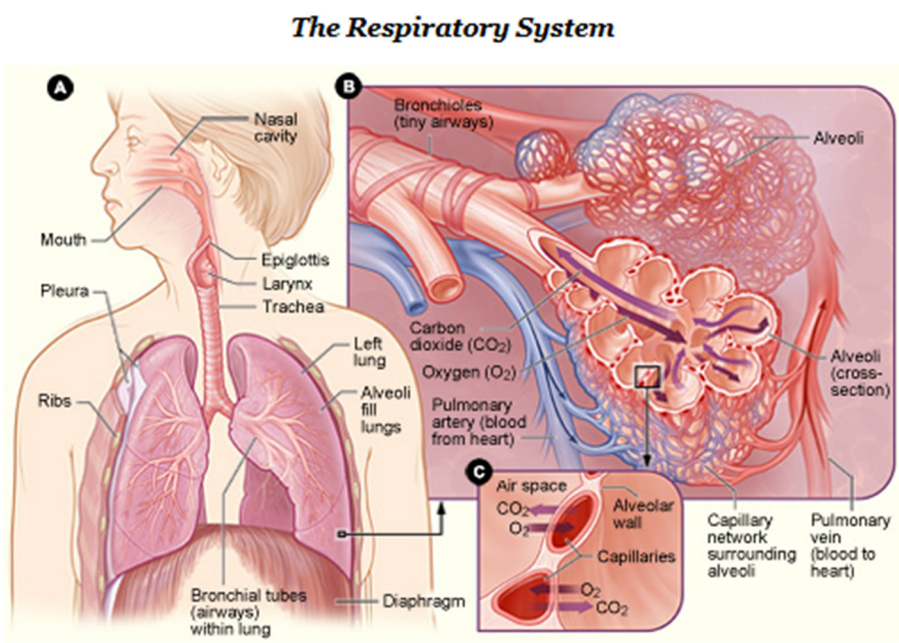

Figure 1: A – Gross anatomy of the airways. B – The acinar airways consists of terminal bronchioles and alveoli that form respiratory units. C – Gaseous exchange involves oxygen diffusing through the alveolar-capillary membrane from the respiratory unit in to the bloodstream, as well as carbon dioxide diffusing out of the bloodstream to the respiratory units. United States National Institute of Health: National Heart, Lung and Blood Institute. Public domain

Each airway branching is termed a generation. Beginning with trachea as generation 0, the human airways branch over 20 times. (Figure 2) (12) The interface between purely conducting and gas-exchanging tissues is formed between the terminal and transitional bronchioles, approximately at generation 15, when the first alveoli appear. The air present in the airways above this point is called anatomic dead space. The airspaces from this point downstream are called distal airspaces; with each branching generation, the alveolar openings increase in number, until they reach the entire luminal surface of an alveolar duct.

Small airways < 2 mm in diameter comprise the distal part of the intrathoracic (conducting) airways, as well as the acinar airways, and they are generally found from the 8^{th} generation onward. (Figure 2) The distance between trachea and alveoli, however, is not constant. The variation in the pathway length gives rise to 2 mm airways being distributed from the fourth to the fourteenth generation. Similarly, the respiratory bronchioles are found between the 8^{th} and 22^{nd} generation. (12-15) Three to five terminal bronchioles support a secondary pulmonary lobule. (16, 17) Each secondary pulmonary lobule is supported by a central feeding artery, and consists of approximately 12-30 acini. (18) The acini, in turn consist of alveolar ducts, sacs and alveoli. (19, 20)

According to a cast model, the inner diameter of human acinar airways was found to be approximately 270 μm – 500 μm, depending on which generation the acinus originated from. The inner diameter of alveolar sacs, however, was found to be approximately 250 μm for all generations. (16, 21)

Each branching increases the cross-sectional area available for the inhaled gas, and consequently, the bulk flow of the inhaled gas is slowed down. Approximately around generation 15, the conducting velocity falls to zero and diffusion takes over as the main mode of transport. (22) Hence, upon a breath, a large volume of gas at a very low flow is accumulated into the distal airspaces, enabling gaseous exchange. In healthy lungs, there is low resistance to airflow in small airways.

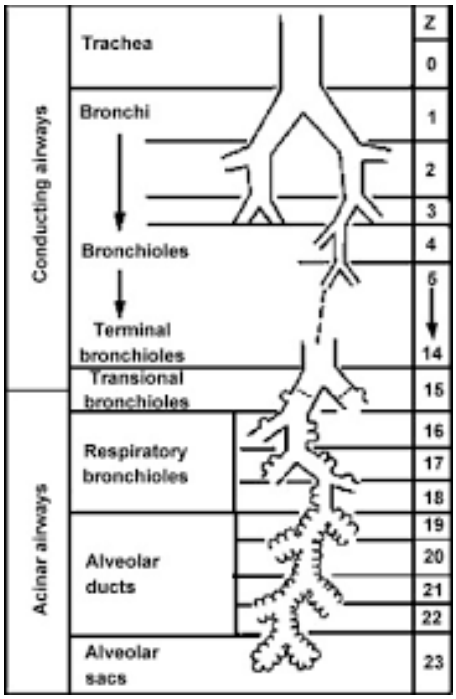

Generation Z	Number per generation $n(Z)$	Diameter $d(Z)$, cm	Length $l(Z)$ cm
0	1	1.8	12.0
1	2	1.22	4.76
2	4	0.83	1.90
3	8	0.56	0.76
4	16	0.45	1.27
5	32	0.35	1.07
6	64	0.28	0.90
7	128	0.23	0.76
8	256	0.186	0.64
9	512	0.154	0.54
10	1024	0.13	0.46
11	2048	0.109	0.39
12	4096	0.095	0.33
13	8192	0.082	0.27
14	16384	0.074	0.23
15	32768	0.066	0.20
16	65536	0.060	0.165
17	131072	0.054	0.141
18	262144	0.050	0.117
19	524288	0.047	0.099
20	1048576	0.045	0.083
21	2097152	0.043	0.070
22	4194304	0.041	0.059
23*	8388608	0.041	0.050*

* Adjusted for complete generation.

Figure 2: Airway generations, their number, diameter and length according to Weibel 1963 (12)

Histologically, the lung parenchyma contains two main components, the bronchial-bronchiolar epithelium and alveolar cells. The former is lined with ciliated epithelial cells, mucus secreting goblet and serous cells, basal as well as neuroendocrine and inflammatory cells. The ciliated cells move the mucus in cephalad direction for clearance. The proportion of goblet and ciliated cells decreases in the terminal bronchioles, while non-ciliated secretory Clara cells increase. Alveoli consist of type I and II pneumocytes, of which the latter secrete surfactant to keep the airspace surface tension low. In the conducting airways, bronchial wall is lined with smooth muscle fibers, which contract to facilitate mucous clearance

Lymph vessels follow the centrilobular artery and bronchovascular structures, draining via peribronchial and hilar nodes to mediastinal nodes. (23)

2.2 Pathophysiology of COPD

Toxic inhaled particles coat the airways from the extrathoracic to acinar airways. Yet the small, < 2 mm airways are the major site of pathology in COPD. In the small airways, the lung is vulnerable to accumulation of toxic particles, partially due to

decreased clearance. Less mucus is secreted, the small airways epithelium is thinner and the cilia decrease in number with increasing generations.

Also, in the case of the common ultra-fine particles, such as combustion emissions from smoking, traffic or biomass burning, slowing of bulk flow and increasing diffusion favors particle deposition in the small airways. The accumulated deposition initiates an inflammatory response and remodeling sequence, leading to edema, scarring and narrowing of bronchioli and bronchi. Furthermore, in the airways, both increased mucus secretion and smooth muscle hypertrophy and metaplasia in the airway epithelium ensue, leading to a decrease in cross-sectional area available for convective gas transport. (24-26) The resistance to flow is inversely proportional to the fourth power of the radius. Hence, even minor decrease in radius may lead to considerable increase in resistance.

In the pathophysiological sequence of COPD, terminal bronchioli shorten and decrease in number, and their cross-sectional area decreases before emphysematous lesions occur. (27) The combination of narrowing of bronchi and bronchioli as well as reduction in their number cause increased resistance in the distal airspaces. (28) The increased resistance leads to progressive gas trapping during expiration, resulting in hyperinflation. (29)

Emphysema formation is thought to be caused by inflammatory cells releasing proteinases and oxidants, which destroy the extracellular matrix in the walls of the acinus. Three subtypes of emphysema are recognized. (30)

1. Centrilobular, which involves dilatation and destruction of respiratory bronchioles, beginning at the center of secondary pulmonary lobule. Most often associated with smoking and often present in the apical parts of the lungs. (31)
2. Panlobular, characterized by uniform destruction of all of the acini within the secondary lobule. (32) Associated with the genetic deficiency of alpha-1-antitrypsin plasma protein and frequently involves the basal parts of the lungs.
3. Paraseptal, which involves regions near lung fissures.

In emphysema, enlarged acini exhibit decreased elastic recoil. (33) Gas enters into the distal lung with inhalation, but the lack of elastic force inhibits the air from exiting. There is also a loss of radial traction on the airways by supporting alveolar walls. This promotes airway collapse during expiration. (34, 35)

Thus, the distal airspaces contribute to increased airflow obstruction in two ways, both by reduced airway lumen, as well as by reduced elastic recoil.

2.3 Lung function tests

2.3.1 Spirometry

Airflow obstruction is the hallmark of chronic obstructive pulmonary disease. The obstruction can be measured by using pulmonary function tests (PFTs), mainly spirometry. A modern version of this device, originally described by Hutchinson in 1846, can be placed in clinical outpatient settings, and the results of the measurements are relatively straightforward to interpret. (36) In spirometry, lung volumes, capacities and flow measurements are made. (Figure 3)

The lung volumes and capacities can be described as either static or dynamic. The static volumes, e.g. vital capacity (VC), total lung capacity (TLC) and residual volume (RV) stay the same irrespective of the rate of air flow in and out of the lungs. The dynamic volumes, such as forced expiratory flow in one second (FEV_1,), and forced vital capacity (FVC), are dependent on air flow.

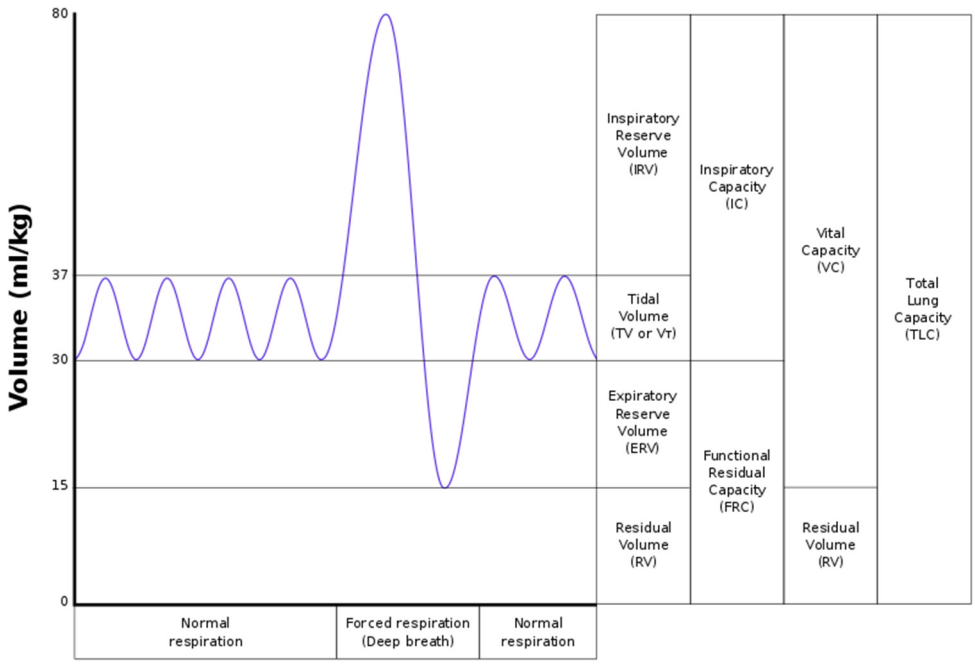

Figure 3: A spirometry output graphic illustrating the lung volumes and capacities. Image: Vihsadas, creative commons attribution license http./commons.

When the ratio of the volume of air that can be forcibly expired from fully inflated lungs in one second (FEV_1), divided by the volume that can forcibly be expired (FVC), reaches below 0.70, obstruction is considered to be present. If obstruction is present, it is further quantified by comparing the FEV_1 to values predicted taking the patient's age, sex and height into consideration. (37) The lung flow/volume loop shape may also assume a concave form, which has been suggested as an early indication of small airways obstruction. (38) (Figure 4) In airway obstruction, peak expiratory flow is also reduced. Considering healthy individuals, the main site of resistance is in the 4^{th} to 8^{th} generations; FEV_1, can be seen mainly as an index of large airways. Hence, the resistance of the small airways must be considerably increased for the disease to give rise to measurable changes in spirometry. (39) To diagnose COPD, spirometry is conducted after inhalation of bronchodilators. In the clinical context, the patients' symptoms are also weighed in when diagnosing and staging COPD. (2)

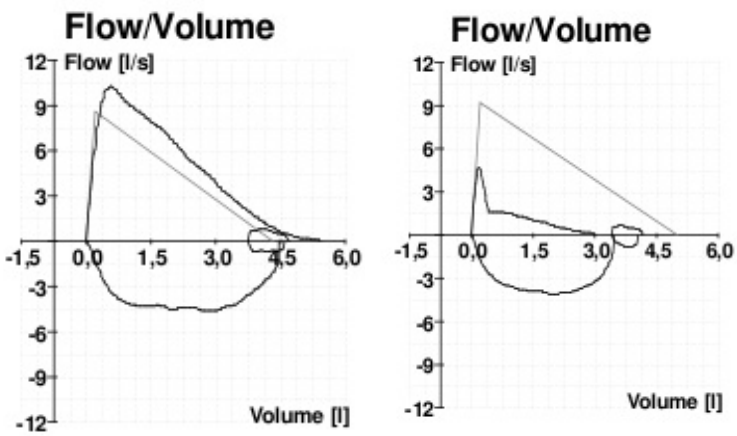

Figure 4: On the left, normal spirometry. On the right, findings indicating obstruction. The smaller ring denotes normal breathing. The larger loop refers to maximal inspiration and expiration. Note the concave flow/volume curve indicating In the case of COPD Http:// commons.wikimedia.org/wiki File:Normal_spirometry.png, File:COPD.png. Public domain

RV, which is a component of TLC, cannot be measured by simple spirometry alone, and to determine TLC, additional instruments are required, usually body pletysmography. Decreased elastic recoil in emphysema, in combination with narrowing of airway lumen, causes an increase in RV, and therefore also TLC.

In advanced centers, additional measurements suggesting small airway disease may be included, e.g. diffusing capacity of carbon monoxide, forced oscillometry, (40) or nitrogen washout. (41)

2.3.2 $D_{L,CO}$

Diffusing capacity for carbon monoxide ($D_{L,CO}$) uses a technique originally described in 1909. The method measures of the diffusion property of the lung, and the test indirectly quantifies the lung's capacity to oxygenate the blood. (42, 43)
The test is performed using a mixture of carbon monoxide and a tracer gas, often helium. The blood haemoglobin has high affinity to carbon monoxide, which readily enters the bloodstream from the gas-exchanging tissue. The patient inhales the test gas maximally through a mouthpiece from RV to TLC, holds her/his breath for 10 seconds, exhales, after which a distal airspace sample is used to analyse the gas mixture. The partial pressure of carbon monoxide in inhaled and exhaled gas mixture are compared. The measured unit is given as mmol min^{-1} kPa^{-1}, but the result is often given as a percentage of predicted value taking anthropometric variables and preferably blood haemoglobin concentration into consideration. In emphysema, the alveolar walls are destroyed, and the active surface area of the alveolar-capillary membrane available for gaseous exchange is reduced. Similarly, the $D_{L,CO}$ is also reduced compared to normal. The test has been found to indicate emphysema in smokers before obstruction is present. An important limitation is that reduced $D_{L,CO}$ is not specific for emphysema. (44)

2.4 Lung imaging methods

2.4.1 Conventional x-ray imaging and computed tomography

In both conventional x-ray and computed tomography, the part of the body being imaged is placed between an X-ray source and a detector or film to record the rays. The x-ray source sends electromagnetic waves, i.e. radiation, through the tissue. As the photons pass through the body, dense objects, such as bone or metal, will readily attenuate photons, leaving the corresponding areas on the detector or film white. Consequently, the probability of a ray attenuating in a less dense structure is lower, and a larger proportion of the photons reach the detector, appearing black in the image. In conventional x-ray, the organs are superimposed on a 2D-image, while in computed tomography, the x-ray source rotates around the patient, scanning the body slice-by-slice, resulting in cross-sectional images. In CT, the images may be reconstructed and viewed in different planes. The conventional x-ray is easily available and less costly than CT, and it generally generates a lower radiation dose of than CT. In CT, the attenuation of X-rays can be quantified by Hounsfield Units (HU), where 0 HU refers to water, -1000 to air and 3000 to bone.

The tissue destruction in emphysema increases the air content within the pulmonary parenchyma, which then becomes more permissible to x-rays than healthy lung

tissue. In plain x-ray, the presence of emphysema is suggested when the classic findings of hyperinflation, flattened diaphragmatic cupola and increased anteroposterior distance are present. (Figure 5) Inhomogeneously distributed emphysema gives rise to local disruptions in parenchymal architecture, which may be detected in chest x-ray. In CT, the lower attenuation and architectural disruption can be better evaluated compared to x-ray, and a clearer regional information can be attained. The three different types of emphysema; centrilobular, panlobular and paraseptal, can be assessed. (45) (Figure 6)

Emphysema is often assessed with high resolution CT (HRCT) (46) In HRCT, thin section slices should be used with appropriate windowing to enable visualization of the pathological findings in the secondary pulmonary lobules. (47) Paired inspiratory and expiratory scans can be used to identify air trapping.

CT is currently the most specific, clinically used method to diagnose emphysema, with superior concordance to pathological specimens over lung function tests including $D_{L,CO}$. (48-50) CT is, however, rarely used for this indication, mainly due to cost, lack of availability and to radiation dose. Also, the interpretation requires radiologist skills. Modern methods can decrease the radiation dose lower, and the clinical praxis may shift to favor CT over PFTs, especially as screening programs for lung cancer are being established and semi-automated image interpretation may become available.

a)

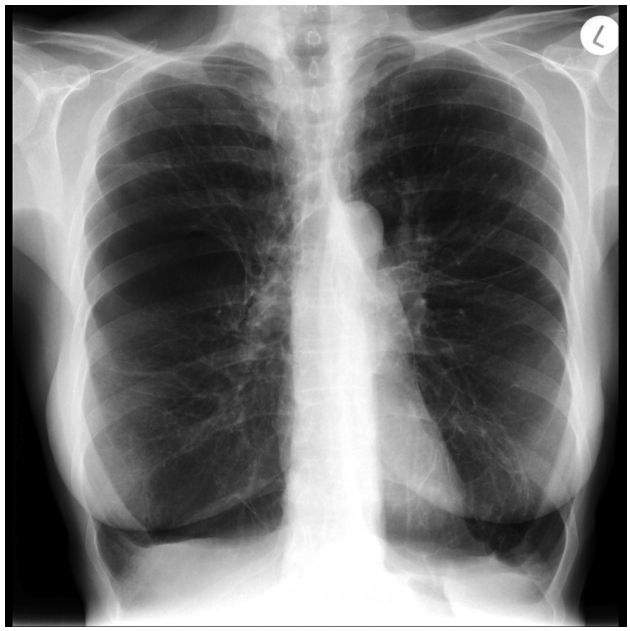

b)

Figure 5: A chest x-ray image of emphysema, s) anteroposterior view. b) lateral view (see text)
Image http://www.radiopaedia.org, dr Andrew Dixon, Creative commons attribution license

a)

b)

c)

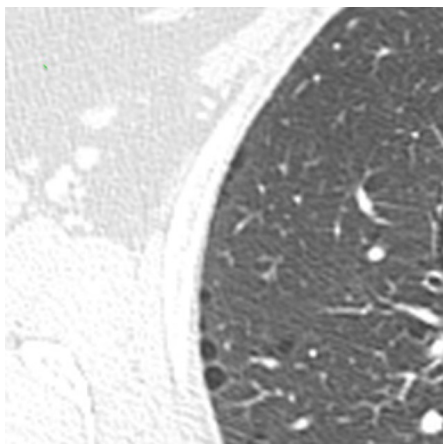

Figure 6: CT appearance of a) centrilobular, b) panlobular and d) paraseptal emphysema. Note the central vascular structure in the secondary pulmonary lobule in the centrilobular (a) emphysema. In panlobular emphysema, (b), larger areas of destruction are seen Images: http//:www.radiopaedia.org. Dr. Dains Cuete, Dr. Abdallah Alqudah, Dr Natalie Jung, Creative commons attribution license

2.4.2 CT densitometry

In CT, each slice has a pre-determined thickness, and hence, each image pixel represents a tiny volume. Such "3D-pixels", called voxels, can be seen to represent a volume sub-unit of the tissue being examined. The x-ray attenuation is indicative of tissue density. Densitometry refers to quantitative, voxel-by-voxel assessment of the tissue's attenuation values (HU). In the case of the lung, determining the attenuation value of each voxel in the lung parenchyma gives indication regarding the lung density, which is decreased in the destroyed, emphysematous tissue. Hayhurst first described 1984 that centrilobular emphysematous subjects had significantly more voxels in the attenuation range between -900 and -1000 HU compared to normal subjects. (51) Direct one-to-one pathologic radiologic correlations to HRCT have since confirmed the findings. (52).

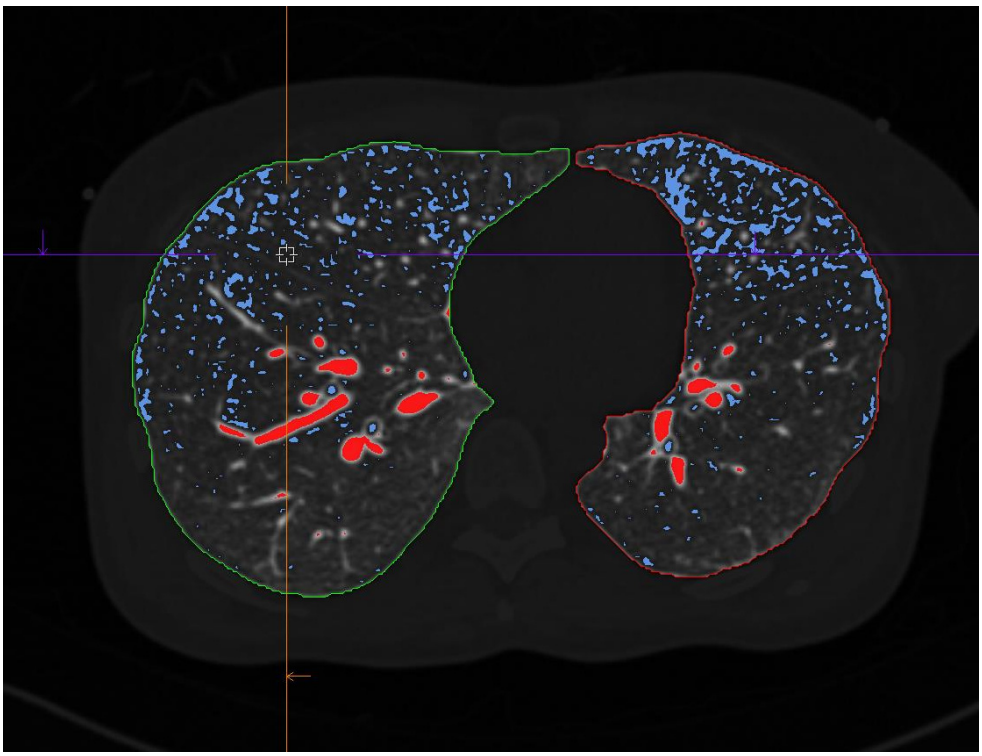

Figure 7: CT-densitometric axial cross-sectional image of the chest. The software delineates right and left lung, and separates them from the thoracic wall and mediastinum. The areas in blue represent voxels with attenuation value below -950 HU. The areas in red correspond to blood vessels, also excluded from analysis.

Muller developed a technique called “density mask”, where voxels below a certain attenuation value are considered emphysematous. (53) This method has also been validated against microscopic and macroscopic pathologic specimens. (54, 55) Currently, the most common mask used is to consider attenuation values below -950 HU as emphysematous. (54) Additionally, the fifteenth percentile of attenuation distribution histogram, termed PD15, has been used as a measure of density by adding 1000 to the HU-value to yield a value in g/L. (56) PD15 has been found as the most robust measure of emphysema progression. (57, 58)
Visually assessed CT has been found to consistently underestimate mild and moderate emphysema. (59) It has been stated that CT densitometry correlates better to pathological specimens than visual assessment. (60) Despite its apparent superiority over the human eye, densitometry has not made it to clinical praxis yet, as there is no consensus what can generally be accepted as cut-off value for emphysema. The results depend highly on radiation dose, scanner, algorithm, post-processing and detector configurations. The lung density values also depend on age, TLC and sex. (61-65)

2.4.3 Magnetic resonance imaging

In magnetic resonance imaging (MRI), the body’s protons are placed under a powerful magnetic field. Many of the protons, with their positive charge, will first align with this magnetic field. The protons are then excited by radio waves to obtain a signal. The signal is then collected and converted to an image

MRI in the lung, however, is complicated by low signal as normal lung tissue has a low proton content. In emphysema, the lungs are hyperinflated and poorly perfused, which further reduces the proton content. To image emphysematous lungs, proton-density weighted, ultra-short echo time technique has been developed, and densitometric analyses similar to CT have been suggested. (66-68) (Figure 8)

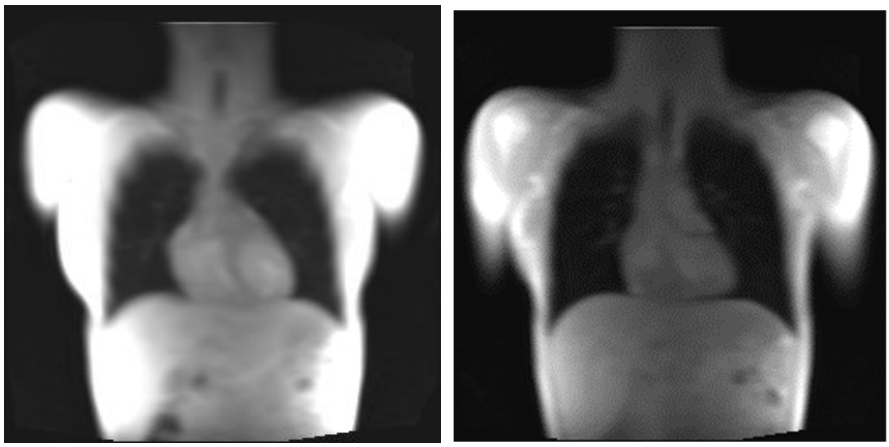

Figure 8: Magnitude images from the short echo-time sequence used for MR densitometry measurements in Paper II.

Visualization of ventilated tissue is made possible by using either oxygen-enhancement or inhalation of hyperpolarized gases, often ^{3}He. Determining the apparent diffusion coefficient (ADC) gives a quantitative measure of free diffusion of gas during a breath-hold. The term unrestricted is used if the molecules can diffuse freely, and conversely, restricted if diffusion availability is low. (69) In the lungs, diffusion becomes effectively restricted by the boundaries of the airspaces. In MRI with hyperpolarized gases, diffusion is highly restricted in the normal lung parenchyma, and almost unrestricted in severe emphysema. Using this method, it is possible to obtain an estimate of the size of alveoli. (70) This method has also been validated against histology. (71) (Figure 9)

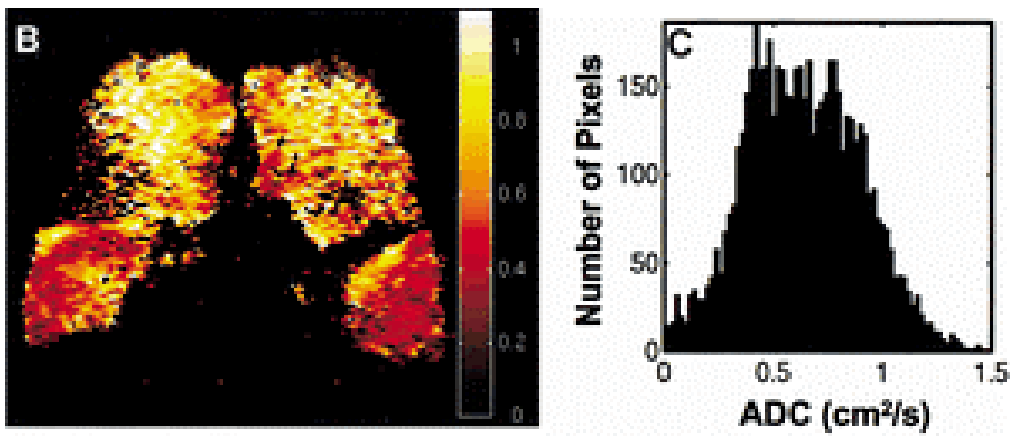

Figure 9: Magnetic resonance imaging of the lungs with hyperpolarized helium showing an ADC-measurement (Image: Sandra Diaz, Hyperpolarized He-diffusion MRI in evaluation of lung structure in emphysema 2008. Validation and development of the method), reprinted with permission

2.4.4 Other methods

Numerous methods to image emphysema and COPD have been developed, describing them comprehensively is beyond the scope of this introduction. (72, 73) To name a few examples, using paired inspiratory and expiratory CTs can air trapping can be identified by using a density mask. (74) CT has also been used to quantify bronchial properties, for example wall thickness or luminal area. (75, 76)

Clinical HRCT can characterize anatomic details as small as approximately seventh to ninth bronchial generation. (77) With micro-CT resolution as low as 3-4 µm can be achieved, and smaller structures, such as terminal bronchioli and alveoli, can be assessed. Micro-CT is not available for in-vivo use, though, due to limited field of view, artefacts from respiration and heart motion, as well as radiation dose. (78-80)

Molecular imaging is a term that refers to techniques, which monitor and record the spatiotemporal distribution of molecular or cellular processes for biochemical, biologic, diagnostic or therapeutic applications. (81) In COPD, quantitative histology and gene expression profiling can be imaged using micro-CT, giving further insight in the pathophysiological process. (82, 83)

In gamma scintigraphy, radioactivity-emitting radionucleids can be imaged as they decay. In single photon emission tomography (SPECT), multiple gamma detectors rotate around a patient. The images can be reconstructed to illustrate radionucleid distribution in three dimensions. This method can be combined with CT to relate the distribution to corresponding anatomical locations using inhaled radiolabelled gases or radiolabelled < 100 nm particles (Technegas). Studies with Technegas indicate that even in the presence of several airflow limitation, the radiolabelled tracer regional distribution pattern mimics that of real gas. (84) Technegas SPECT has been shown to identify regional differences in emphysema. (85) Also, finding early emphysema by detecting perfusion heterogeneity in ventilation/perfusion methods has been suggested. (86, 87)

Synchrotron real time x-ray imaging has enabled in vivo alveolar dimension measurements in mice, including measuring the contraction and expansion of alveoli during respiration. (88)

2.5 Inhaled particles

2.5.1 Particle size

A nanometer refers to a size unit of one billionth of a meter, or 10^{-9} m. The term nanoparticle generally refers to engineered particles under 100 nm in size. In air pollution context, particles under 100 nm are termed ultra-fine particles. For comparison, the term fine particle is used for particles between 0.1-2.5 μm (100 and 2,500 nm); and coarse particle refers to a particle between 2.5-10 μm (2500 - 10000 nm) in diameter. (89)

2.5.2 Particle deposition in the lungs

The respiratory system is adapted to successfully clearing inhaled particles away from the gaseous exchanging regions. Simplifying, particles of different sizes are removed at various depths of the respiratory system. Generally, the largest particles (>10 μm) are removed already at the nose and larynx levels, whereas smaller particles may deposit further distally. Particles roughly below 500 nm reach the alveoli in significant amounts. Very small particles, below 5-10 nm, however, also have a high deposition in extrathoracic airways due to their rapid movement by diffusion.

Upon contact with the airway wall, particles generally do not bounce, but deposit instead. In this context, deposition refers to a particle adhering to a surface. The most important methods of deposition of airborne particles in the lungs are impaction, interception, sedimentation and diffusion (Figure 10). (90)

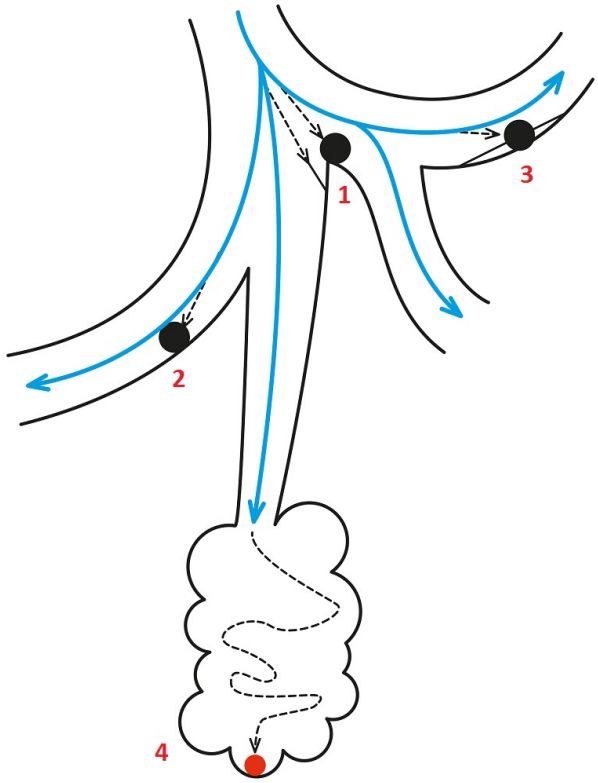

Figure 10: Particle deposition modes. 1 inertial impaction, 2 gravitational settling, 3 interception, 4 diffusion (see text).

The largest particles deposit by *impaction*, which means they cannot, due to their mass, follow changes of the direction of flow, and at each change of flow direction they continue with their inertia, eventually impacting on the airway surface. This often leads to greater deposition at hot spots near bifurcations. Deposition by *interception* refers to a particle, which is able to follow the air flow, coming in contact with the airway surface due to its size. Further down the bronchial tree, as the bulk flow grows closer to zero, *gravitational settling* and *diffusion* take over as the main mechanisms of transportation. In gravitational settling, particles are pulled under gravity toward dependent sites. The smallest particles undergo Brownian motion, which refers to a random motion of small particles in still air, which is caused by the particles being hit by the surrounding, much smaller gas molecules. (91) Brownian diffusion refers to particles or gas undergoing Brownian motion, while moving from a region of high concentration to a region of low concentration. (The Latin origin of the word diffusion means “to spread out”.) (69) Nanoparticles deposit almost exclusively by Brownian diffusion. The diffusion rate is proportional

to the size of the particles; the smaller the particle/molecule, the higher the diffusion rate. (69, 90)

The likelihood of nanoparticles' deposition in the airways depends on the diffusion distances as well as the time the aerosol resides in the distal airspaces. Keeping the residence time constant, the deposition will be reflective of diffusion distance. (92)

2.5.3 Hypothesis

The main hypothesis of this thesis is that the nanoparticles' deposition property can be used to differentiate persons who have emphysematous, enlarged distal airspaces from those who do not have emphysema. (Figure 11) The term recovery is used to describe the fraction of inhaled particles that returns back with the exhaled gas mixture. Persons with enlarged airspaces will have longer diffusion distances relative to normal. We therefore expect the deposition in these persons to be lower than normal and thus, we expect the recovery to be higher than normal.

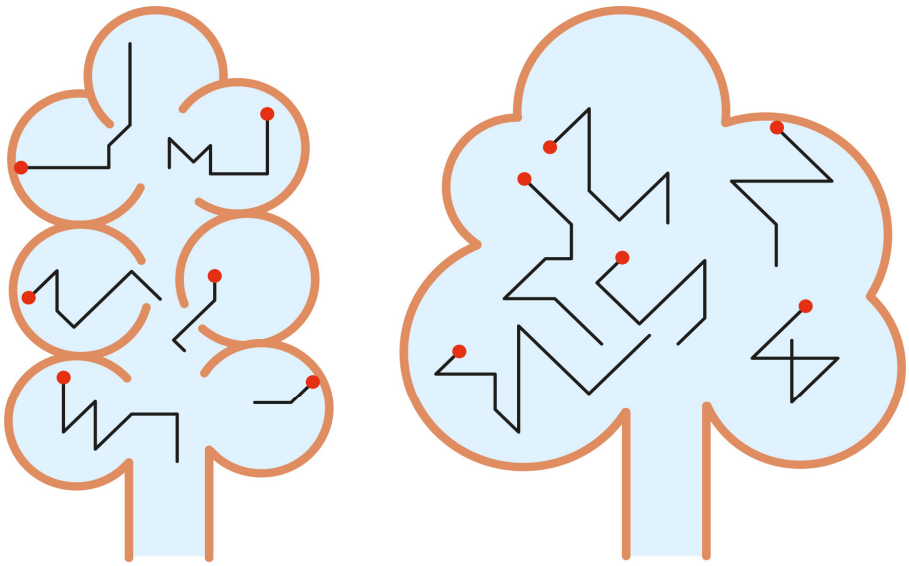

Figure 11: A schematic diagram exemplifying the recovery difference in healthy and emphysematous tissue. On the left, a normal alveolus with shorter diffusion distances, many particles deposit, giving a **low** recovery in exhaled air. On the right, emphysematous alveolus with larger diffusion distances; fewer particles deposit, yielding a **high** recovery in exhaled air.

The previous literature regarding empirical studies of nanoparticle deposition in COPD-patients is scarce. (93-96) According to a theoretical model, nanoparticles in the size range of 50 µm deposit mainly in the distal airspaces, and their deposition is not dependent on the flow rate. (Figure 12) (11)

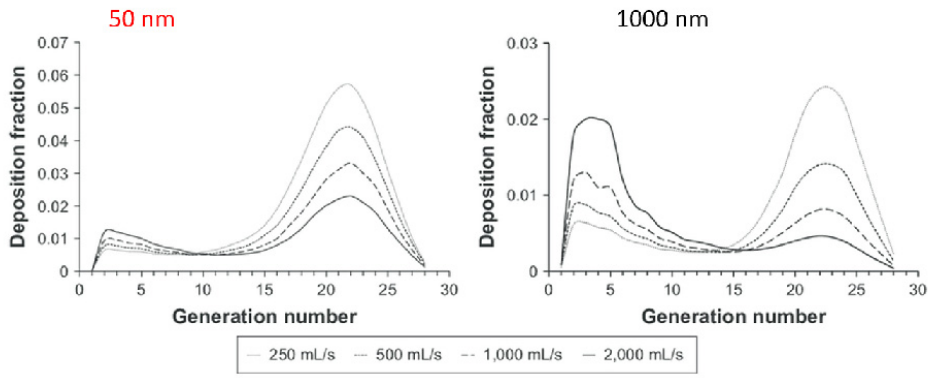

Figure 12: Deposition fraction at different generations of the respiratory tract for 50 nm particles (left) and 1000 nm particles (right) as calculated with the Multiple Path Particle Dosimetry model for a healthy adult during oral breathing without breath-hold. (IRCP 1994) (92)

2.5.4 Airspace Dimension Assessment with nanoparticles

To test the hypothesis, an apparatus to measure nanoparticle recovery was constructed as a collaboration between Lund University Faculty of Engineering and Department of Translational Medicine. (Figure 13) (97)

In the apparatus, termed Airspace Dimension Assessment (AiDA), nanoparticles are generated and led to a reservoir. During the measurements, the patient sits comfortably and breathes several cycles of completely particle-free air from a mouthpiece and then exhales to residual volume. A maximal inhalation to TLC ensues; at the beginning of this inhalation, computer-controlled valves close, and aerosol is led from the reservoir to the mouthpiece. The patient holds her or his breath for a predetermined time period, and then exhales. Particle concentration in inhaled gas, and in a sample of exhaled gas from distal airspaces at a given volumetric depth, are measured. (Figure 14) (92, 97) For a detailed description, see section 4.4.

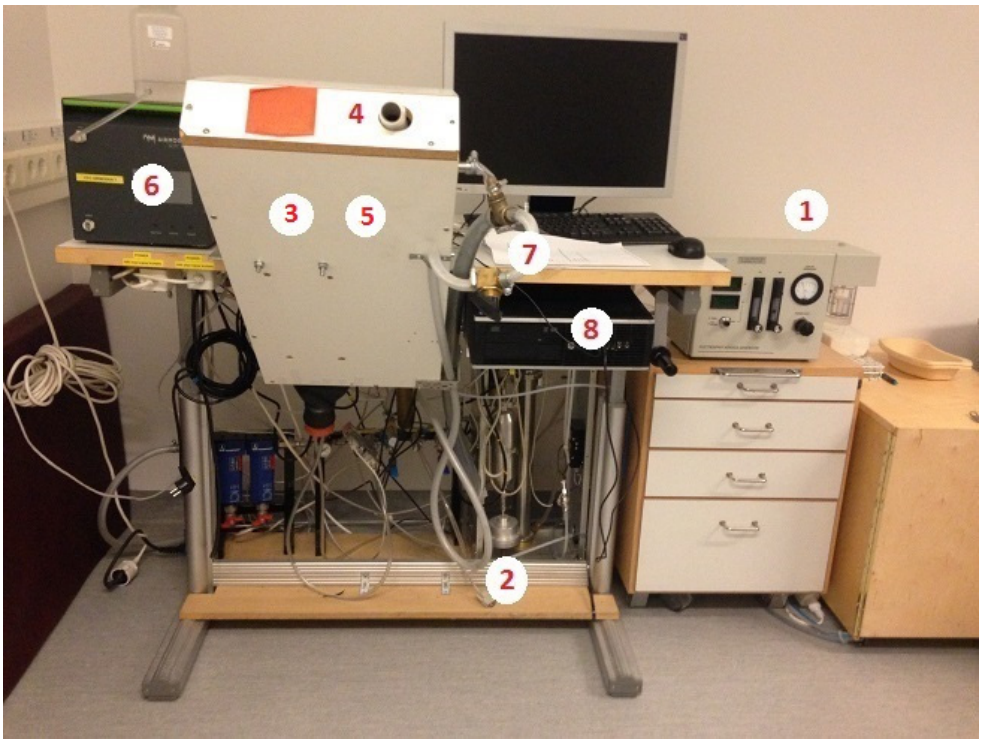

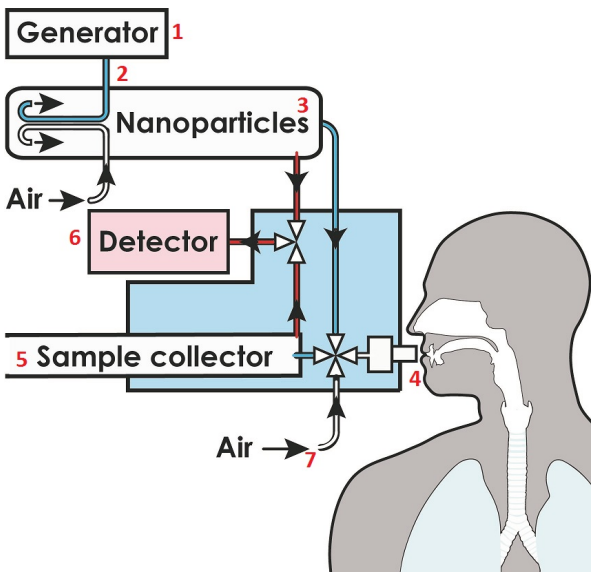

Figure 13: The AiDA prototype and a schematic illustration (1) Particle generator (2) Differential mobility analyzer (DMA) ensures uniform particle concentration (3)The aerosol reservoir where the nanoparticles are mixed with particle-free air (4) Mouthpiece (5) Sample collector, (6) Particles are detected by a condensation particle counter (CPC) (7) Filtered, particle-free air (8) Computer

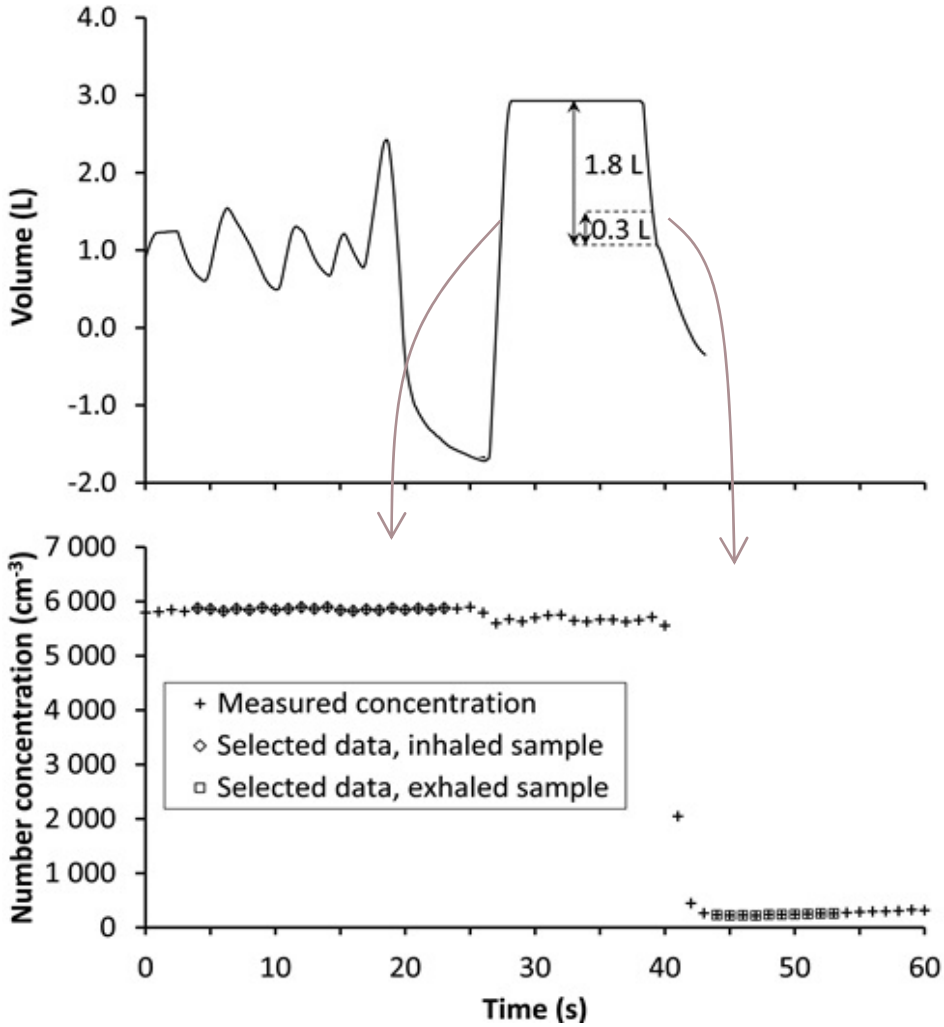

Figure 14: Recovery is measured as the fraction of particles returning with the exhaled gas mixture. The sampled air mixture is chosen from a volumetric lung depth distal to conducting airways. Volumetric depth refers to the volume of exhaled gas from TLC.

Nanoparticle recovery can be used to calculate the airspace radius as described by Löndahl. (92) Briefly, an exponential decay curve is fitted to the recovery values obtained by a series of breath holds of varying duration (Figure 15). The airspace radius, r_{AiDA}, is calculated from the half-life of this decay, according to:

$$r = 2.89\sqrt{D}t_{½}$$

where *D* is the diffusion coefficient given by the Stokes-Einstein equation, and it is affected by temperature, viscosity, and particle size. (90-92) The larger the D-value, the faster the diffusion process is.

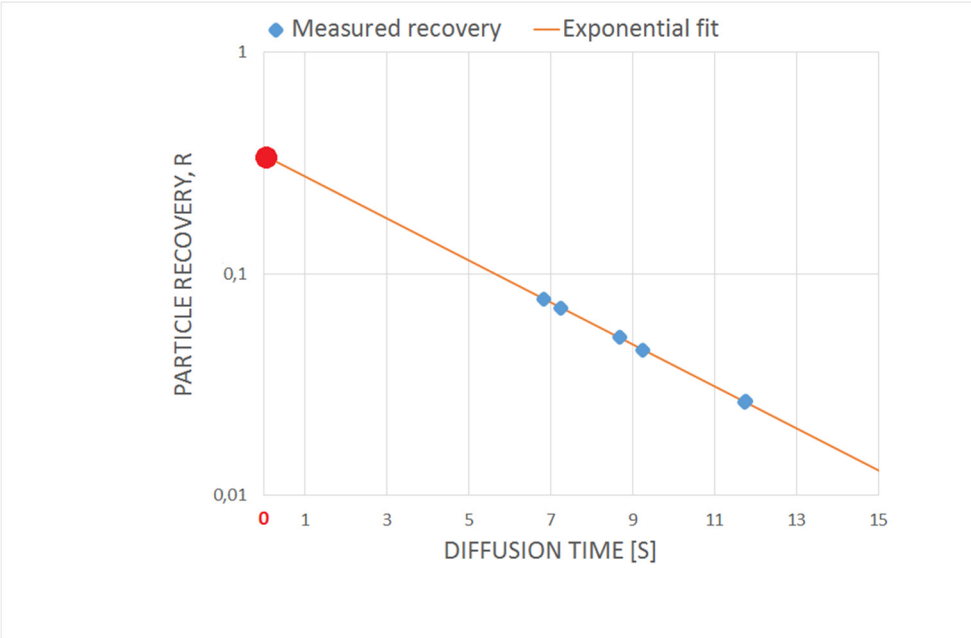

Figure 15: Example data from an AiDA-measurement in Paper II. Exhaled nanoparticle recovery over time and extrapolation line, (logarithmic scale). The extrapolation line is used to determine the particle half-life. R(0) is the recovery value at the y-intercept of the extrapolation line, i.e. recovery at time = 0. R(0) is indicated with a red dot.

As the D depends on the particle size, the particles in AiDA must have a very narrow size distribution. This is achieved by a differential mobility analyzer (DMA), in which an electric field is generated to separate particles of a desired size.

The radius here should not be understood as a specific anatomical model, but rather an expression of average diffusion distance in the airspaces at a given volumetric lung depth. As the nanoparticles mainly deposit in the distal airspaces (Figure 12), their average diffusion distance is reflective of the diffusion distances in this region.

The AiDA mean radius is not an arithmetic mean, but a geometric mean, which slightly overemphasizes larger values. Recovery measurements with at least two different breath-hold times are needed to calculate the half-life, and hence, the radius. (92, 98)

Extrapolating the exponential decay curve to the y-intercept yields a theoretical recovery value for a breath-hold time zero. (Figure 15) This variable has been suggested to have biological properties. (92) The significance of this finding is presently not known.

AiDA has been found to have high precision of ± 7 μm for repeated measurements of the same subject. Also, in healthy subjects, r_{AiDA} value has been found to be constant over a range of volumetric depths. (98)

2.5.5 Aerosol Derived Airway Morphometry

Studies of lung deposition of aerosols to measure lung dimensions have been conducted as early as 1968 by Palmes. (99) Micron and submicron size particle inhalation tests have since been proposed to assess distal airway dimensions. A technique termed Aerosol Derived Airway Morphometry (ADAM) harnesses the particles' gravitational sedimentation property. After a series of breath-hold inhalations, the particle recovery at different breath-hold times is used to estimate distal airspace diameter. (100) The method has been validated against pathological specimens, compared to a lung model and lung function indices, and it has been shown to detect emphysema. (101-104) Differences between ADAM and AiDA are discussed in section 6.2.

2.5.6 Particle clearance

Clearance refers to the body's actions to remove particles. In the extrathoracic airways, insoluble particles are cleared mechanically, i.e. by sneezing, coughing or swallowing. In the intrathoracic region, mucociliary clearance is used, where particles fasten in secreted mucus. The epithelial cilia then undergo rhythmic contractions to propel the mucus towards the pharynx, where it is either coughed or ingested. (105) Towards the deeper generations of the conducting airways, cilia decrease in number, and the mucociliary clearance progressively decreases. In the alveolar region, the particles are cleared by macrophages. (106)
Translocation refers to the process of particles entering the bloodstream from the lungs, and migrating to extrapulmonary organs. There is no evidence of quantitatively significant translocation of 35 nm carbon nanoparticles in humans. (107) However, more studies on different nanoparticle materials and their clearance are warranted. (108)

3 Aims

The overall aim of this thesis was to investigate the potential of the Airspace Dimension Assessment with nanoparticles (AiDA) as a method to describe distal airspace morphology, as well as to assess the technique as a possible biomarker for emphysema.

Paper I

The aim of this study was to explore the difference in nanoparticle recovery between COPD-patients and never-smoking controls. A secondary aim was to examine, whether the recovery values correlate with the extent of emphysema as measured by computed tomography (CT) densitometry and diffusing capacity for carbon monoxide ($D_{L,CO}$).

Paper II

The aim of this study was to determine whether the AiDA-derived airspace radius correlates with pulmonary density as measured by MRI in healthy volunteers.

Paper III

The aim of this study was to examine the distal airspace morphology using the AiDA method in a subjectively healthy population without known pulmonary disease or self-reported symptoms; to investigate the variability of the AiDA measures in a general population sample, as well as to explain the variability in terms of anthropometry, lung function and imaging-derived measures. A secondary aim was to examine the AiDA values relative to smoking history.

Paper IV

The aim of this study was to evaluate AiDA as a possible biomarker for emphysema by determining if AiDA can differentiate persons with CT-verified emphysema from those without emphysema in a general population sample. A secondary aim was to determine if persons with emphysema defined by quantitative imaging or lung function parameters have larger AiDA radius relative to non-emphysematous persons. A tertiary aim was to investigate the role of comorbidities.

4 Material and Methods

4.1 Study populations

Paper I

The study group consisted of 23 patients with COPD. The control group consisted of a conveniency sample of 20 never-smokers without a history of pulmonary disease. The control group was similar to the COPD group with respect to age and sex ratio. A total of four COPD-patients were excluded due to poor quality of AiDA measurements; three due to inhaled volume below 2/3 of vital capacity, and one due to too long breath-hold time (>17 seconds). One prospective control person was excluded due to spirometry values indicating GOLD stage 2 COPD. Hence, 19 COPD-patients and 19 controls were eligible for analysis.

Paper II

The study group consisted of 25 prospectively recruited healthy, never-smoking volunteers between 21 and 64 years of age. Four persons were excluded due to poor quality of AiDA measurements; two due to dispersion in data points with a deviation from theoretical model with intra-individual correlation less than 0.95. Another person was excluded due to large intra-individual variation at the 5 second inhalation, and another had to abort the measurement due to air leakage at the instrument mouthpiece. Additional two individuals did not perform AiDA-measurements or pulmonary function tests due to logistical reasons. This resulted in a total of 19 individuals eligible for analysis.

Papers III-IV

The data for this prospective study were obtained from the Swedish CArdioPulmonary bioImage Study (SCAPIS), a national population-based study with 30 154 participants between 50 and 64 years of age. (8) In total, 744 individuals examined at the SCAPIS local site at Malmö, Sweden, underwent AiDA measurements.

In Paper III, a subset of the population was used. A healthy normal population was defined according to principles given by Johannessen et al, excluding persons with a history of respiratory disease or symptoms. (9) Respiratory illness was defined as

an affirmative answer to the question: “Have you been diagnosed with chronic obstructive pulmonary disease, chronic bronchitis, emphysema, asthma, tuberculosis or other pulmonary disease?” Self-reported respiratory symptoms were defined as an affirmative answer to any of the following questions: “Do you cough even when you do not have a common cold?”, “Do you experience wheezing or whistling in your lungs?”, or “Do you experience shortness of breath when hurrying on level ground or walking up a slight incline?” Of the initial 744 individuals, 55 were excluded due to previously diagnosed respiratory illness, and an additional 199 due to self-reported respiratory symptoms. Nineteen individuals were excluded due to missing study questionnaire data. This resulted in 471 eligible participants, of which 68 were excluded due to poor quality of AiDA measurements, as stated under section 4.4. Hence, a total of 403 individuals were included.

In Paper IV, 126 of the 744 examined individuals were excluded due to poor quality of AiDA measurements, according to the criteria stated under section 4.4. This resulted in 618 persons eligible for analysis.

4.2 Lung function tests

Papers I-IV

The subjects underwent conventional lung function tests performed according to the European Respiratory Society/American Thoracic Society guidelines. Postbronchodilator FEV_1, vital capacity (VC) and $D_{L,CO}$ values were measured (Jaeger MasterScreen PFT, IntraMedic, Sollentuna, Sweden). In Papers I and II the lung function variables were presented as percentage of predicted values and in papers III and IV both as percentage of predicted and as raw values. (37)

4.3 Lung imaging methods

Paper I

The COPD group underwent a low radiation dose CT scan of the chest in suspended full inspiration using a multidetector-row scanner (Siemens Somatom Definition Flash; Siemens Healthineers, Forchheim, Germany) with a detector configuration of 128 × 0.6, automatic tube voltage selection (Care kV, ref kV 120), automatic tube current modulation (CareDose 4D, ref mAs 15), pitch 1.2 and rotation time 0.5 seconds. Images were obtained using B20f, 1 mm slice thickness / 1 mm increment, as well as I70f, (SAFIRE level 1), 2 mm / 2.5 mm. A computer-assisted tissue density analysis was carried out using *syngo.via* Pulmo 3D software version VA,

which automatically separated the lungs from adjacent organs. The extent of emphysema was estimated using two densitometric measures:

1. The relative volume of voxels with x-ray attenuation values below -950 Hounsfield Units (RV-950) (53)
2. The lung density at the 15th percentile of the attenuation distribution histogram, termed partial density (PD15). (54, 55) This value, given as g/L, was used to represent tissue density in correlation analyses. (55, 56, 60)

The CT scans were also visually assessed by a radiologist with 9 years of experience (SD) and a radiology resident (HLA) with 2 years of experience. The extent of emphysema was graded as absent, mild, moderate or severe. Also, the presence of bullous emphysema, bronchiectasis and extensive bronchial wall thickening were evaluated. To avoid radiation exposure, the control group did not undergo CT.

Paper II

All subjects underwent a MRI of the chest on a 1.5 Tesla Siemens Magnetom AvantoFit (Siemens Healthcare, Erlangen, Germany), with an 18 channel body coil and a 32 channel spine matrix. Coronal proton density (PD) maps were measured with the Snapshot FLASH pulse sequence to correct for T1. (68) The imaging matrix was 128 × 64 zero filled to 256 × 256; field of view 450 mm square; slice thickness 1.5 cm; echo time = 0.67 ms; repetition time = 3.0 ms; and flip angle = 7°. All measurements were preceded by instructions for breath-hold after a tidal inspiration and subjects were given at least 10 seconds of free breathing to restore magnetization equilibrium between measurements. The data were processed in MatLab R2014b (MathWorks, Natick, MA, USA). The lungs were segmented in three dimensions (3D) using the magnitude images, followed by manual removal of major vessels. Segmentations were considered successful when each slice clearly included the signal magnitude gradient representing the border of the lung.

For each subject, a radiologist (HLA) selected three slices ventral to the airway bifurcation and manually placed a region of interest (ROI) representing the left ventricular blood in each image. For each image, the lung PD was normalized to the mean signal intensity of the ventricular ROI. (66) Since MRI measurements were made at tidal inspiration – which is a poorly defined lung volume – the volume of the lung at the MRI acquisition, V_{MRI}, was calculated (as the size of the total segmented lung). Assuming the lungs simply inflate without changing tissue or blood content, density values at total lung capacity (TLC) can be calculated by multiplying density values with V_{MRI}/TLC. This TLC-corrected PD was called PD(TLC). Furthermore, all voxels with a density value higher than 60% of the ventricular blood were considered blood vessels and hence, discarded from the analysis.

Three imaging variables were used to quantify lung density. These variables were originally developed for computed tomography, (56, 58) and later adopted to MRI: (66)

1. Mean lung density (MLD) represents the mean PD(TLC) of the entire segmented lung volume in three central slices.
2. The 15th percentile proton density (PD15) was calculated from the PD(TLC) histogram of all voxels in the selected lung slices.
3. The relative area under 7.5% PD (RA7.5). Here, a density mask analogous to CT in papers I, III and IV is applied; this is the fraction of lung voxels in the selected slices, with a PD(TLC) less than 7.5% of the ventricular blood signal intensity.

Papers III-IV

All subjects underwent a low radiation dose CT of the chest in full inspiration using a multidetector-row scanner (Siemens Somatom Definition Flash; Siemens Healthineers, Forchheim, Germany) with a detector configuration of 128 × 0.6, tube voltage 120 kV (Care kV off), tube current modulation (CareDose 4D, ref mAs 30), pitch 0.9, rotation time 0.5 seconds. Images were reconstructed according to the following kernels B31f, B20f, I30f (SAFIRE level 3), 0.6 mm slice thickness / 0.6 mm increment, as well as B35f 0.6 mm / 0.4 mm. The images were interpreted visually by one of four chest radiologists, who had between 9 and 35 years of experience. Emphysema was defined by the Fleischner society's guidelines and recorded as present or absent (109) If present, a modified Goddard score was obtained; each lung was divided into an upper, middle and lower section. For each section, a score between 0 and 3 was assigned, where 0 represented no emphysema, 1 represented 0 – 25% emphysema, 2 denoted a 25 – 50% emphysema, and 3 represented above 50% emphysema. The scores were added, yielding a maximum score of 18. (110) The images were further assessed using syngo.via pulmo 3D software version VA, and the CT-densitometric values described under Paper I were obtained. Emphysema was considered present if 7% or 5% of the voxels fell under the threshold HU-value. (111) CT-derived total lung capacity TLC (CTV) was calculated as the volumetric sum of the CT voxels containing lung tissue. (112, 113) Additionally, left upper lobe apical segmental bronchus thickness was measured. (75)

4.4 Airspace Dimension Assessment with nanoparticles

Papers I-IV

Nanoparticle recovery was measured using Airspace Dimension Assessment with nanoparticles (AiDA) method. (92, 97) The apparatus generated a monodisperse aerosol containing 50 nm polystyrene latex nanospheres using an electrospray aerosol generator (TSI model 3480; TSI Inc, Shoreview, MN, USA), followed by size selection by a differential mobility analyser (Model 3071; TSI GmbH, Aachen, Germany), and dilution with particle-free air. The aerosol was generated into a 10 L semi-flexible container. A constant flow of aerosol through the container was maintained to ensure a uniform particle concentration. A condensation particle counter (CPC, Model 3760; TSI Inc., Aachen, Germany) was used to measure the particle concentration in the inhaled and exhaled aerosol. The inhalation system in AiDA was temperature-controlled at 35°C to prevent water vapor condensation. All aerosol containing volumes and tubings were made of electrically conducting or antistatic material to minimize deposition due to electrostatic attraction. In addition, the inhaled aerosol particles were singly (positively) charged, and thus only weakly interacting with electrical fields. The particles were hydrophobic to avoid hygroscopic particle growth. (114)

The measurements were carried out in a sitting position, using a protocol similar to that of measuring $D_{L,CO}$ (43) The subject at first inhaled several breaths of particle-free air through a mouthpiece connected to a computer-controlled four-way valve (as used in Master Screen PFT; Jaeger, Germany) and then exhaled to residual volume. The valves closed, leading nanoparticle aerosol from a reservoir to the mouthpiece. The subject then performed an inhalation to total lung capacity (TLC), held his or her breath a predetermined time, and finally exhaled into a sample collector.

After accounting for particle losses within the instrument, particle concentration values in the inhaled and exhaled aerosol were used to determine recovery. The volumetric lung depth for the exhaled sample was chosen to be 1100–1300 mL. This is considered deep enough to measure beyond the dead space, but shallow enough for most subjects, including elderly, to be able to reach. The diffusion that takes place at either end of the breath-hold is accounted for, analogous to the procedure for measuring $D_{L,CO}$ (43).

In Paper I, three repeated measurements at the nominal breath-hold of 10 seconds were conducted. In papers II-IV, two repeats of three different nominal breath-hold times (5, 7 and 10 seconds) were conducted.

In Paper I, the results are given only as recovery. In papers II-IV, the multiple breath-hold times are used to calculate the airspace radius as described by Löndahl. (92) I.e. an exponential decay curve was fitted to the recovery values obtained by a series of breath holds of varying duration. The airspace radius was calculated from the half-life of this decay as given under 2.5.4.

Extrapolating the exponential decay curve to the y-intercept yields a theoretical recovery value for a breath-hold time zero. This value is recorded and investigated in papers II and III.

Technical quality

In Paper I, the measurements were considered of acceptable technical quality if the subject inhaled up to 2/3 of their vital capacity, and if the total breath-hold-time did not exceed 17 seconds. Paper II, which featured only healthy volunteers, measurements were considered of acceptable technical quality if the subject inhaled up to 2/3 of their vital capacity, and the measured values correlated with a theoretical model with a R^2-value exceeding 0.95. In Papers III and IV, the measurements were considered of sufficient technical quality if the subjects performed at least four valid breathing manoeuvers, no instrumental errors were detected and the correlation coefficient r, between breath-hold time and log recovery was above 0.9.

Exposure

Papers I-IV: The study protocol resulted in an exposure to aerosol with a particle number concentration of 10^4 particles cm^{-3} and a deposited particle mass of <0.03 μg in the lungs.

4.5 Statistical analysis

In all the papers, a p-value of less than 0.05 was considered statistically significant. The analyses were conducted using IBM SPSS v. 22-24, Armonk, NY.

Paper I

Data were, unless otherwise specified, reported as mean, standard deviation and range. Student's t-test was used for sex differences. The recovery values were reported as mean and intra-individual standard deviation of three technically acceptable tests. The intra-individual variability was evaluated by coefficient of variation. The difference between the groups was assessed with independent sample *t*-tests. Relationships between the parameters were evaluated using the Spearman's ρ correlation.

Paper II

In this study, the data were, unless otherwise specified, reported as mean, standard deviation, and range. Student's t-test was used for sex differences. For the investigated variables and the subjects with complete and acceptable measurements, Spearman's (ρ) was presented with p-values to assess correlation. The 95% confidence intervals (95% CI) for the AiDA parameters were calculated from the estimated standard error and the two-sided t-distribution with 4 degrees of freedom.

Paper III

The distributions of each variable were examined for skewness and kurtosis to test normality. To improve the fit, logarithmic transformations were investigated. No outliers were excluded. To assess the variability within the population, coefficient of variation was used. Linear regression models were used to evaluate the variation in both r_{AiDA} and R(0); standardized beta coefficients and their p-values were given. Collinearity was tested by tolerance and variation inflation factor (VIF). ANOVA and T-test were used for smoking subgroup analysis.

Paper IV

The distributions of each variable were examined for skewness and kurtosis to test normality. Means, standard deviations, minimum and maximum values were recorded. No outliers were excluded. The analyses were conducted with and without one outlier with a rAiDA value of 516 µm. Student's t-test was used to determine differences in r_{AiDA} between emphysematous and non-emphysematous subjects. The percentage of emphysema/COPD were investigated according to tertiles of r_{AiDA} in the population. Logistic regression models were used to investigate differences in r_{AiDA} odds ratios between COPD/emphysema subjects and healthy controls. In each analysis, missing data were reported. T-test in emphysema/COPD –indices between those who had missing AiDA values and those who did not were conducted to detect possible selection bias. A power calculation was made based on the results of paper I to allow sufficient power in paper IV.

5 Results

Paper I

In this proof-of-concept study the 19 COPD patients were found to have significantly higher mean nanoparticle recovery relative to the 19 controls, 0.128 ± 0.063 vs 0.074 ± 0.058; p = 0.010. Also, recovery correlated significantly with CT densitometry variables RV-950 (ρ = 0.586, p = 0.008) and PD15 (ρ = -0.665, p = 0.003). This indicates increasing recovery with decreasing lung density. Recovery was found to correlate with $D_{L,CO}$ (% predicted) both when considering the COPD group alone (ρ = -0.668, p = 0.002), as well as together with the controls (ρ = -0.506, p = 0.001) (Figure 16). No significant correlation between recovery and FEV_1 was found.

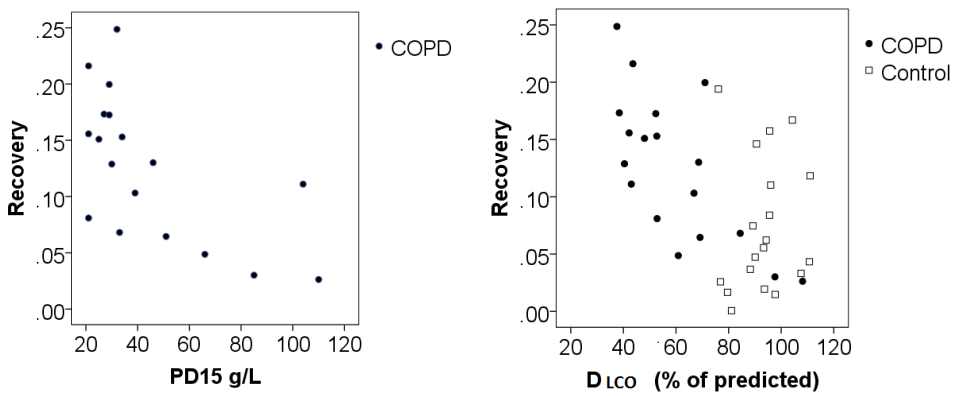

Figure 16: Recovery over tissue density (PD15) and $D_{L,CO}$.

Paper II

This study was the first empirical study to report AiDA-derived distal airspace radius (r_{AiDA}) values. The mean r_{AiDA} in the study group of 19 healthy volunteers aged 21-64 years was 272 ± 31 µm. The radius correlated with MR densitometric variables RA7.5 (ρ = 0.603, p = 0.006) and PD15 (ρ = - 0.584, p = 0.008). The results indicate increasing radius with decreasing lung density. A correlation to age was suggested, ρ = 0.452, although the finding was not established at the required level of significance (p = 0.052). The zero second recovery value R(0), or the

intercept of the exponential decay curve, was found to correlate significantly with age and FEV_1.

Paper III

The study group consisted of 403 persons 50-64 years of age, without respiratory disease or symptoms, participating in a nationally representative cross-sectional study (SCAPIS). In this group, the mean distal airspace radius was 293 ± 36 µm, which is approximately in line with other comparative methods. In the linear regression models, the radius was minimally influenced by weight and height. In regression models adjusted for age and anthropometry, the radius increased with increasing pack years (standard $\beta = 0.12$, $p = 0.02$). The ever-smoking men had a significantly larger radius compared to never-smoking men. (Table 1)

Table 1:
Differences between never- and ever-smoking men

	Never (N=92)		**Ever (N=90)**		
	Mean	SD	Mean	SD	p-value
TLC (CTV) (L)	6.3	1.2	6.1	1.2	NS
VC (% pred)	107	13	105	13	NS
FEV_1 (% pred)	108	13	105	15	NS
FEV_1/VC	0.80	0.06	0.76	0.07	0.005
FEV_1/VC (% pred)	104	8.3	101	9.3	0.01
$D_{L,CO}$ (% pred)	97	13	93	17	NS
PD15 (g/L)	84	19	90	22	NS
r_{AiDA} (µm)	289	33	302	40	0.03
ln r_{AiDA}	-1.25	0.11	-1.21	0.13	0.03
R(0)	0.55	0.21	0.53	0.19	NS

In women, no significant differences between never- and ever-smokers were found with respect to any of the listed variables, including FEV1/VC and FEV1/VC %. (Never-smokers N=90, ever-smokers N=130)
Never-smoker = a person with an accumulated tobacco consumption of less than one pack-year.
Ever-smoker = a person who is either a former smoker or an active smoker.

Paper IV

The r_{AiDA} values in a group of 618 individuals aged 50-64 years participating in the population-based SCAPIS-study were approximately normally distributed. (Figure 17) There was visually detected emphysema on CT in 47 individuals. The r_{AiDA} value in this group was significantly larger (326 ± 49 µm), compared to non-emphysematous individuals (291 ± 36 µm). The results were unchanged even if the outlier in figure 17 is excluded. Logistic regression analysis found increasing odds of emphysema with increasing r_{AiDA}. Odds ratio per 1 µm for emphysema, adjusted for age, sex, height and weight was 1.021 (1.013 – 1.028), $p < 0.0001$. Similar results were found when emphysema was defined by abnormal CT densitometry or $D_{L,CO}$ values. In table 2, the results are compared to other studies measuring distal airspaces.

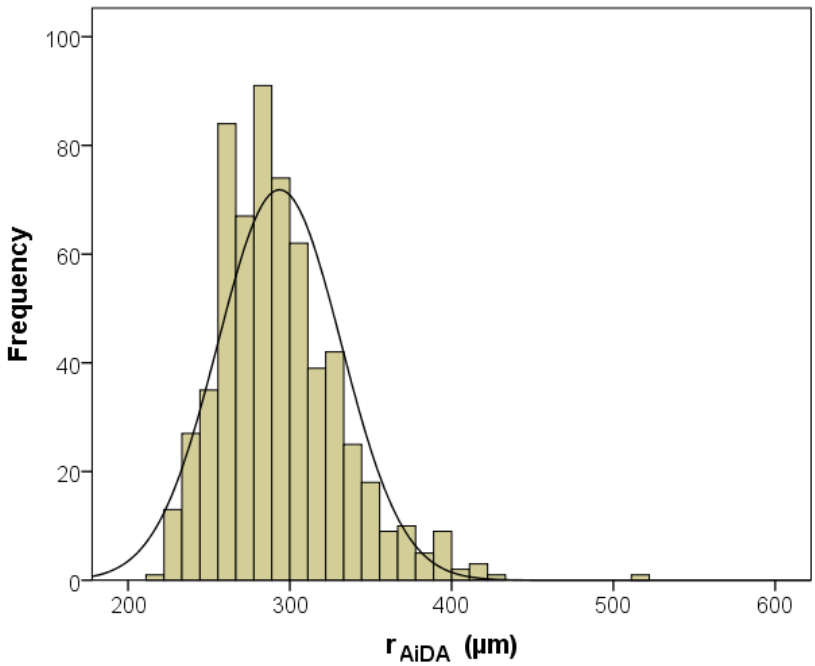

Figure 17: Frequency table of rAiDA
There was one female outlier value with r_{AiDA} of 516 mm. This person had moderate emphysema on CT with a modified Goddard score of 8 (of 16). She had COPD stage 2 according to spirometric GOLD-criteria ($FEV_1/VC < 0.7$ and FEV_1 of 55% of predicted). She also had a $D_{L,CO}$ of 49% of predicted. This person was an active smoker with a >52 pack year smoking history. She also reported experiencing dyspnoea, cough, wheezing and increased phlegm.

Table 2: Distal airspace diameter measured by different methods

STUDY	Method	Site of measurement	Number of subjects	Average diameter, non-emphysematous lung	Average diameter, emphysematous lung	Comment
Matsuba Thurlbeck 1972	Pathologic specimens	Small airways	Non-emphysematous N = 20, Emphysematous N = 12	723 µm	744 ± 60 µm	The results were corrected for lung inflation. No statistically significant difference between the groups. No SD given for the control subjects.
Hogg 2012	Micro CT	Terminal bronchi lumen	Controls N = 4 CLE N = 4 PLE N = 8	424 ± 48 µm	CLE: 52 ± 30 µm PLE: 210 ± 48 µm	
Tanabe 2017	Micro-CT	Preterminal bronchiolar internal diameter	Controls N = 7 CLE N = 6 PLE N = 7	570 ± 110 µm	CLE: 280 ± 120 µm PLE: 520 ± 170 µm	
Thurlbeck 1967	Pathologic specimens	Lm	Non-emphysematous N = 7, Emphysematous N = 44	283 µm	~800 µm	The results were corrected for lung inflation. No SD given for the control subjects.
Tanabe 2017	Micro-CT	Lm	Same as above	336 ± 37 µm	CLE: 766 ± 259 µm PLE: 698 ± 240 µm	
Hogg 2009	Micro-CT	Lm		Normally distributed mean alveolar dimension in the range of 150-600 µm	Right shifted distribution with alveolar dimension in the range of 150-1200 µm	These results were labeled preliminary, no N given
Woods 2006	^{3}He MRI	Lm	Controls N = 6 COPD N = 6	200 µm	410 µm	No SD given.
Chen 2016	^{3}He MRI	Lm	Healthy N = 5 COPD N = 1	~200 µm	314 µm	No mean value for healthy given.
Kohlhaufl 1999	ADAM	Distal airspaces	Non-emphysematous N = 30 Emphysematous N = 20	330 ± 100 µm	840 ± 530 µm	
The present study	AiDA	Distal airspaces	Non-emphysematous N = 563 Emphysematous N = 47	582 ± 72 µm	652 ± 96 µm	Diameter = 2 x radius.

CLE = centrilobular emphysema, PLE = panlobular emphysema, Lm = mean linear intercept, a measure of alveolar/acinar structures, ADAM = aerosol derived airway morphometry, AiDA = airspace dimension assessment with nanoparticles

6 Discussion

6.1 Disposition

Nanoparticles are able to penetrate to the distal lung. They behave like gases, undergoing stochastic, Brownian motion. In airspaces, they deposit mainly by diffusion, and the likelihood of their deposition depends on the diffusion distance. This diffusion distance can be quantified by AiDA and given as a radius, which in papers II-IV measures around 250-350 micrometers. As the pathway length from trachea to alveoli varies, however, the radius should not be understood as a specific anatomic site, but rather a geometric mean diffusion distance in the airways, measured at a given volumetric depth. The exact anatomical site at which the particles deposit is presently not known. As showed by Jakobsson, however, the radius is constant over a large range of volumetric depths distal to the purely conducting airways. (98)

The distal airspace dimensions in healthy individuals in Papers III and IV were generally in line with the previous literature, although considerable caution should be exercised in interpreting these findings, as there are vast differences in methodology, sample size, lung inflation and study design. The geometric rather than arithmetic mean used gives proportionally more weight to larger radii, which may be the reason why AiDA gives slightly higher radii compared to the other methods presented in paper IV.

Presently, it is not known how diseased lung will affect the signal, as the distribution of ventilated areas are less uniform. Areas completely not ventilated, such as those shown as black in Figure 9 (hyperpolarized helium), likely do not contribute to the diffusion distance measurements. Although further studies in diseased lungs should be undertaken, it should be noted that AiDA has showed significant differences between both healthy and persons with moderate-to-advanced COPD as in Paper I as well as between persons with and without mild-to-moderate emphysema in Paper IV.

The explorative correlation analysis shows the R(0) value may reflect biological properties

6.2 Comparing AiDA to other methods

Spirometry is the method currently used for diagnosis of COPD. Spirometry has very limited ability to differentiate between bronchial disease and emphysema. Also, the sensitivity for emphysema is low. AiDA has similarities with $D_{L,CO}$, being dependent on distribution of inhaled gas and diffusion within the airways. In contrast, AiDA is independent of transfer across the air-blood interface, haemoglobin concentration, recent smoking and altitude. The instrument is potentially simpler, as no compressed gases are needed.

With CT, the emphysematous regions of the lung are identified irrespective of ventilation. This is, however, not the case for AiDA, $D_{L,CO}$ nor ADC, which all depend on distribution of inhaled particles or gas to the affected regions. There may, therefore, be differences between the types of emphysema found with the two methods; AiDA may reflect homogeneously distributed emphysema in ventilated regions, while being less accurate detecting poorly ventilated regions, such as bullae.

AiDA, like ADC,, is based on diffusion in airspaces. AiDA, however, does not provide regional information like ADC, and it can be measured at maximum inhalation, which is difficult for ADC. AiDA is also much easier to perform and potentially much cheaper and could be made more widely available. SPECT with radiolabeled technetium also uses nanoparticles' ability to penetrate to distal lung. Technegas, however, is less uniform in size, leading to more dispersion in the mode of particle deposition. Under ideal circumstances, the image approximates the regional distribution of ventilation. Airway obstruction may, however, result in central deposition in hotspots at larger airways. Compared to SPECT, AiDA, again gives no regional information, and in AiDA there is no radiation dose, SPECT with technegas also produces an image that may be difficult to quantify, reproduce and requires a specialist to interpret, instead of a single radius estimate figure.

Both AiDA and Aerosol Derived Airway Morphometry (ADAM) use particle recovery to quantify distal airspace dimensions. ADAM uses larger particles with gravitational settling as the main mode of deposition. However, especially at high flow rates the large, micron-sized particles also deposit by impaction (Figure 12), Impaction in conducting airways adds uncertainties in particle penetrance, especially in the diseased lung. To minimize this effect, long breaths with constant low flow rates were mandated, making the measurement protocol practically challenging, especially for the elderly and patients with airway obstruction. Also, the ADAM technique normally requires determining static lung volumes, which leads to a longer protocol with additional measurements in a plethysmograph. An advantage ADAM has over AiDA is that the particles in ADAM are counted at the

mouthpiece and hence, ADAM is able to measure airspace dimensions in more proximal airways than AiDA (92)

6.3 Biomarkers

As briefly described in the introduction, for the pulmonologist of the first-half of twenty-first century, there is an increasingly wide selection of methods available with potential to give insights in pathological changes, pathogenesis or possibly diagnostics of emphysema. There is, however, a challenge translating these results in diagnostics at everyday practice. In their joint action statement, the American and European Thoracic Societies prompt research in future COPD biomarkers that can relate anatomical and physiological findings to patient-centered outcomes, such as symptoms. (115) Mannino has in 2018 suggested the following criteria for the optimum COPD biomarker, after which he states that no current biomarkers fulfil the criteria. (7):

1. Usable in a primary care setting
2. Easy to perform or administer
3. Able to find disease in early stages
4. Able to detect and classify different phenotypes of disease

The method suggested in this thesis may be able to fit the described niche. Criterion 2 is fulfilled as the measurement procedure is similar to that of $D_{L,CO}$, and does not require special training beyond what is expected of health care technicians. As for criterion 3, the method was able to differentiate between healthy and emphysematous subjects, even though most subjects in paper IV had early stages of the disease, although more studies are needed to validate this. As for criterion 4, we believe that in ventilated areas, airflow obstruction will not affect the gas distribution, which is why we believe AiDA may give information about emphysema irrespective of the bronchial component of COPD. (84, 116) This is supported by the lack of correlation to FEV_1 in Paper 1, although more studies are needed. As for criterion 1, we are presently relying on a prototype of the apparatus, but the technology is comparatively simple, and highly reproducible down to 7 µm. (97, 98) The subsequent, simpler prototypes aim at being placed in clinical outpatient settings, including primary care. A simple apparatus could be an advantage considering that a large proportion of the disease burden is in mid-to low income countries with comparatively limited healthcare resources.

The relationship between increased OR for emphysema with the presence of respiratory symptoms in Paper IV suggests AiDA could be suitable for evaluating persons with respiratory symptoms.

6.4 Methodological aspects

Internal validity of a study refers to the test's ability to measure the effect it was set out to measure. *External validity* refers to the extent the conclusions of a study apply outside the context of that study.

Internal validity, in turn, may be compromised by *systematic or random errors*. Common systematic errors can be explained in terms of *confounding, selection bias* and *information bias*, and the researchers should address these issues in study design and data analysis. In Paper I, the study and control groups are chosen to be of the same age and male/female ratio to reduce confounding. In Papers III and IV, several potential confounders are accounted for in the regression models. Information bias refers to systematic distortion in data collection, for example due to instrumental errors. All the equipment used in the studies was regularly calibrated to reduce instrumental error. As the AiDA technology is at a developing stage, however, errors of the prototype instruments may have introduced a bias, as exemplified by the number of persons excluded in papers III and IV due to invalid measurements. Measuring the distal airspace sample at a set volumetric depth for all individuals may lead to the sampled air to represent different part of the airways in persons with large lungs compared to persons with small lungs, which may have introduced a bias. The MRI method used to determine tissue density in Paper II is under development, and the method is not yet standardized, which may have introduced an instrumental error. Also, the MRI method included a normalization of PD to TLC, which is an approximation that may again have introduced a bias.

The concept information bias also includes misclassification of outcomes. The golden standard against which AiDA was compared to in papers I, III and IV was CT. Early emphysema diagnostics, however, is challenging, as the findings may be subtle. In literature, there is poor intra- and inter-observer agreement in visual diagnostics of emphysema. (117) Due to differences in calibration, scanning and processing, here is no currently accepted cutoff-value of RV-950 what can be considered as emphysematous. The percent cutoff values of 5% and 7% used in Paper IV are arbitrary, and lead to possible misclassification of outcomes. (111) Furthermore, to reduce exposure, the studies were conducted using low radiation dose, possibly compromising the diagnostic quality. (In Papers III and IV this resulted in artefacts, which were later minimized by using an iterative reconstruction algorithm. The densitometry analysis was conducted using a kernel I30f instead of

original B20f.) (118) All in all, in Paper IV, there may have been persons labeled as emphysematous, who did not have emphysema, and vice versa. As to selection bias, the participation rate to SCAPIS local site in Malmö was approximately 50%. While the figure is comparatively high, there may yet have been bias regarding to the persons who chose to participate.

Random errors, in turn, are due to chance and can be reduced by increasing the sample size. Papers I and II are explorative, proof-of-concept studies, where the number of subjects is limited. Conclusions from these studies should be cautiously expressed. The preliminary results from Paper I enabled a tentative power calculation to be made for the subsequent studies, reducing the random error.

While the he cross-sectional study design in papers III and IV increases the N and gives more insight in the method, the study is still not enough to validate AiDA as a new biomarker, as external validity remains to be explored. The correlations and associations in the exploratory analyses suggested in this thesis are only suggestive that similar findings will be made in another cohort. To establish external validity, AiDA, like any biomarker associated with diagnosing, staging or prognosis of a disease, should be tested in at least one other confirmatory cohort.

6.5 Developing a diagnostic method

Validating a diagnostic method requires a study specifically designed for this purpose. The study should be undertaken in an appropriate spectrum of patients, such as those a clinician would see in practice. It could be possible to consider AiDA as a potential screening test among smokers, in which case a study in such a target population should be conducted. There should be an independent, blind comparison with reference to a golden standard. Furthermore, the standard should be applied regardless of the index test result. To prove the results are reliable and replicable, the new test should ideally be validated in a second, independent group of patients. (119)

In diagnostic tests, there are two types of results commonly reported. The test's accuracy is given as specificity and sensitivity, defined as the test's ability to find true positives for the condition, i.e. sensitivity, and the ability to find true negatives for the same condition, i.e. specificity. A perfect test finds no false positives and misses no persons with the condition (finds no false negatives). A receiver-operator curve (ROC) is often plotted between specificity and 1-sensitivity. The closer the area under graph (AUC) is to one, the closer the test is to this ideal. The STARD-statement describes the methodological and reporting steps that should be taken in diagnostic studies. (119) Furthermore, post-test probabilities may be used to affect the management of a specific patient.

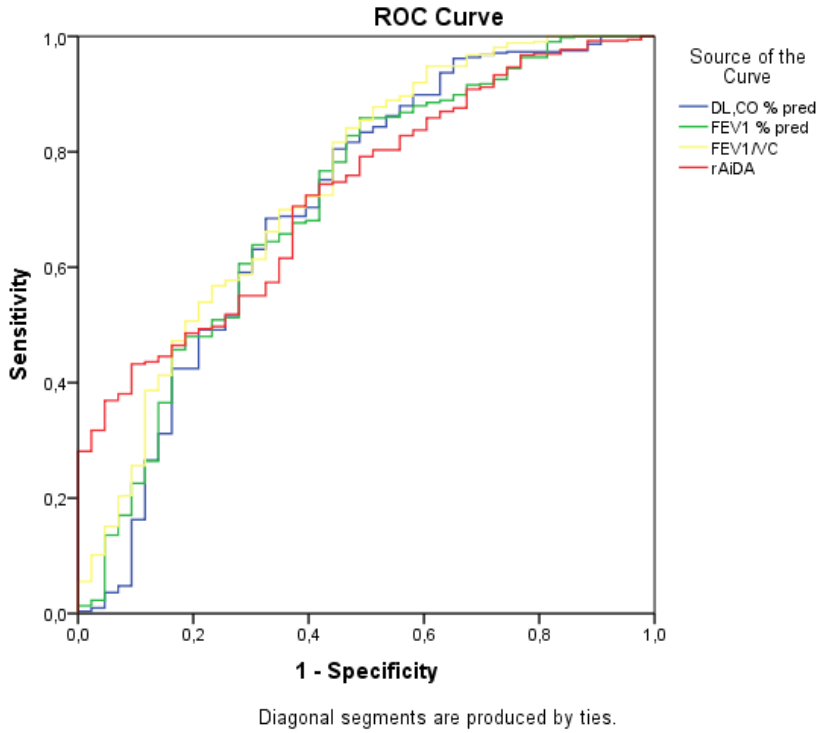

Figure 18: ROC-kurvor. AUC for $D_{L,CO}$=0.707, FEV_1 % = 0.710 , FEV_1/VC=0.739 and r_{AiDA} =0.728

AiDA is not at this point suggested as a screening tool in unselected populations, and hence, no AUC values were given in Paper IV. In Figure 18, however, AiDA is compared to other methods to diagnose emphysema using the data from Paper IV. The comparatively low AUC-values for all the listed tests reflect the unselected study population, where no disease was suspected and the prevalence of emphysema was low. These results are considered preliminary, but they do indicate AiDA's feasibility as a potential diagnostic tool.

Forecasting which emerging medical technologies become successful, and which problems may arise in the implementation, leading to product failure is difficult. Developing a new diagnostic method should be exercised with an open mindset, anticipating and reacting to possible theoretical or concrete product failures. (120)

6.6 Ethical considerations

6.6.1 Exposure to nanoparticles

Nanoparticles are present in ambient air, leading to exposure to inhaled nanoparticles in everyday life settings. In Europe, the average inhaled nanoparticle number exposure per day is 500-10 000 cm^{-3}in rural settings, and 7500-25 000 cm^{-3} in urban settings. In busy streets, the mean European average is 31 500 cm^{-3}. (121) Assuming a mean deposition probability of 0.5, this corresponds to a dose of 3×10^{11} particles per day, or 1.2×10^{10} particles deposited per hour; which, in turn, translates to every alveolar cell having an average daily exposure of eight nanoparticles. (122)

Inhalation is the most common route of exposure to engineered nanoparticles. The toxicity is a function of hazard and exposure. (123) The exposure to nanoparticles as per the study protocol was low. The total cumulative exposure to particles is very low, comparative to relative to inhaling a few breaths of relatively clean urban air. (124) Furthermore, between the measurements, the subjects inhaled completely particle-free air, which reduced the total nanoparticle exposure. The particles consisted of latex nanospheres, chosen for their low toxicity potential.

6.6.2 Exposure to radiation

The subjects in Papers I, III and IV were exposed to ionizing radiation. To keep the radiation dose as low as reasonably achievable, low radiation dose protocols were used. The subjects in Paper II were investigated using MRI, avoiding ionizing radiation.

In Paper I, low radiation dose was applicable, as full dose was not required to find the desired correlations. In Papers III and IV, the subjects were recruited from general population. The participants were actively approached to participate in the study, they did not approach health care with a concern they wished to address, which is why the radiation dose was kept very low. In future validation studies, however, especially in a diagnostic accuracy study, a proper HRCT as golden standard should preferably be used in order to reduce the risk of misclassification of outcomes.

7 Conclusions

The Airspace Dimension Assessment with nanoparticles (AiDA) method reflects distal airspace properties and shows potential as a diagnostic biomarker for emphysema.

Paper I

A significant nanoparticle recovery difference was found between COPD-patients and never-smoking controls. Recovery correlated with the extent of disease as measured with existing methods to evaluate distal airspaces, computed tomography (CT) densitometry and diffusing capacity for carbon monoxide ($D_{L,CO}$). This offers a proof-of-concept for the AiDA method as a potential biomarker.

Paper II

The radius correlated with pulmonary density as measured by MRI in healthy volunteers. The finding suggests AiDA may reflect changes in distal airspaces that result in decreased tissue density.

Paper III

The mean distal airspace radius measured in a subjectively healthy population without respiratory disease had a relatively narrow variation. The AiDA radius was generally in line with other comparative methods. The radius was minimally influenced by weight and height. The radius increased with decreasing lung density and decreasing diffusing capacity for carbon monoxide. A part of the variation may be explained by smoking-related changes.

Paper IV

In an unselected cross-sectional population, the individuals with visually detected emphysema had a significantly larger radius compared to non-emphysematous individuals. The results hold when emphysema was defined by using other indices. Comorbidities did not give rise to significant changes in the AiDA radius.

8 Future perspectives

As outlined above, further validation in different cohorts and a diagnostic accuracy study should be performed. Presently, the distal airspace morphological features obtained from the test are inferred using other in vivo measurements, such as $D_{L,CO}$, or PD15; a study relating the AiDA-obtained dimensions to pathological specimens should be conducted, if methodologically feasible. Studies comparing predominantly bronchial and predominantly emphysematous phenotypes of the disease should be undertaken. Testing young-to-middle age persons with alpha-1-antitrypsin deficiency would give insights in AiDA's ability to differentiate early emphysema from healthy lung. The role of the R(0) value should be further investigated. Testing persons with other diseases involving the small airways, for example interstitital disease or bronchiolitis obliterans organizing pneumonia, should be considered. The technical development should include standardized and automated measures of quality control.

Emphysema can be considered a human-made disease, arising by exposure to mainly anthropogenic noxious inhalants. Emphysema thus presents a different existential context from diseases of microbiological origin, such as tuberculosis, in which humanity can be considered a victim of circumstances rather than an active subject of the pathogenesis. *Technological optimism* refers to an ideology presented in the 1970s, suggesting humans will overcome the challenges of pollution and overpopulation through technology. This view has since been challenged, and considered unrealistically optimistic. (125) Recently, a careful case-study of optimistic mechanisms has been suggested as a more cautious and moderate way to encounter challenges of the first half of the twenty-first century. (126) It is too early to say if the method presented in this thesis could be of use in the struggle against emphysema, but more studies are under way.

9 Acknowledgements

I would like to acknowledge the following people for their contributions to this thesis, I am very thankful for each and every one of you.

The biggest recognition goes to the main supervisor of this thesis, Per Wollmer and the co-supervisors Jakob Löndahl, Sandra Diaz and Sophia Zackrisson, I am grateful for all the work, time and effort you have invested in this thesis. The AiDA method has been developed by Jakob Löndahl and Per Wollmer. I am happy to have had the chance to follow and contribute to the early stages of this innovation.

Many others have contributed with their subject expertise and work – I would specifically like to thank Jonas Jakobsson, Simon Kindvall, Eeva Piitulainen, Gunnar Engström, Hanna Nicklasson, Madeleine Petersson Sjögren, Veronica Ideböhn, Marcus Söderberg, Lars-Erik Olsson, Francisco Sánchez Montiel, Lars Bååth, Hanna Markstad, Lisa Ander Olsson and Catharina Adlercreutz.

Thanks for all the encouraging support to Anita Strömbeck, Barbara Elmståhl, Leena Lehti, Jan Holst, Eufrozina Selariu, Fredrik Holmquist, Krister Askaner, Linda Johnson and Li Sturesdotter.

The project would not have been possible without the support of a network of contributors, helping with time, resources, materials and practical matters. I owe thanks to Carin Cronberg, Peter Hochbergs, Olle Ekberg, Pia Maly-Sundgren, Anetta Bolejko, Krystyna Gralla, Haris Zilic, Elisabet Andersson, Matias Varonen and Eva Prahl.

Special thanks to my teachers Elina Näsäkkälä, Saija Kaartinen and Nicholas Botting.

I would like to express my gratitude to the participants of each study.

Above all, I would like thank my family and friends, near and far - especially Jeff, Adam and Aaron.

References

1. Snider GL. Emphysema: the first two centuries--and beyond. A historical overview, with suggestions for future research: Part 1. The American review of respiratory disease. 1992;146(5 Pt 1):1334-44.
2. Vogelmeier CF, Criner GJ, Martinez FJ, Anzueto A, Barnes PJ, Bourbeau J, et al. Global Strategy for the Diagnosis, Management, and Prevention of Chronic Obstructive Lung Disease 2017 Report. GOLD Executive Summary. American journal of respiratory and critical care medicine. 2017;195(5):557-82.
3. Adeloye D, Chua S, Lee C, Basquill C, Papana A, Theodoratou E, et al. Global and regional estimates of COPD prevalence: Systematic review and meta–analysis. Journal of Global Health. 2015;5(2):020415.
4. Global, regional, and national life expectancy, all-cause mortality, and cause-specific mortality for 249 causes of death, 1980-2015: a systematic analysis for the Global Burden of Disease Study 2015. Lancet (London, England). 2016;388(10053):1459-544.
5. Gordon L. Snider JK, William M. Thurlbeck, and Zakir H. Bengali. The Definition of Emphysema. American Review of Respiratory Disease. 1985 132:1:182-5.
6. Thurlbeck WM. Overview of the pathology of pulmonary emphysema in the human. Clinics in chest medicine. 1983;4(3):337-50.
7. Mannino DM. Biomarkers for chronic obstructive pulmonary disease diagnosis and progression: insights, disappointments and promise. Current opinion in pulmonary medicine. 2018.
8. Price DB, Yawn BP, Jones RCM. Improving the differential diagnosis of chronic obstructive pulmonary disease in primary care. Mayo Clinic proceedings. 2010;85(12):1122-9.
9. From the Global Strategy for the Diagnosis MaPoC, Global Initiative for Chronic Obstructive Lung Disease (GOLD) 2019. Available from: http://goldcopd.org.
10. Pleasants RA, Riley IL, Mannino DM. Defining and targeting health disparities in chronic obstructive pulmonary disease. Int J Chron Obstruct Pulmon Dis. 2016;11:2475-96.
11. Human respiratory tract model for radiological protection. A report of a Task Group of the International Commission on Radiological Protection. Annals of the ICRP. 1994;24(1-3):1-482.
12. Weibel ER. Morphometry of the Human Lung.. New York: Springer Verlag and Academic Press 1963.

13. Horsfield K, Cumming G. Morphology of the bronchial tree in man. J Appl Physiol. 1968;24(3):373-83.
14. Tatsis G, Horsfield K, Cumming G. Distribution of dead space volume in the human lung. Clinical science (London, England : 1979). 1984;67(5):493-7.
15. Leong P, Tran A, Rangaswamy J, Ruane LE, Fernando MW, MacDonald MI, et al. Expiratory central airway collapse in stable COPD and during exacerbations. Respiratory research. 2017;18(1):163-.
16. Haefeli-Bleuer B, Weibel ER. Morphometry of the human pulmonary acinus. The Anatomical Record. 1988;220(4):401-14.
17. Webb WR. Thin-section CT of the secondary pulmonary lobule: anatomy and the image--the 2004 Fleischner lecture. Radiology. 2006;239(2):322-38.
18. Hochhegger B, Langer FW, Irion K, Souza A, Moreira J, Baldisserotto M, et al. Pulmonary Acinus: Understanding the Computed Tomography Findings from an Acinar Perspective. Lung. 2019.
19. Berend N, Rynell AC, Ward HE. Structure of a human pulmonary acinus. Thorax. 1991;46(2):117-21.
20. Tsuda A, Filipovic N, Haberthür D, Dickie R, Matsui Y, Stampanoni M, et al. Finite element 3D reconstruction of the pulmonary acinus imaged by synchrotron X-ray tomography. Journal of Applied Physiology. 2008;105(3):964-76.
21. Weibel ER, Sapoval B, Filoche M. Design of peripheral airways for efficient gas exchange. Respiratory Physiology & Neurobiology. 2005;148(1):3-21.
22. Verbanck S, Paiva M. Gas mixing in the airways and airspaces. Comprehensive Physiology. 2011;1(2):809-34.
23. Rosai and Ackerman's Surgical Pathology. 11th Edition ed. Goldblum Jea, editor: Elsevier; 2017.
24. Baraldo S, Turato G, Saetta M. Pathophysiology of the small airways in chronic obstructive pulmonary disease. Respiration; international review of thoracic diseases. 2012;84(2):89-97.
25. Turato G, Zuin R, Miniati M, Baraldo S, Rea F, Beghe B, et al. Airway inflammation in severe chronic obstructive pulmonary disease: relationship with lung function and radiologic emphysema. American journal of respiratory and critical care medicine. 2002;166(1):105-10.
26. Cosio MG, Hale KA, Niewoehner DE. Morphologic and morphometric effects of prolonged cigarette smoking on the small airways. The American review of respiratory disease. 1980;122(2):265-21.
27. Hogg JC, McDonough JE, Sanchez PG, Cooper JD, Coxson HO, Elliott WM, et al. Micro-computed tomography measurements of peripheral lung pathology in chronic obstructive pulmonary disease. Proceedings of the American Thoracic Society. 2009;6(6):546-9.
28. Hogg JC, Chu F, Utokaparch S, Woods R, Elliott WM, Buzatu L, et al. The nature of small-airway obstruction in chronic obstructive pulmonary disease. The New England journal of medicine. 2004;350(26):2645-53.

29. O'Donnell DE, Laveneziana P. Physiology and consequences of lung hyperinflation in COPD. European Respiratory Review. 2006;15(100):61-7.
30. Lynch DA, Austin JH, Hogg JC, Grenier PA, Kauczor HU, Bankier AA, et al. CT-Definable Subtypes of Chronic Obstructive Pulmonary Disease: A Statement of the Fleischner Society. Radiology. 2015;277(1):192-205.
31. Leopold JG, Gough J. The centrilobular form of hypertrophic emphysema and its relation to chronic bronchitis. Thorax. 1957;12(3):219-35.
32. Wyatt JP, Fischer VW, Sweet HC. Panlobular emphysema: anatomy and pathodynamics. Diseases of the chest. 1962;41:239-59.
33. Macklem PT. The pathophysiology of chronic bronchitis and emphysema. The Medical clinics of North America. 1973;57(3):669-70.
34. Hogg JC. Pathophysiology of airflow limitation in chronic obstructive pulmonary disease. Lancet (London, England). 2004;364(9435):709-21.
35. Robins AG. Pathophysiology of emphysema. Clinics in chest medicine. 1983;4(3):413-20.
36. Hutchinson J. On the capacity of the lungs, and on the respiratory functions, with a view of establishing a precise and easy method of detecting disease by the spirometer. Medico-chirurgical transactions. 1846;29:137-252.
37. Miller MR, Hankinson J, Brusasco V, Burgos F, Casaburi R, Coates A, et al. Standardisation of spirometry. The European respiratory journal. 2005;26(2):319-38.
38. Johns DP, Das A, Toelle BG, Abramson MJ, Marks GB, Wood-Baker R, et al. Improved spirometric detection of small airway narrowing: concavity in the expiratory flow-volume curve in people aged over 40 years. Int J Chron Obstruct Pulmon Dis. 2017;12:3567-77.
39. McNulty W, Usmani OS. Techniques of assessing small airways dysfunction. European clinical respiratory journal. 2014;1:10.3402/ecrj.v1.25898.
40. Grimby G, Takishima T, Graham W, Macklem P, Mead J. Frequency dependence of flow resistance in patients with obstructive lung disease. The Journal of clinical investigation. 1968;47(6):1455-65.
41. Verbanck S, Schuermans D, Meysman M, Paiva M, Vincken W. Noninvasive assessment of airway alterations in smokers: the small airways revisited. American journal of respiratory and critical care medicine. 2004;170(4):414-9.
42. Hughes JMB, Bates DV. Historical review: the carbon monoxide diffusing capacity (DlCO) and its membrane (Dm) and red cell (Θ·Vc) components. Respiratory Physiology & Neurobiology. 2003;138(2):115-42.
43. Macintyre N, Crapo RO, Viegi G, Johnson DC, van der Grinten CP, Brusasco V, et al. Standardisation of the single-breath determination of carbon monoxide uptake in the lung. The European respiratory journal. 2005;26(4):720-35.
44. Harvey BG, Strulovici-Barel Y, Kaner RJ, Sanders A, Vincent TL, Mezey JG, et al. Risk of COPD with obstruction in active smokers with normal spirometry and reduced diffusion capacity. The European respiratory journal. 2015;46(6):1589-97.

45. Foster WL, Jr., Gimenez EI, Roubidoux MA, Sherrier RH, Shannon RH, Roggli VL, et al. The emphysemas: radiologic-pathologic correlations. Radiographics : a review publication of the Radiological Society of North America, Inc. 1993;13(2):311-28.
46. Webb WR. High-resolution CT of the lung parenchyma. Radiologic clinics of North America. 1989;27(6):1085-97.
47. Verschakelen JA. Imaging of the small airways. Seminars in respiratory and critical care medicine. 2003;24(5):473-88.
48. Bergin C, Müller N, Nichols DM, Lillington G, Hogg JC, Mullen B, et al. The Diagnosis of Emphysema. American Review of Respiratory Disease. 1986;133(4):541-6.
49. Thurlbeck WM, Muller NL. Emphysema: definition, imaging, and quantification. AJR American journal of roentgenology. 1994;163(5):1017-25.
50. Remy-Jardin M, Remy J, Boulenguez C, Sobaszek A, Edme JL, Furon D. Morphologic effects of cigarette smoking on airways and pulmonary parenchyma in healthy adult volunteers: CT evaluation and correlation with pulmonary function tests. Radiology. 1993;186(1):107-15.
51. Hayhurst MD, MacNee W, Flenley DC, Wright D, McLean A, Lamb D, et al. Diagnosis of pulmonary emphysema by computerised tomography. Lancet (London, England). 1984;2(8398):320-2.
52. Hruban RH, Meziane MA, Zerhouni EA, Khouri NF, Fishman EK, Wheeler PS, et al. High resolution computed tomography of inflation-fixed lungs. Pathologic-radiologic correlation of centrilobular emphysema. The American review of respiratory disease. 1987;136(4):935-40.
53. Muller NL, Staples CA, Miller RR, Abboud RT. "Density mask". An objective method to quantitate emphysema using computed tomography. Chest. 1988;94.
54. Gevenois PA, de Maertelaer V, De Vuyst P, Zanen J, Yernault JC. Comparison of computed density and macroscopic morphometry in pulmonary emphysema. American journal of respiratory and critical care medicine. 1995;152(2):653-7.
55. Gevenois PA, De Vuyst P, de Maertelaer V, Zanen J, Jacobovitz D, Cosio MG, et al. Comparison of computed density and microscopic morphometry in pulmonary emphysema. American journal of respiratory and critical care medicine. 1996;154(1):187-92.
56. Gould GA, MacNee W, McLean A, Warren PM, Redpath A, Best JJ, et al. CT measurements of lung density in life can quantitate distal airspace enlargement–an essential defining feature of human emphysema. The American review of respiratory disease. 1988;137.
57. Parr DG, Sevenoaks M, Deng C, Stoel BC, Stockley RA. Detection of emphysema progression in alpha 1-antitrypsin deficiency using CT densitometry; methodological advances. Respir Res. 2008;9:21.
58. Madani A, Zanen J, de Maertelaer V, Gevenois PA. Pulmonary emphysema: objective quantification at multi-detector row CT--comparison with macroscopic and microscopic morphometry. Radiology. 2006;238(3):1036-43.

59. Miller RR, Muller NL, Vedal S, Morrison NJ, Staples CA. Limitations of computed tomography in the assessment of emphysema. The American review of respiratory disease. 1989;139(4):980-3.
60. Bankier AA, De Maertelaer V, Keyzer C, Gevenois PA. Pulmonary emphysema: subjective visual grading versus objective quantification with macroscopic morphometry and thin-section CT densitometry. Radiology. 1999;211(3):851-8.
61. Walsdorff M, Van Muylem A, Gevenois PA. Effect of total lung capacity and gender on CT densitometry indexes. The British journal of radiology. 2016;89(1058):20150631-.
62. Knudson RJ, Clark DF, Kennedy TC, Knudson DE. Effect of aging alone on mechanical properties of the normal adult human lung. Journal of applied physiology: respiratory, environmental and exercise physiology. 1977;43(6):1054-62.
63. Gevenois PA, Scillia P, de Maertelaer V, Michils A, De Vuyst P, Yernault JC. The effects of age, sex, lung size, and hyperinflation on CT lung densitometry. AJR American journal of roentgenology. 1996;167(5):1169-73.
64. Kirby M, van Beek EJR, Seo JB, Biederer J, Nakano Y, Coxson HO, et al. Management of COPD: Is there a role for quantitative imaging? European Journal of Radiology. 2017;86:335-42.
65. Crossley D, Renton M, Khan M, Low EV, Turner AM. CT densitometry in emphysema: a systematic review of its clinical utility. International journal of chronic obstructive pulmonary disease. 2018;13:547-63.
66. Zhang W-J, Cristinacce PLH, Bondesson E, Nordenmark LH, Young SS, Liu Y-Z, et al. MR Quantitative Equilibrium Signal Mapping: A Reliable Alternative to CT in the Assessment of Emphysema in Patients with Chronic Obstructive Pulmonary Disease. Radiology. 2015;275(2):579-88.
67. Takahashi M, Togao O, Obara M, van Cauteren M, Ohno Y, Doi S, et al. Ultra-short echo time (UTE) MR imaging of the lung: comparison between normal and emphysematous lungs in mutant mice. Journal of magnetic resonance imaging : JMRI. 2010;32(2):326-33.
68. Jakob PM, Hillenbrand CM, Wang T, Schultz G, Hahn D, Haase A. Rapid quantitative lung (1)H T(1) mapping. Journal of magnetic resonance imaging : JMRI. 2001;14(6):795-9.
69. Gillespie DT SE. Simple Brownian Diffusion: An Introduction to the Standard Theoretical Models. 1 edition ed: Oxford University Press;; 2012.
70. Chan H-F, Stewart NJ, Parra-Robles J, Collier GJ, Wild JM. Whole lung morphometry with 3D multiple b-value hyperpolarized gas MRI and compressed sensing. Magnetic resonance in medicine. 2017;77(5):1916-25.
71. Woods JC, Choong CK, Yablonskiy DA, Bentley J, Wong J, Pierce JA, et al. Hyperpolarized 3He diffusion MRI and histology in pulmonary emphysema. Magn Reson Med. 2006;56(6):1293-300.
72. Galban CJ, Han MK, Boes JL, Chughtai KA, Meyer CR, Johnson TD, et al. Computed tomography-based biomarker provides unique signature for diagnosis of COPD phenotypes and disease progression. Nature medicine. 2012;18(11):1711-5.

73. Bodduluri S, Reinhardt JM, Hoffman EA, Newell JD, Jr., Bhatt SP. Recent Advances in Computed Tomography Imaging in Chronic Obstructive Pulmonary Disease. Annals of the American Thoracic Society. 2018;15(3):281-9.
74. Capaldi DP, Zha N, Guo F, Pike D, McCormack DG, Kirby M, et al. Pulmonary Imaging Biomarkers of Gas Trapping and Emphysema in COPD: (3)He MR Imaging and CT Parametric Response Maps. Radiology. 2016;279(2):597-608.
75. Nakano Y, Muro S, Sakai H, Hirai T, Chin K, Tsukino M, et al. Computed tomographic measurements of airway dimensions and emphysema in smokers. Correlation with lung function. American journal of respiratory and critical care medicine. 2000;162(3 Pt 1):1102-8.
76. Lynch DA, Al-Qaisi MA. Quantitative computed tomography in chronic obstructive pulmonary disease. Journal of thoracic imaging. 2013;28(5):284-90.
77. Goldin JG. Quantitative CT of the lung. Radiologic clinics of North America. 2002;40(1):145-62.
78. Hogg JC, McDonough JE, Suzuki M. Small airway obstruction in COPD: new insights based on micro-CT imaging and MRI imaging. Chest. 2013;143(5):1436-43.
79. Rueckel J, Stockmar M, Pfeiffer F, Herzen J. Spatial resolution characterization of a X-ray microCT system. Applied Radiation and Isotopes. 2014;94:230-4.
80. McDonough JE, Yuan R, Suzuki M, Seyednejad N, Elliott WM, Sanchez PG, et al. Small-airway obstruction and emphysema in chronic obstructive pulmonary disease. The New England journal of medicine. 2011;365(17):1567-75.
81. Thakur ML, Lentle BC. Joint SNM/RSNA Molecular Imaging Summit Statement. Journal of nuclear medicine : official publication, Society of Nuclear Medicine. 2005;46(9):11n-3n, 42n.
82. Suzuki M, Sze MA, Campbell JD, Brothers JF, 2nd, Lenburg ME, McDonough JE, et al. The cellular and molecular determinants of emphysematous destruction in COPD. Scientific reports. 2017;7(1):9562.
83. Vasilescu DM, Phillion AB, Tanabe N, Kinose D, Paige DF, Kantrowitz JJ, et al. Nondestructive cryomicro-CT imaging enables structural and molecular analysis of human lung tissue. Journal of applied physiology (Bethesda, Md : 1985). 2017;122(1):161-9.
84. Crawford AB, Davison A, Amis TC, Engel LA. Intrapulmonary distribution of 99mtechnetium labelled ultrafine carbon aerosol (Technegas) in severe airflow obstruction. The European respiratory journal. 1990;3(6):686-92.
85. Nagao M, Murase K, Ichiki T, Sakai S, Yasuhara Y, Ikezoe J. Quantitative analysis of technegas SPECT: evaluation of regional severity of emphysema. Journal of nuclear medicine : official publication, Society of Nuclear Medicine. 2000;41(4):590-5.
86. Alford SK, van Beek EJ, McLennan G, Hoffman EA. Heterogeneity of pulmonary perfusion as a mechanistic image-based phenotype in emphysema susceptible smokers. Proceedings of the National Academy of Sciences of the United States of America. 2010;107(16):7485-90.

87. Bajc M, Markstad H, Jarenbäck L, Tufvesson E, Bjermer L, Jögi J. Grading obstructive lung disease using tomographic pulmonary scintigraphy in patients with chronic obstructive pulmonary disease (COPD) and long-term smokers. Annals of nuclear medicine. 2015;29(1):91-9.
88. Chang S, Kwon N, Kim J, Kohmura Y, Ishikawa T, Rhee CK, et al. Synchrotron x-ray imaging of pulmonary alveoli in respiration in live intact mice. Scientific reports. 2015;5:8760.
89. Gwinn MR, Vallyathan V. Nanoparticles: health effects--pros and cons. Environ Health Perspect. 2006;114(12):1818-25.
90. Hinds W. Aerosol technology: Properties, Behavior, and Measurement of Airborne Particles 2nd edition. 1999.
91. Liu D-L. Chapter 1 - Particle Deposition onto Enclosure Surfaces. In: Kohli R, Mittal KL, editors. Developments in Surface Contamination and Cleaning. Oxford: William Andrew Publishing; 2010. p. 1-56.
92. Löndahl J, Jakobsson JK, Broday DM, Aaltonen HL, Wollmer P. Do nanoparticles provide a new opportunity for diagnosis of distal airspace disease? International journal of nanomedicine. 2017;12:41-51.
93. Anderson PJ, Wilson JD, Hiller FC. Respiratory tract deposition of ultrafine particles in subjects with obstructive or restrictive lung disease. Chest. 1990;97(5):1115-20.
94. Brown JS, Zeman KL, Bennett WD. Ultrafine particle deposition and clearance in the healthy and obstructed lung. American journal of respiratory and critical care medicine. 2002;166(9):1240-7.
95. Löndahl J, Swietlicki E, Rissler J, Bengtsson A, Boman C, Blomberg A, et al. Experimental determination of the respiratory tract deposition of diesel combustion particles in patients with chronic obstructive pulmonary disease. Particle and Fibre Toxicology. 2012;9(1):1-8.
96. Moller W, Felten K, Sommerer K, Scheuch G, Meyer G, Meyer P, et al. Deposition, retention, and translocation of ultrafine particles from the central airways and lung periphery. American journal of respiratory and critical care medicine. 2008;177(4):426-32.
97. Jakobsson JK, Hedlund J, Kumlin J, Wollmer P, Londahl J. A new method for measuring lung deposition efficiency of airborne nanoparticles in a single breath. Scientific reports. 2016;6:36147.
98. Jakobsson JKF, Wollmer P, Londahl J. Charting the human respiratory tract with airborne nanoparticles - evaluation of the Airspace Dimension Assessment technique. Journal of applied physiology (Bethesda, Md : 1985). 2018.
99. Palmes ED. Use of aerosols to measure pulmonary dimensions. Journal of the Air Pollution Control Association. 1968;18(10):671.
100. Gebhart J, Heyder J, Stahlhofen W. Use of aerosols to estimate pulmonary air-space dimensions. Journal of applied physiology: respiratory, environmental and exercise physiology. 1981;51(2):465-76.
101. Nikiforov AI, Lippmann M, Palmes ED. Validation of an in vivo Aerosol Probe Technique by Measurements of Deposition and Morphometry in Excised Human Lungs. The Annals of Occupational Hygiene. 1988;32(inhaled_particles_VI):33-9.

102. Brand P, Letzel S, Buchta M, Scheuch G, Windorfer K, Hilla W, et al. Can aerosol-derived airway morphometry detect early, asymptomatical lung emphysema? Journal of aerosol medicine : the official journal of the International Society for Aerosols in Medicine. 2003;16(2):143-51.
103. Lehnigk B, Schleiss M, Brand P, Heyder J, Magnussen H, Jorres RA. Aerosol-derived airway morphometry (ADAM) in patients with lung emphysema diagnosed by computed tomography--reproducibility, diagnostic information and modelling. European journal of medical research. 2007;12(2):74-83.
104. Blanchard JD, Heyder J, O'Donnell CR, Brain JD. Aerosol-derived lung morphometry: comparisons with a lung model and lung function indexes. Journal of applied physiology (Bethesda, Md : 1985). 1991;71(4):1216-24.
105. Bustamante-Marin XM, Ostrowski LE. Cilia and Mucociliary Clearance. Cold Spring Harbor perspectives in biology. 2017;9(4):a028241.
106. Semmler-Behnke M, Takenaka S, Fertsch S, Wenk A, Seitz J, Mayer P, et al. Efficient elimination of inhaled nanoparticles from the alveolar region: evidence for interstitial uptake and subsequent reentrainment onto airways epithelium. Environ Health Perspect. 2007;115(5):728-33.
107. Wiebert P, Sanchez-Crespo A, Falk R, Philipson K, Lundin A, Larsson S, et al. No significant translocation of inhaled 35-nm carbon particles to the circulation in humans. Inhalation toxicology. 2006;18(10):741-7.
108. Stone V, Miller MR, Clift MJD, Elder A, Mills NL, Møller P, et al. Nanomaterials Versus Ambient Ultrafine Particles: An Opportunity to Exchange Toxicology Knowledge. Environmental health perspectives. 2017;125(10):106002-.
109. Hansell DM, Bankier AA, MacMahon H, McLoud TC, Muller NL, Remy J. Fleischner Society: glossary of terms for thoracic imaging. Radiology. 2008;246(3):697-722.
110. Goddard PR, Nicholson EM, Laszlo G, Watt I. Computed tomography in pulmonary emphysema. Clinical radiology. 1982;33(4):379-87.
111. Casaburi R, Gorek Dilektasli A, Porszasz J, Stringer WW, Bhatt S, Washko G, et al. Establishing clinically meaningful cutoffs for %emphysema and %gas trapping in quantitative chest CT scans. European Respiratory Journal. 2015;46(suppl 59):OA2944.
112. Iwano S, Okada T, Satake H, Naganawa S. 3D-CT volumetry of the lung using multidetector row CT: comparison with pulmonary function tests. Academic radiology. 2009;16(3):250-6.
113. Kauczor HU, Heussel CP, Fischer B, Klamm R, Mildenberger P, Thelen M. Assessment of lung volumes using helical CT at inspiration and expiration: comparison with pulmonary function tests. American Journal of Roentgenology. 1998;171(4):1091-5.
114. Löndahl J, Möller W, Pagels JH, Kreyling WG, Swietlicki E, Schmid O. Measurement techniques for respiratory tract deposition of airborne nanoparticles: a critical review. Journal of aerosol medicine and pulmonary drug delivery. 2014;27(4):229-54.

115. Celli BR, Decramer M, Wedzicha JA, Wilson KC, Agusti A, Criner GJ, et al. An official American Thoracic Society/European Respiratory Society statement: research questions in COPD. The European respiratory journal. 2015;45(4):879-905.
116. Kirby M, Svenningsen S, Kanhere N, Owrangi A, Wheatley A, Coxson HO, et al. Pulmonary ventilation visualized using hyperpolarized helium-3 and xenon-129 magnetic resonance imaging: differences in COPD and relationship to emphysema. Journal of applied physiology (Bethesda, Md : 1985). 2013;114(6):707-15.
117. Mascalchi M, Diciotti S, Sverzellati N, Camiciottoli G, Ciccotosto C, Falaschi F, et al. Low agreement of visual rating for detailed quantification of pulmonary emphysema in whole-lung CT. Acta radiologica (Stockholm, Sweden : 1987). 2012;53(1):53-60.
118. Wang R, Sui X, Schoepf UJ, Song W, Xue H, Jin Z, et al. Ultralow-Radiation-Dose Chest CT: Accuracy for Lung Densitometry and Emphysema Detection. American Journal of Roentgenology. 2015;204(4):743-9.
119. Bossuyt PM, Reitsma JB, Bruns DE, Gatsonis CA, Glasziou PP, Irwig L, et al. STARD 2015: an updated list of essential items for reporting diagnostic accuracy studies. Bmj. 2015;351:h5527.
120. Apreda R, Bonaccorsi A, dell'Orletta F, Fantoni G. Expert forecast and realized outcomes in technology foresight. Technological Forecasting and Social Change. 2019;141:277-88.
121. Putaud JP, Van Dingenen R, Alastuey A, Bauer H, Birmili W, Cyrys J, et al. A European aerosol phenomenology – 3: Physical and chemical characteristics of particulate matter from 60 rural, urban, and kerbside sites across Europe. Atmospheric Environment. 2010;44(10):1308-20.
122. Geiser M, Kreyling WG. Deposition and biokinetics of inhaled nanoparticles. Particle and Fibre Toxicology. 2010;7(1):2.
123. Oberdörster G, Kuhlbusch TAJ. In vivo effects: Methodologies and biokinetics of inhaled nanomaterials. NanoImpact. 2018;10:38-60.
124. Hussein T, Londahl J, Paasonen P, Koivisto AJ, Petaja T, Hameri K, et al. Modeling regional deposited dose of submicron aerosol particles. The Science of the total environment. 2013;458-460:140-9.
125. Basiago A. The limits of technological optimism. Environmentalist. 1994;14:(17.).
126. Cvitanovic C, Hobday AJ. Building optimism at the environmental science-policy-practice interface through the study of bright spots. Nature Communications. 2018;9(1):3466.

Paper I

Clin Physiol Funct Imaging (2018) **38**, pp1008–1014 doi: 10.1111/cpf.12517

Deposition of inhaled nanoparticles is reduced in subjects with COPD and correlates with the extent of emphysema: proof of concept for a novel diagnostic technique

H. L. Aaltonen[1,2], J. K. Jakobsson[3], S. Diaz[1,2], S. Zackrisson[1,2], E. Piitulainen[4], J. Löndahl[3] and P. Wollmer[1,2]

[1]Department of Medical Imaging and Physiology, Skåne University Hospital, [2]Department of Translational Medicine, Lund University, [3]Division of Ergonomics and Aerosol Technology, Department of Design Sciences, Faculty of Engineering LTH, Lund University, and [4]Department of Respiratory Medicine and Allergology, Lund University, Lund, Sweden

Correspondence
Per Wollmer, Department of Medical Imaging and Physiology, Skåne University Hospital, SE-20502 Malmö, Sweden
E-mail: per.wollmer@med.lu.se

Accepted for publication
Received 2 February 2018;
accepted 5 March 2018

Key words
AiDA; COPD; CT densitometry; emphysema; nanoparticles; respiratory diagnostics

Summary

Background: The diagnosis of chronic obstructive pulmonary disease (COPD) is often based on spirometry, which is not sensitive to early emphysema. We have recently described a method for assessing distal airspace dimensions by measuring recovery of nanoparticles in exhaled air after a single-breath inhalation followed by breath-hold. Recovery refers to the non-deposited particle fraction. The aim of this study was to explore differences in the recovery of exhaled nanoparticles in subjects with COPD and never-smoking controls. A secondary aim was to determine whether recovery correlates with the extent of emphysema.

Method: A total of 19 patients with COPD and 19 controls underwent three repeats of single-breath nanoparticle inhalation followed by breath-hold. Particle concentrations in the inhaled aerosol, and in an alveolar sample exhaled after breath-hold, were measured to obtain recovery.

Findings: The patients with COPD had a significantly higher mean recovery than controls, $0{\cdot}128 \pm 0{\cdot}063$ versus $0{\cdot}074 \pm 0{\cdot}058$; $P = 0{\cdot}010$. Also, recovery correlated significantly with computed tomography (CT) densitometry variables ($P<0{\cdot}01$) and diffusing capacity for carbon monoxide ($D_{L,CO}$; $P = 0{\cdot}002$).

Interpretation: Higher recovery for emphysema patients, relative to controls, is explained by larger diffusion distances in enlarged distal airspaces. The nanoparticle inhalation method shows potential to be developed towards a tool to diagnose emphysema.

Introduction

Chronic obstructive pulmonary disease (COPD) is a common global cause of morbidity and mortality, with a large disease burden in developing countries (Adeloye *et al.*, 2015). As observed already by Burrows *et al.* (1966), patients with COPD may have a predominantly bronchial disease or emphysema. The diagnosis is currently based on a history of exposure to noxious inhalants, symptoms of cough or shortness of breath, and spirometric evidence of airflow obstruction after bronchodilation (Celli & MacNee, 2004). Spirometry is, however, relatively insensitive to early emphysema (Kuwano *et al.*, 1990; Tylen *et al.*, 2000; Regan *et al.*, 2015). There is evidence suggesting early diagnosis and intervention are beneficial for preserving lung function and reducing healthcare costs (Camilli *et al.*, 1987; Zhou *et al.*, 2010; Tawara *et al.*, 2015). Hence, there is a need for a simple, easily accessible diagnostic method to detect emphysema. In this paper, we investigate a new, single-breath nanoparticle inhalation method, which could potentially be used to find early emphysema in clinical outpatient settings (Jakobsson *et al.*, 2016; Löndahl *et al.*, 2017).

Due to their small size, inhaled nanoparticles easily traverse to distal airspaces, where they are deposited almost exclusively by diffusion (Schulz *et al.*, 1992; Verbanck & Paiva, 2011). The probability of deposition there depends on the residence time in the lung, and the distance to a surface. If time is kept constant, we expect enlarged distal airspaces to give rise to a lower than normal nanoparticle deposition. The term recovery is used to describe the fraction of particles returned with the exhaled gas; it is defined as the ratio of the particle number concentration in the expired gas to the particle number

concentration in inhaled gas. ('Human respiratory tract model for radiological protection. A report of a Task Group of the International Commission on Radiological Protection' 1994; Hinds, 1999) Thus, in emphysematous, enlarged distal airspaces, nanoparticle recovery is expected to be increased relative to normal. In a previous study, the method has shown to correlate with pulmonary tissue density in healthy volunteers (Aaltonen *et al.*, 2018).

The aim of this proof-of-concept study was to explore the difference in nanoparticle recovery between patients with COPD and never-smoking controls in an alveolar gas sample. A secondary aim was to examine whether the recovery values correlate with the extent of emphysema measured by computed tomography (CT) densitometry and diffusing capacity for carbon monoxide ($D_{L,CO}$). We also investigated the relationship between recovery and forced expiratory flow in one second (FEV_1).

Method

The study group consisted of 23 patients with COPD prospectively recruited from the Department of Respiratory Medicine at Skåne University Hospital in Malmö, Sweden, as well as a local primary healthcare clinic. COPD was defined using Global Initiative for Chronic Obstructive Lung Disease (GOLD) criteria. (From the Global Strategy for the Diagnosis) The control group consisted of a conveniency sample of 20 never-smokers without a history of pulmonary disease. The control group was similar to the COPD patients with respect to age and gender; the controls were subjectively healthy with no history of pulmonary disease. Never-smoker was defined as having no previous history of regular cigarette smoking for more than 1 year. The participants were recruited between March 2014 and September 2015.

Nanoparticle recovery was measured using Airspace Dimension Assessment with nanoparticles (AiDA) method (Fig. 1). The instrument, the procedure as well as the theoretical background are described in detail elsewhere (Jakobsson *et al.*, 2016; Löndahl *et al.*, 2017). Briefly, each measurement was carried out in sitting position during an inhalation followed by breath-holding for a given time, using a protocol similar to that of measuring $D_{L,CO}$ (Macintyre *et al.*, 2005). The subject first inhaled several breaths of particle-free air through a mouthpiece connected to a computer-controlled four-way valve (as used in Master Screen PFT; Jaeger, Germany) and then exhaled to residual volume. The valves closed, leading nanoparticle aerosol from a reservoir to the mouthpiece. The subject then performed an inhalation to total lung capacity (TLC), held his breath for ten seconds and finally exhaled into a sample collector. The AiDA apparatus generated a monodisperse aerosol containing 50 nm polystyrene latex nanospheres using an electrospray aerosol generator (TSI model 3480; TSI Inc, Shoreview, MN, USA), followed by size selection by a differential mobility analyser (Model 3071; TSI GmbH, Aachen, Germany), and dilution with particle-free air. The aerosol was generated into a 10-l semi-flexible container. A constant flow of aerosol through the container was maintained to ensure a uniform particle concentration. A condensation particle counter (CPC, Model 3760; TSI Inc., Aachen, Germany) was used to measure the particle concentration in the inhaled and exhaled aerosol. The inhalation system in AiDA was temperature-controlled at 35°C to prevent water vapour condensation. All aerosol containing volumes and tubings were made of electrically conducting or antistatic material to minimize deposition due to electrostatic attraction. In addition, the inhaled aerosol particles were singly (positively) charged, and thus only weakly interacting with electrical fields. The particles were hydrophobic to avoid hygroscopic particle growth (Löndahl *et al.*, 2014).

After accounting for particle losses within the instrument, particle concentration values in the inhaled and exhaled aerosol were used to determine recovery. The volumetric lung depth for the exhaled sample was chosen to be 1100–1300 ml. All subjects performed three repeated measurements, lasting approximately one minute each. The recovery values were normalized to 13s-effective breath-hold time, analogous to the procedure for measuring $D_{L,CO}$ (Macintyre *et al.*, 2005). The protocol resulted in an exposure to aerosol with a particle number concentration of 10^4 particles cm^{-3} and a deposited particle mass of <0·03 μg in the lungs.

The COPD group underwent CT scans of the chest. The scans were performed in suspended full inspiration using a multidetector-row scanner (Siemens Somatom Definition Flash; Siemens Healthcare, Forchheim, Germany), generating an exposure of 120 kV/15 mAs. A computer-assisted tissue density analysis was carried out using *syngo.via* Pulmo 3D software version VA, which automatically separated the lungs from adjacent organs. The extent of emphysema was estimated using two densitometric measures:

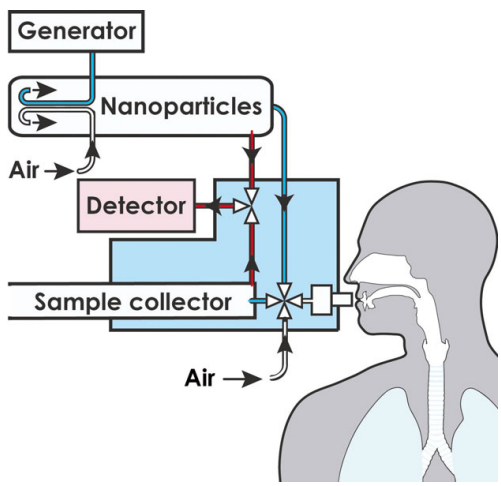

Figure 1 The AiDA apparatus. More detailed description is given by Jakobsson and colleagues (Jakobsson *et al.*, 2016). [Colour figure can be viewed at wileyonlinelibrary.com]

1 The relative volume of voxels with x-ray attenuation values below -950 Hounsfield Units (RV-950)
2 The lung density at the 15th percentile of the attenuation distribution histogram, termed partial density (PD15), given as gram per litre (Müller *et al.*, 1988; Gevenois *et al.*, 1995, 1996).

The CT scans were also visually assessed by a radiologist with 9 years of experience and a radiology resident with 2 years of experience. The extent of emphysema was graded as absent, mild, moderate or severe. Also, the presence of bullous emphysema, bronchiectasis and extensive bronchial wall thickening was evaluated.

Each subject underwent conventional lung function tests performed according to the European Respiratory Society/American Thoracic Society guidelines. Postbronchodilator FEV_1, vital capacity (VC) and $D_{L,CO}$ values were measured (Jaeger MasterScreen PFT, IntraMedic, Sollentuna, Sweden). Lung function variables were presented as percentage of predicted values (Miller *et al.*, 2005).

The study was approved by the Regional Ethical Review Board in Lund, Sweden, and the local radiation protection committee; it was performed in accordance to the Declaration of Helsinki, including informed written consent from all subjects. All investigations were conducted in Skåne University Hospital, Malmö, Sweden.

Data analysis was performed with IBM SPSS Statistics 22 (2013). Data were, unless otherwise specified, reported as mean, standard deviation and range. Chi-squared test was used for sex differences. The recovery values were reported as mean and intra-individual standard deviation of three technically acceptable tests. The intra-individual variability was evaluated by coefficient of variation. The difference between the groups was assessed with independent sample *t*-tests. Relationships between the parameters were evaluated using the Spearman's ρ correlation. The requested level of significance was P less than 0·05 for all statistical tests.

Results

Of the 23 COPD subjects initially included, four were excluded due to poor quality of AiDA measurements. Of these, three due to inhaled volume below 2/3 of vital capacity and one due to effective breath-hold time exceeding 17 s were excluded. One control subject was excluded due to spirometry indicating GOLD stage 2 COPD. Thus, 19 COPD subjects and 19 controls were eligible for analysis (Table 1).

Nanoparticle recovery was significantly higher (and thus, deposition lower) in the COPD group relative to controls (Table 1, Fig. 2). The coefficient of variation for the recovery measurements was 11% (12% for the COPD group and 10% for controls).

The recovery of nanoparticles correlated with extent of emphysema as assessed with both CT and $D_{L,CO}$ (Fig. 3). Considering the COPD group, in which CT was available, significant correlations were found between recovery and RV-950 ($\rho = 0{\cdot}586$; $P = 0{\cdot}008$), as well as between recovery and PD15 ($\rho = -0{\cdot}665$, $P = 0{\cdot}003$). A significant correlation between recovery and $D_{L,CO}$, expressed as a percentage of predicted, was observed when considering only the COPD group ($\rho = -0{\cdot}668$; $P = 0{\cdot}002$). A similar result was obtained when all subjects were considered ($\rho = -0{\cdot}506$; $P = 0{\cdot}001$). No significant correlation between recovery and FEV_1 was found, neither considering only the COPD group ($\rho = -0{\cdot}084$, $P = 0{\cdot}732$) nor all subjects ($\rho = -0{\cdot}285$, $P = 0{\cdot}083$; Fig. 3).

Table 1 Patient characteristics and results. Means and standard deviations are shown.

	COPD	Healthy subjects	*P*-value
N	19	19	
Age (yrs)	67 ± 7	64 ± 6	NS
Sex (M/F)	7/12	10/9	NS
Height (cm)	168 ± 9	173 ± 10	NS
Weight (kg)	73 ± 12	78 ± 14	NS
Smoker/former smoker/never-smoker	2/13/4[a]	0/0/19	
VC% of predicted	103 ± 24	109 ± 20	<0·0001
FEV_1% of predicted	52 ± 20	109 ± 15	<0·0001
FEV_1/VC	0·41 ± 0·12	0·80 ± 0·05	<0·0001
$D_{L,CO}$% of predicted	60 ± 21[b]	93 ± 10	<0·0001
GOLD-stage by spirometry 0/1/2/3/4	0/1/7/9/2	19/0/0/0/0	
CT: RV - 950 (%)	20 ± 11		
CT: PD15 (g l^{-1})	45 ± 28		
CT: Emphysema by visual assessment[c] Absent/mild/moderate/severe	0/4/4/11		
CT: Bullae Absent/minor/severe	11/4/4		
Recovery (R)	0·128 ± 0·063	0·074 ± 0·058	0·010

[a]All four never-smokers in the COPD group had alpha-1-antitrypsin deficiency.
[b]$D_{L,CO}$ is missing for one COPD subject.
[c]Five subjects had extensive bronchiectasis or bronchial wall thickening.

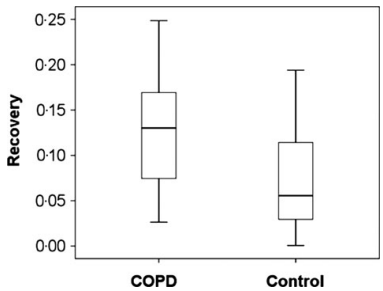

Figure 2 Median recovery as measured by the AiDA method. (COPD group N = 19, median recovery 0·130, range (0·068–0·172); control group N = 19, median recovery 0·130, range (0·056–0·118).

A significant correlation was found between $D_{L,CO}$ and PD15 ($\rho = 0{\cdot}517$, $P = 0{\cdot}028$), but the correlation between $D_{L,CO}$ and RV-950 was not statistically significant ($\rho = 0{\cdot}406$; $P = 0{\cdot}095$).

Discussion

This is the first experimental study showing nanoparticle deposition may be able to separate emphysema patients from healthy subjects. Mathematical models have suggested that nanoparticle deposition would be lower in emphysema subjects compared to healthy individuals (Sturm & Hofmann, 2004). Presently, there are only a few experimental studies of nanoparticle deposition in patients with COPD (Anderson *et al.*, 1990; Brown *et al.*, 2002; Möller *et al.*, 2008; Löndahl *et al.*, 2012). In most of these studies, the patients have not been characterized with respect to bronchial disease and emphysema. In a previous study, diesel exhaust particle deposition was lower in patients with COPD than healthy individuals, with the largest difference in the interval 20–50 nm (Löndahl *et al.*, 2012). For this reason, we selected 50 nm particles to maximize a putative difference. The volumetric lung depth for the measurements was chosen to be deep enough to represent respiratory zone, yet shallow enough to ensure that elderly and patients with pulmonary illness would be able to comply with the protocol.

The most important factor influencing aerosol deposition probability in the lungs is the size of the particles. ('Human respiratory tract model for radiological protection. A report of a Task Group of the International Commission on Radiological Protection' 1994) Hydrophobic spherical particles larger than about 0·3 μm deposit mainly by gravitational settling and inertial impaction, while particles below this size belong to the diffusion-dominated size regime (Löndahl *et al.*, 2014). Unlike gas molecules, aerosol particles generally do not bounce after contact with a surface. Deposition by gravitational settling is highest in horizontally oriented narrow airspaces with long particle residence times. Deposition by impaction is, on the other hand, most efficient in the branching conducting airways with high flow velocities. Deposition

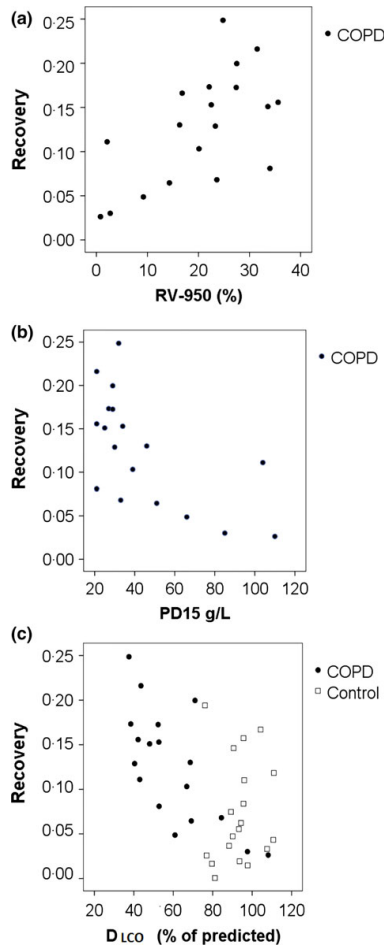

Figure 3 Nanoparticle recovery correlates with (a) RV − 950 (N = 19, P = 0·008, ρ = 0·586); and (b) PD15 (N = 19, P = 0·003, ρ = −0·665), (c) $D_{L,CO}$ as per cent of predicted COPD group (N = 19, P = 0·002, ρ = −0·668). All subjects (N = 38, P = 0·001, ρ = −0·506). [Colour figure can be viewed at wileyonlinelibrary.com]

by diffusion onto surfaces in the lungs does not depend on airway orientation with respect to the gravitational field or on change in direction of the airflow, but only on distance and residence time. Short distances and long residence times increase nanoparticle deposition. Nanoparticles in the range 10–300 nm deposit mainly in the gas exchange region of the lungs, beyond generation 15. Micrometre-sized particles have a more complex deposition pattern, which can be high in the conducting airways, especially during fast breathing manoeuvres or in patients with airflow obstructions (Löndahl *et al.*, 2017).

As the probability of deposition of nanoparticles in the lungs depends on the aerosol residence time and distance to

the wall, recovery should reflect diffusion distances in the distal airspaces, given controlled residence time. Recovery in this study is determined by measuring particle concentration in an alveolar sample of exhaled gas.

Methods currently used to detect emphysema in a clinical setting include CT and $D_{L,CO}$. In computed tomography, distal airspace enlargement gives rise to low lung density, which is detected as low x-ray attenuation. The percentile density CT densitometric method has been shown to correlate with the extent of emphysema in pathologic specimens (Gould *et al.*, 1988). In this study, there was a significant correlation between recovery and densitometric variables RV-950 and PD15, suggesting recovery may reflect the extent of emphysema (Fig. 3). There may, however, be differences between the types of emphysema likely to be found with CT and AiDA; nanoparticle recovery may reflect homogeneously distributed emphysema in ventilated regions, while poorly ventilated, heterogeneously emphysematous regions, such as bullae, may not affect recovery. This could explain part of the scatter in the correlation between the CT variables and recovery. The number of patients with bullous emphysema in this study (five) was too small to allow for analysis. Reduced $D_{L,CO}$, in combination with airflow obstruction, indicates the presence of emphysema. Reduced $D_{L,CO}$ may, however, also have other causes, and when spirometry is normal, the finding is non-specific. In this study, we found a highly significant correlation between nanoparticle recovery and $D_{L,CO}$ (Fig. 3). This is to be expected, as some of the determinants of the uptake of carbon monoxide are also important for AiDA – both techniques depend on bulk flow delivery and diffusion in distal airspaces (Macintyre *et al.*, 2005). The $D_{L,CO}$ method, however, also depends on diffusion across the alveolar–capillary membrane and into the red blood cell, as well as on reaction with haemoglobin – factors not expected to affect the AiDA measurements. Thus, conceptually, nanoparticle recovery may reflect distal airspace enlargement more specifically than $D_{L,CO}$, although further studies are required to investigate this relationship.

Previous studies have shown a correlation between the CT percentile density method (PD15) and $D_{L,CO}$ (Gould *et al.*, 1991). In this study, recovery tended to show stronger correlation to PD15 than $D_{L,CO}$ did. Furthermore, recovery correlated significantly with RV-950, while $D_{L,CO}$ did not. These findings might indicate that recovery reflects distal airspace enlargement more specifically than $D_{L,CO.}$ The findings, however, need to be further investigated in larger studies.

The correlation between recovery and FEV_1 was not significant. This finding could signal that recovery may reflect the emphysematous component of the COPD rather than bronchial abnormalities; nanoparticle recovery is considered to have a low sensitivity to changes in direction of the airflow and does not deposit by impaction (Löndahl *et al.*, 2017). Patients with predominantly bronchial disease could, therefore, be expected to have similar recovery results to healthy subjects. Larger studies in patients with bronchial wall thickening and bronchiectasis should be carried out to investigate this relationship.

In healthy subjects, AiDA has shown highly repeatable results with a within-session coefficient of variation of 5% (Jakobsson *et al.*, 2016). The present study yielded a higher coefficient of variation of 11% for nanoparticle recovery, possibly due to differences in subject demographics and higher morbidity; many subjects were elderly, and many patients had moderate to severe COPD. One patient was paraplegic and performed the measurements from a wheelchair. Also, the resistance of the breathing circuit was somewhat high, which may explain why adequate measurements could not be obtained in all subjects. In future studies, the ergonomics of the apparatus should be further improved to facilitate better measurement quality. Nevertheless, the variability may be considered equal to comparative methods, such as $D_{L,CO}$ (Macintyre *et al.*, 2005).

Analyses of deposition patterns of micrometre-sized particles have previously been suggested as a tool to find emphysema. These methods, extensively discussed by Löndahl *et al.* (2017) are conceptually different, as micrometre-sized particles deposit mainly by sedimentation. They have not yet resulted in widespread clinical applications, presumably due to cumbersome measurement procedures. The AiDA method is simpler in comparison. Also, as the AiDA method uses relatively simple technology, it could be made available in primary care, as well as in areas with limited healthcare resources.

As the measurements consist of three repeats of a single-breath-hold inhalation, together with several cycles of particle-free air, the protocol resulted in a low exposure to nanoparticles, comparable to <3‰ of daily particle number exposure, and <0·7‰ of daily particle mass exposure in a relatively clean urban setting (Hussein *et al.*, 2013; Johnston *et al.*, 2013). Similar particles, but at a higher concentration, have previously been extensively used in determining mucociliary clearance (Foord *et al.*, 1975). Wiebert and colleagues showed no evidence of quantitatively important translocation of nanoparticles to the systemic circulation from the lungs (Wiebert *et al.*, 2006).

This study is the first to explore the possible use of nanoparticles as an indicator of COPD. As such, it has obvious limitations. The sample size is small. As the study is exploratory in nature, and previous experimental data in the field are very limited, no statistical power analysis was performed. Also, in this study, we did not attempt to separate the results between patients with mainly conductive airway disease from those with parenchymal destruction.

Several aspects of the AiDA technique require further research, for example the optimal particle diameter, breath-hold time and sample volume. To evaluate AiDA as a possible diagnostic tool, a diagnostic study has to be performed; specificity, sensitivity and discrimination value as well as the role of comorbidities should be assessed. From a clinical point of view, detection of emphysema may be most interesting at an early stage of COPD. In this study, only a few patients had mild disease. A diagnostic study among subjects with possible early emphysema, such as smokers, should be conducted. Additionally, the information from the AiDA measurements in this study is given as particle recovery rather than airspace

dimension. It is, however, possible to estimate airspace radius in millimetres from the recovery values according to method described by Löndahl *et al.* (2017). This calculation requires a minimum of two repeats of the above-described measurements at different breath-hold time periods, which was not performed in this study – the approach should, however, be incorporated in future studies. Also, the effect of bronchial disease, asthma and interstitial lung disease to the recovery of nanoparticles should be investigated.

Conclusion

The patients with COPD have significantly higher recovery of nanoparticles in exhaled gas after a single-breath aerosol inhalation followed by standardized breath-hold compared to never-smoking healthy controls. Recovery is significantly correlated to physiological and radiological parameters of emphysema. In this limited-sample proof-of-concept study, nanoparticle recovery analysis shows potential to be developed towards a tool to diagnose emphysema. Further studies in larger samples are needed to further investigate and validate the AiDA method.

Acknowledgment

The authors would like to acknowledge Hanna Nicklasson, Dept of Translational Medicine, Lund, Sweden, for performing AiDA measurements and recruiting volunteers.

Disclosures

The following organizations are gratefully acknowledged for financial support: The Swedish Research Council (project 621-2011-3560), the Crafoord foundation, the Swedish Governmental Agency for Innovation Systems (VINNOVA), the ERA-NET project EuroNanoMed2, the Swedish Heart and Lung Foundation, governmental funding of clinical research within the National Health Services, Lund University as well as Skåne Region. Please contact the authors for data sharing enquiries.

Conflict of interest

Jakob Löndahl and Per Wollmer have a patent pending for the AiDA technology, a device and method for pulmonary function measurement, application number PCT/EP2013/073977. The other authors report no conflict of interests.

Author contributions

HLA, JKJ, JL and PW designed the study. All authors reviewed and had input to the protocol. EP and HLA recruited the subjects. JKJ and JL contributed to the measurements. SD and HLA designed the CT protocol and reviewed the CT images. All authors took part in the data analysis. HLA wrote the first version of the manuscript. All authors had input to the manuscript and approved the final version.

References

From the Global Strategy for the Diagnosis, MaPoC, Global Initiative for Chronic Obstructive Lung Disease (GOLD). (2017). Available from: http://goldcopd.org.

Aaltonen HL, Kindvall S, Jakobsson JK, *et al.* Airspace dimension assessment with nanoparticles reflects lung density as quantified by MRI. *Int J Nanomedicine* (2018). In press.

Adeloye D, Chua S, Lee C, *et al.* ; Global Reference Health Epidemiology Group. Global and regional estimates of COPD prevalence: systematic review and meta–analysis. *J Glob Health* (2015); **5**: 020415.

Anderson PJ, Wilson JD, Hiller FC. Respiratory tract deposition of ultrafine particles in subjects with obstructive or restrictive lung disease. *Chest* (1990); **97**: 1115–1120.

Brown JS, Zeman KL, Bennett WD. Ultrafine particle deposition and clearance in the healthy and obstructed lung. *Am J Respir Crit Care Med* (2002); **166**: 1240–1247.

Burrows B, Fletcher CM, Heard BE, *et al.* The emphysematous and bronchial types of chronic airways obstruction. A clinicopathological study of patients in London and Chicago. *Lancet* (1966); **1**: 830–835.

Camilli AE, Burrows B, Knudson RJ, *et al.* Longitudinal changes in forced expiratory volume in one second in adults. Effects of smoking and smoking cessation. *Am Rev Respir Dis* (1987); **135**: 794–799.

Celli BR, MacNee W. Standards for the diagnosis and treatment of patients with COPD: a summary of the ATS/ERS position paper. *Eur Respir J* (2004); **23**: 932–946.

Foord N, Black A, Walsh M. Pulmonary deposition of inhaled particles with diameters in the range 2.5 to 7.5 micron. *Inhaled Part* (1975); **4**(Pt 1): 137–149.

Gevenois PA, de Maertelaer V, De Vuyst P, *et al.* Comparison of computed density and macroscopic morphometry in pulmonary emphysema. *Am J Respir Crit Care Med* (1995); **152**: 653–657.

Gevenois PA, De Vuyst P, de Maertelaer V, *et al.* Comparison of computed density and microscopic morphometry in pulmonary emphysema. *Am J Respir Crit Care Med* (1996); **154**: 187–192.

Gould GA, MacNee W, McLean A, *et al.* CT measurements of lung density in life can quantitate distal airspace enlargement–an essential defining feature of human emphysema. *Am Rev Respir Dis* (1988); **137**: 380–392.

Gould GA, Redpath AT, Ryan M, *et al.* Lung CT density correlates with measurements of airflow limitation and the diffusing capacity. *Eur Respir J* (1991); **4**: 141–146.

Hinds W. *Aerosol technology: properties, Behavior, and Measurement of Airborne Particles*, 2nd edn. (1999). Wiley, New York.

Human respiratory tract model for radiological protection. A report of a Task Group of the International Commission on Radiological Protection. *Ann ICRP* (1994); **24**: 1–482.

Hussein T, Löndahl J, Paasonen P, *et al.* Modeling regional deposited dose of submicron aerosol particles. *Sci Total Environ* (2013); **458–460**: 140–149.

Jakobsson JK, Hedlund J, Kumlin J, *et al.* A new method for measuring lung deposition efficiency of airborne nanoparticles in a single breath. *Sci Rep* (2016); **6**: 36147.

Johnston H, Pojana G, Zuin S, *et al.* Engineered nanomaterial risk. Lessons learnt from completed nanotoxicology studies: potential solutions to current and future challenges. *Crit Rev Toxicol* (2013); **43**: 1–20.

Kuwano K, Matsuba K, Ikeda T, *et al.* The diagnosis of mild emphysema. Correlation of computed tomography and pathology scores. *Am Rev Respir Dis* (1990); **141**: 169–178.

Löndahl J, Swietlicki E, Rissler J, *et al.* Experimental determination of the respiratory tract deposition of diesel combustion particles in patients with chronic obstructive pulmonary disease. *Part Fibre Toxicol* (2012); **9**: 1–8.

Löndahl J, Möller W, Pagels JH, *et al.* Measurement techniques for respiratory tract deposition of airborne nanoparticles: a critical review. *J Aerosol Med Pulm Drug Deliv* (2014); **27**: 229–254.

Löndahl J, Jakobsson JK, Broday DM, *et al.* Do nanoparticles provide a new opportunity for diagnosis of distal airspace disease? *Int J Nanomedicine* (2017); **12**: 41–51.

Macintyre N, Crapo RO, Viegi G, *et al.* Standardisation of the single-breath determination of carbon monoxide uptake in the lung. *Eur Respir J* (2005); **26**: 720–735.

Miller MR, Hankinson J, Brusasco V, *et al.* Standardisation of spirometry. *Eur Respir J* (2005); **26**: 319–338.

Möller W, Felten K, Sommerer K, *et al.* Deposition, retention, and translocation of ultrafine particles from the central airways and lung periphery. *Am J Respir Crit Care Med* (2008); **177**: 426–432.

Müller NL, Staples CA, Miller RR, *et al.* "Density mask". An objective method to quantitate emphysema using computed tomography. *Chest* (1988); **94**: 782–787.

Regan EA, Lynch DA, Curran-Everett D, *et al.* Clinical and radiologic disease in smokers with normal spirometry. *JAMA Intern Med* (2015); **175**: 1539–1549.

Schulz H, Heilmann P, Hillebrecht A, *et al.* Convective and diffusive gas transport in canine intrapulmonary airways. *J Appl Physiol* (1992); **1985**: 1557–1562.

Sturm R, Hofmann W. Stochastic simulation of alveolar particle deposition in lungs affected by different types of emphysema. *J Aerosol Med* (2004); **17**: 357–372.

Tawara Y, Senjyu H, Tanaka K, *et al.* Value of systematic intervention for chronic obstructive pulmonary disease in a regional Japanese city based on case detection rate and medical cost. *Int J Chron Obstruct Pulmon Dis* (2015); **10**: 1531–1542.

Tylen U, Boijsen M, Ekberg-Jansson A, *et al.* Emphysematous lesions and lung function in healthy smokers 60 years of age. *Respir Med* (2000); **94**: 38–43.

Verbanck S, Paiva M. Gas mixing in the airways and airspaces. *Compr Physiol* (2011); **1**: 809–834.

Wiebert P, Sanchez-Crespo A, Falk R, *et al.* No significant translocation of inhaled 35-nm carbon particles to the circulation in humans. *Inhal Toxicol* (2006); **18**: 741–747.

Zhou Y, Hu G, Wang D, *et al.* Community based integrated intervention for prevention and management of chronic obstructive pulmonary disease (COPD) in Guangdong, China: cluster randomised controlled trial. *BMJ* (2010); **341**: c6387.

Paper II

International Journal of Nanomedicine

Dovepress
open access to scientific and medical research

Open Access Full Text Article

ORIGINAL RESEARCH

Airspace Dimension Assessment with nanoparticles reflects lung density as quantified by MRI

H Laura Aaltonen[1,2,*]
Simon S Kindvall[3,*]
Jonas K Jakobsson[4]
Jakob Löndahl[4]
Lars E Olsson[3,5]
Sandra Diaz[1,2]
Sophia Zackrisson[1,2]
Per Wollmer[1,2]

[1]Department of Medical Imaging and Physiology, Skåne University Hospital, Malmö, Sweden; [2]Department of Translational Medicine, Lund University, Malmö, Sweden; [3]Department of Medical Radiation Physics, Lund University, Malmö, Sweden; [4]Department of Design Sciences, Lund University, Lund, Sweden; [5]Department of Hematology, Oncology and Radiation Physics, Skåne University Hospital, Malmö, Sweden

*These authors contributed equally to this work

Correspondence: H Laura Aaltonen
Email laura.aaltonen@med.lu.se

Background: Airspace Dimension Assessment with inhaled nanoparticles is a novel method to determine distal airway morphology. This is the first empirical study using Airspace Dimension Assessment with nanoparticles (AiDA) to estimate distal airspace radius. The technology is relatively simple and potentially accessible in clinical outpatient settings.

Method: Nineteen never-smoking volunteers performed nanoparticle inhalation tests at multiple breath-hold times, and the difference in nanoparticle concentration of inhaled and exhaled gas was measured. An exponential decay curve was fitted to the concentration of recovered nanoparticles, and airspace dimensions were assessed from the half-life of the decay. Pulmonary tissue density was measured using magnetic resonance imaging (MRI).

Results: The distal airspace radius measured by AiDA correlated with lung tissue density as measured by MRI ($\rho = -0.584$; $p = 0.0086$). The linear intercept of the logarithm of the exponential decay curve correlated with forced expiratory volume in one second (FEV_1) ($\rho = 0.549$; $p = 0.0149$).

Conclusion: The AiDA method shows potential to be developed into a tool to assess conditions involving changes in distal airways, eg, emphysema. The intercept may reflect airway properties; this finding should be further investigated.

Keywords: nanoparticles, respiratory diagnostics, distal airspaces, airspace dimension assessment with nanoparticles, magnetic resonance densitometry

Introduction

Distal airspaces are often evaluated by pulmonary function testing (PFT), including diffusing capacity for carbon monoxide ($D_{L,CO}$), or computed tomography (CT). In clinical praxis, however, there are no precise methods to quantify morphological changes in peripheral lungs, which makes diagnosing disease in these areas challenging. Various experimental methods used in research settings have been proposed to evaluate this region, including magnetic resonance imaging (MRI), and deposition studies of inhaled micron-sized particles.

A non-invasive method to estimate distal airspace radius by a series of single breath-hold nanoparticle inhalations has recently been described.[1,2] This method, termed Airspace Dimension Assessment with nanoparticles (AiDA), is based on nanoparticle deposition behavior in distal airspaces. Nanoparticles deposit almost exclusively by diffusion; in a given time, the likelihood of deposition depends on the diffusion distance.[3] Deposition can be given as particle recovery, ie, the ratio of the particle number concentration in the exhaled air to the particle number concentration in inhaled air. Hence, individuals with increased diffusion distances are expected to show increased recovery. In a proof-of-concept study, COPD-patients showed significantly higher nanoparticle recovery compared to healthy never-smokers.[22]

submit your manuscript | www.dovepress.com
Dovepress
http://dx.doi.org/10.2147/IJN.S160331

This is the first study to estimate distal airspace radius using a nanoparticle recovery method. Similar attempts have been previously conducted with larger, micron-sized particles.[4,5] The nanoparticle-based model, however, is not exactly comparable to micron-size models. While the main deposition mechanism for nanoparticles is diffusion, larger particles deposit mainly by gravitational settling and inertial impaction. Hence, in nanoparticle studies, fewer particles are lost in conductive airways. Also, there is reason to assume that nanoparticles penetrate into more peripheral airways than micron-sized particles, especially in diseased lungs. Nanoparticle versus micron-size particle recovery methods are extensively discussed by Löndahl.[1] A crucial difference between the two methods is that in AiDA, a simpler measurement procedure can be used, allowing for measurements without a set breathing flow rate. The deposition of nanoparticles is essentially independent of flow during inhalation.[2] The use of micron-size particles, on the other hand, requires inspiratory flow to be low (<1 L/s) and constant – conditions that are difficult to achieve, especially in patients with lung disease.

The AiDA measurements give rise to a low exposure to nanoparticles. The subjects in the current study were exposed to <0.05% of daily mass and <0.60% of daily particle number exposure in a comparatively clean urban setting.[6]

The AiDA method allows recovery to be further analyzed to estimate airspace radius in millimeters, by using half-life of exponential decay. Also, as described by Löndahl,[1] the y-intercept of the logarithm of the recovery may carry biological information. The radius estimate, as well as the intercept, still remains to be investigated empirically.

The aim of this study was to investigate if the airspace radius, as measured by AiDA, correlates with pulmonary density as measured by MRI in healthy volunteers. A secondary aim is to explore the possible physiological significance of the intercept of the exponential particle decay curve.

Methods

Subjects

The study group consisted of 25 prospectively recruited healthy, never-smoking volunteers 21–64 years of age. They were allowed an accumulated tobacco consumption of less than one pack-year.

The study was approved by the Regional Ethical Review Board in Lund, Sweden (2014/327), and it was performed in accordance to the Declaration of Helsinki, including obtaining informed written consent from all subjects.

Airspace Dimension Assessment with nanoparticles (AiDA)

Nanoparticle recovery measurements were conducted according to the AiDA method. The apparatus as well as the theoretical background is described in detail elsewhere.[1,2] The measurements were performed in a sitting position, using a protocol and breathing manoeuver similar to measuring $D_{L,CO}$.[7] The subjects inhaled nanoparticles through a mouthpiece to total lung capacity, held their breath for a given amount of time, and exhaled to residual volume. The particle concentrations in the inhaled and exhaled gas were measured to determine particle recovery as the ratio between the exhaled and inhaled concentrations. The exhaled aerosol analysis was conducted from a sample obtained from a lung depth of 1,100–1,300 mL. The subjects performed two repeated measurements at three different breath-hold times; 5, 7 and 10 seconds. The breath-hold time figures refer to the time the valves in the breathing circuit remained closed. Some diffusion occurs also during inhalation and exhalation. We therefore calculated an effective breath-hold time analogous to the practice for measurement of $D_{L,CO}$.[7]

The apparatus generated a monodisperse aerosol containing 50 nm polystyrene latex nanospheres by an electrospray aerosol generator (TSI model 3480; TSI Inc, Shoreview, MN, USA). Background particles smaller than 50 nm were removed by a differential mobility analyzer (DMA Model 3071; TSI Inc). The method accounts for particle losses within the instrument, humidity, and particle charge.

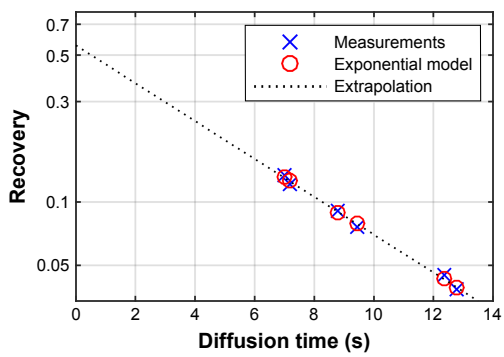

Figure 1 Example data and fit from volunteer AiDA measurement of exhaled nanoparticle concentration (recovery) as a function of diffusion/breath hold-time. Six consecutive inhalations are used to calculate the exponential nanoparticle deposition. Only subjects where $R^2>0.95$ are included, indicating a very good fit between measurements and model.
Abbreviation: AiDA, Airspace Dimension Assessment with nanoparticles.

Nanoparticle recovery was used to calculate the airspace radius as described by Löndahl.[1] Briefly, an exponential decay curve is fitted to the recovery values obtained by a series of breath holds of varying duration (Figure 1). The airspace radius is calculated from the half-life of this decay, according to:

$$r = 2.89\sqrt{D}t_{1/2}$$

where D is the diffusion coefficient given by the Stokes-Einstein equation, based on temperature, viscosity, and particle size.

Extrapolating the exponential decay curve to the y-intercept yields a theoretical recovery value for a breath-hold time zero (Figure 1).[1] To further explore the possible biological information carried by the intercept, correlation analysis to assess relationship between the available anthropometric variables and lung function tests was carried out.

The protocol resulted in a particle number exposure of 10^4 particles/cm^3 and a deposited particle mass of about 0.02 µg in the lungs.

MRI

AiDA should be compared to existing methods to determine distal airspace abnormalities. Enlarged alveoli and reduced perfusion result in a concurrent decrease in proton density, which can be measured in a quantitative manner by MRI.[8–10]

All MRI measurements were made on a 1.5 Tesla Siemens Magnetom AvantoFit (Siemens Healthcare, Erlangen, Germany), with an 18 channel body coil and a 32 channel spine matrix. Coronal proton density (PD) maps were measured with the Snapshot FLASH pulse sequence to correct for T1.[11] The imaging matrix was 128 × 64 zero filled to 256 × 256; field of view 450 mm square; slice thickness 1.5 cm; echo time = 0.67 ms; repetition time = 3.0 ms; and flip angle = 7°. All measurements were preceded by instructions for breath-hold after a tidal inspiration and subjects were given at least 10 seconds of free breathing to restore magnetization equilibrium between measurements. Data processing was made in MatLab R2014b (MathWorks, Natick, MA, USA). The lungs were segmented in three dimension (3D) using the magnitude images, followed by manual removal of major vessels. Segmentations were considered successful when each slice clearly included the signal magnitude gradient representing the border of the lung.

For each subject, a clinical radiologist (HLA) selected three slices ventral to the airway bifurcation and manually placed a region of interest (ROI) representing the left ventricular blood in each image. For each image, the lung PD was normalized to the mean signal intensity of the ventricular ROI.[10] Since MRI measurements were made at tidal inspiration – which is a poorly defined lung volume – the volume of the lung at the MRI acquisition, V_{MRI}, is calculated (as the size of the total segmented lung). Assuming the lungs simply inflate without changing tissue or blood content, density values at total lung capacity (TLC) can be calculated by multiplying density values with V_{MRI}/TLC. This TLC-corrected PD was called PD(TLC). Furthermore, all voxels with a density value higher than 60% of the ventricular blood were considered blood vessels and hence, discarded from the analysis.

We used three imaging variables to quantify lung density. These variables were originally developed for computed tomography,[12,13] and later adopted to MRI:[10]

(1) Mean lung density (MLD) represents the mean PD(TLC) of the entire segmented lung volume in three central slices.
(2) The 15th percentile proton density (PD_{15}) was calculated from the PD(TLC) histogram of all voxels in the selected lung slices.
(3) The relative area under 7.5% PD ($RA_{7.5}$), also known as the density mask,[14] is the fraction of lung voxels in the selected slices, that have a PD(TLC) less than 7.5% of the ventricular blood signal intensity.

PFT

The subjects underwent conventional lung function testing performed according to the European Respiratory Society/American Thoracic Society guidelines,[15] using a Jaeger MasterScreen PFT (IntraMedic, Sollentuna, Sweden). The measurements were performed without bronchodilation. Total lung capacity (TLC), residual volume (RV), forced expiratory volume in one second (FEV_1), and $D_{L,CO}$ values were obtained. Lung function variables are presented as percentage of predicted values.

Statistics

Statistical evaluation was done in MatLab R2014b (MathWorks) and IBM SPSS Statistics 22 (2013). Data are, unless otherwise specified, reported as mean, standard deviation, and range. The Chi-square test was used for sex differences. For the investigated variables and the subjects with complete and acceptable measurements, Spearman's rank of variables test (ρ) is presented with p-values to assess correlation. The requested level of significance was p less than 0.05 for all statistical tests.

The 95% confidence intervals (95% CI) for the AiDA-parameters are calculated from the estimated standard error and the two-sided t-distribution with 4 degrees of freedom.

Results

Two conditions had to be fulfilled in order for the AiDA-measurement to be considered valid; the inhaled volume had to exceed 2/3 of vital capacity (VC), and the measured values had to correlate with a theoretical model with a coefficient of determination larger than 0.95. All subjects fulfilled the first condition, while two displayed intra-individual correlation less than 0.95, and were subsequently excluded. Furthermore, one subject displayed large intra-individual variation at the 5 second inhalation, and another had to abort the measurement due to air leakage at the instrument mouthpiece; these subjects were also excluded. This resulted in 19 persons being eligible for analysis. Two individuals did not perform pulmonary function tests or AiDA due to logistical reasons.

General demographics, MRI and AiDA values for the study group are presented in Table 1. The sample consisted of 10 females and 9 males.

The only variable displaying a significant sex difference ($p<0.05$) was height. Linear regressions of AiDA versus MLD, PD_{15} and $RA_{7.5}$, are presented in Figure 2A–C.

All MRI-derived proton density variables show a significant correlation with the AiDA radius (Table 2). Overall, a high PD_{15} and MLD are associated with a low radius; conversely, a high $RA_{7.5}$ is associated with a large radius.

The findings suggest there may be a correlation between AiDA radius and age, although this was not established at the required level of significance ($p = 0.052$). No correlation between AiDA radius could be seen with the variables height, weight, or BMI ($p>0.15$). Similarly, no significant correlations were found between AiDA radius and pulmonary function parameters FEV_1, $D_{L,CO}$, TLC, RV, or VC, each measured as percentage of predicted ($p>0.37$).

The intercept correlates significantly with FEV_1, measured as percent of predicted (Figure 3). No significant correlations were established between the intercept and the pulmonary function parameters $D_{L,CO}$, TLC, RV, or VC, given as percentage of predicted ($p>0.3$).

The correlation between the intercept and age was found to be significant (Table 2). In contrast, no significant correlations were found between the intercept and the other available anthropometric variables height, weight, or BMI ($p>0.4$). Finally, no correlation between the airspace radius and the intercept was found ($p = 0.46$).

Table 1 Demographics, AiDA, MRI and PFTs

	Mean	SD	Min	Max
Age (years)	42.0	15.4	21	64
Height (cm)	175	10	155	188
Weight (kg)	75.5	10.9	54	104
BMI (kg/m^2)	24.7	2.6	20.5	29.4
TLC (%predicted)	109	9	94	133
RV (%predicted)	101	14	74	133
FEV_1 (%predicted)	109	15	85	141
VC (%predicted)	118	12	98	148
AiDA – radius (mm)	0.272	0.031	0.237	0.347
Intercept	0.482	0.147	0.173	0.711
MLD (% blood)	9.78	1.74	7.48	13.1
PD_{15} (% blood)	7.17	1.42	5.18	9.90
$RA_{7.5}$ (% voxels)	27.48	21.6	0.28	62.4

Abbreviations: AiDA, Airspace Dimension Assessment with nanoparticles; MRI, magnetic resonance imaging; PFTs, pulmonary function tests; BMI, body mass index; TLC, total lung capacity; RV, residual volume; FEV_1, forced expiratory volume in one second; VC, vital capacity; MLD, mean lung density; PD_{15}, 15th percentile proton density; $RA_{7.5}$, relative area under 7.5% PD.

Discussion

In this study, the airspace radius measured with AiDA correlates with tissue density measured with MRI; decreasing tissue density corresponds to increasing distal airspace size. Moreover, the intercept, which may reflect time-independent particle losses in the airways, was shown to correlate with FEV_1 and age.

We chose healthy, never smoking volunteers for this exploratory study, as we believe long-standing effects of smoking and pulmonary disease may affect the particle deposition behavior. It is, however, difficult to recruit completely tobacco-naïve individuals; hence they were permitted a limited previous exposure to cigarettes (less than one pack-year). Lung tissue density varies in the population, with age, sex, and height. Lung tissue decreases and becomes less elastic with age,[16,17] and women have denser lungs than men.[18] Also, persons with larger lungs have lower lung density than persons with smaller lungs.[19] Zeman found that distal airspace dimension, as estimated with micron-size particles, increased with age.[5] Our results suggest the AiDA radius increases with age; the correlation, however, was outside the threshold of statistical significance. The limited sample size and the presence of outliers make it difficult to draw any conclusions regarding correlation to anthropometric measures as well as sex differences. The study is exploratory in nature with few comparable previous studies available. Hence, no prior power analysis was conducted.

When it comes to spirometry, the lack of correlation is less surprising, as the subjects were healthy volunteers. Further studies with larger sample sizes and persons with distal airways abnormalities are needed.

We chose MR densitometry over other available quantitative imaging methods, mainly computed tomography, to avoid exposing the volunteers to ionizing radiation. Sev-

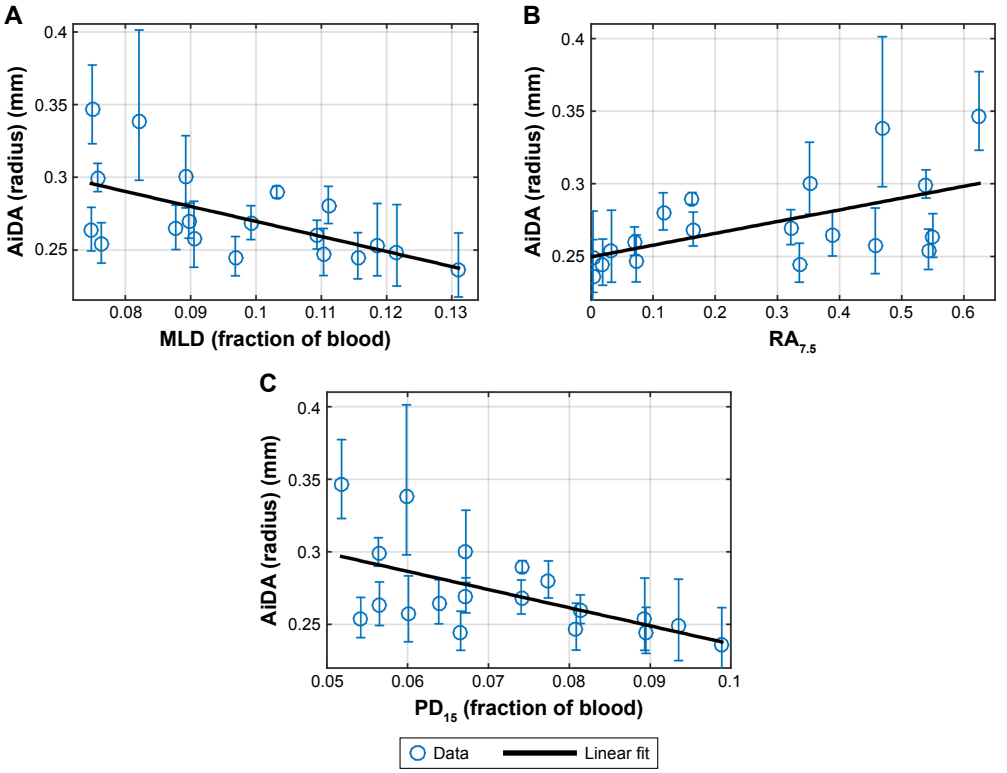

Figure 2 Linear regressions of AiDA radius (with 95% CI) as a function of quantitative MRI density measures: (**A**) mean lung density, (**B**) relative area under 7.5%, (**C**) 15th percentile proton density.
Abbreviations: AiDA, Airspace Dimension Assessment with nanoparticles; MLD, mean lung density; PD_{15}, 15th percentile proton density; $RA_{7.5}$, relative area under 7.5% PD.

eral volunteers were young, and we plan to conduct repeated measurements over time. Although we use a sub-millisecond echo time, our PD is not completely independent of T2* (signal loss due to magnetic field gradients). This will give us approximately 35% lower PD values compared to a spin-echo method, as well as contribute with approximately 5% additional intra-subject variability considering a 1,300–1,500 µs spread in T2*.[20] As we have only examined healthy volunteers, where very low lung density values are not expected, these T2* issues are acceptable. However, in a patient

Table 2 Correlation of AiDA versus MRI densitometric variables as well as intercept versus age and FEV_1

	Spearman's ρ	*p*-value
Airspace radius vs		
PD_{15}	−0.584	0.0086
$RA_{7.5}$	0.603	0.0062
MLD	−0.626	0.0041
Age	0.452	0.0522
Intercept vs		
FEV_1	0.549	0.0149
Age	0.614	0.0051

Abbreviations: AiDA, Airspace Dimension Assessment with nanoparticles; MRI, magnetic resonance imaging; FEV_1, forced expiratory volume in one second; PD_{15}, 15th percentile proton density; $RA_{7.5}$, relative area under 7.5% PD; MLD, mean lung density.

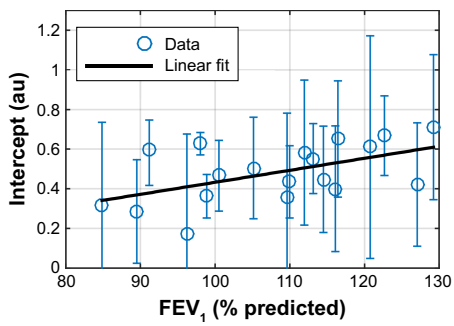

Figure 3 Linear regression of AiDA intercept, with 95% confidence intervals, as a function of FEV_1 (% of predicted).
Abbreviations: AiDA, Airspace Dimension Assessment with nanoparticles; FEV_1, forced expiratory volume in one second.

population suffering from pulmonary tissue degradation, a spin-echo or ultra-short echo time sequence is preferred. We chose to normalize the proton density to the left ventricle and not to skeletal muscle, as has been done previously,[10] for two reasons. First, the heart is more central than most visible muscle and the coil sensitivity profile will be more similar to the lung. Second, postural muscles have been shown to vary in CT-attenuation with age and sex,[21] which may be true for MRI PD as well, whereas the proton density of left ventricular blood can be considered more equal between subjects of varying age and sex.

Considering $RA_{7.5}$, it must be noted that the true cut-off (here set to 7.5%) should be determined as the detection limit of emphysema. Since there are no emphysema patients in this study, the value 7.5% is calculated only from the expected lung signal intensity at TLC, including a T2*-dependent signal loss compared to Zhang et al.[10]

The intercept was shown to correlate with FEV_1 and age. This value reflects particle losses during the breathing manoeuver, possibly implicating particle losses in the airways during convective transport.[1] Currently, the biological implications of the findings are uncertain; there are no other previous studies regarding the intercept. The losses can be expected to occur in the bronchi, bronchioles, and the gas-exchange region; our findings of FEV_1 correlating to the intercept seem to support this notion. Further studies are required.

The nanoparticles are presently not visualized; a study with radiolabelled nanoparticles to show where exactly the particles deposit is needed.

In this study, a high correlation with the theoretical model was achieved, with r^2 larger than 0.95 in all but two subjects, implying satisfying measurement precision.

Conclusion

This is the first study of AiDA in a healthy cohort showing that the estimated radius correlates with tissue density. This suggests the method could be further developed into a tool to diagnose conditions that involve changes in tissue density, such as emphysema. Moreover, the intercept from the AiDA analysis correlated with FEV_1, suggesting that the method may give information regarding the bronchial component of COPD as well.

Acknowledgments

The following organizations are gratefully acknowledged for financial support: The Swedish Research Council (project 2011-3560); the Crafoord foundation; the Swedish Governmental Agency for Innovation Systems (VINNOVA); the ERA-NET project EuroNanoMed2; the Swedish Heart and Lung Foundation and governmental funding of clinical research within the National Health Services; Allmänna sjukhusets i Malmö stiftelse för bekämpande av cancer; and Stiftelsen för cancerforskning vid onkologiska kliniken vid Universitetssjukhuset MAS. The funders of the study had neither involvement in the study design, data collection, data interpretation, writing of the report, nor in the decision to submit the paper for publication. The funders of the study had no commercial interests. Please contact the authors for data sharing enquiries.

The authors would like to acknowledge Hanna Nicklasson, Department of Translational Medicine, Lund, Sweden, for performing the AiDA-measurements.

Author contributions

All authors contributed toward data analysis, drafting and revising the paper and agree to be accountable for all aspects of the work.

Disclosure

Jakob Löndahl and Per Wollmer have a patent pending for the AiDA technology. The other authors report no conflicts of interest in this work.

References

1. Löndahl J, Jakobsson JK, Broday DM, Aaltonen HL, Wollmer P. Do nanoparticles provide a new opportunity for diagnosis of distal airspace disease? *Int J Nanomedicine*. 2017;12:41–51.
2. Jakobsson JK, Hedlund J, Kumlin J, Wollmer P, Londahl J. A new method for measuring lung deposition efficiency of airborne nanoparticles in a single breath. *Sci Rep*. 2016;6:36147.
3. Hinds W. *Aerosol Technology: Properties, Behavior, and Measurement of Airborne Particles*. 2nd ed. New York: Wiley; 1999.
4. Blanchard JD. Aerosol bolus dispersion and aerosol-derived airway morphometry: assessment of lung pathology and response to therapy, Part 1. *J Aerosol Med*. 1996;9(2):183–205.
5. Zeman KL, Bennett WD. Measuring alveolar dimensions at total lung capacity by aerosol-derived airway morphometry. *J Aerosol Med*. 1995; 8(2):135–147.
6. Hussein T, Londahl J, Paasonen P, et al. Modeling regional deposited dose of submicron aerosol particles. *Sci Total Environ*. 2013; 458–460:140–149.
7. Macintyre N, Crapo RO, Viegi G, et al. Standardisation of the single-breath determination of carbon monoxide uptake in the lung. *Eur Resp J*. 2005;26(4):720–735.
8. Takahashi M, Togao O, Obara M, et al. Ultra-short echo time (UTE) MR imaging of the lung: comparison between normal and emphysematous lungs in mutant mice. *J Magn Reson Imaging*. 2010;32(2):326–333.
9. Ma W, Sheikh K, Svenningsen S, et al. Ultra-short echo-time pulmonary MRI: evaluation and reproducibility in COPD subjects with and without bronchiectasis. *J Magn Reson Imaging*. 2015;41(5):1465–1474.
10. Zhang W-J, Hubbard Cristinacce PL, Bondesson E, et al. MR quantitative equilibrium signal mapping: a reliable alternative to CT in the assessment of emphysema in patients with chronic obstructive pulmonary disease. *Radiology*. 2015;275(2):579–588.

11. Jakob PM, Hillenbrand CM, Wang T, Schultz G, Hahn D, Haase A. Rapid quantitative lung (1)H T(1) mapping. *J Magn Reson Imaging*. 2001; 14(6):795–799.
12. Gould GA, MacNee W, McLean A, et al. CT measurements of lung density in life can quantitate distal airspace enlargement – an essential defining feature of human emphysema. *Am Rev Respir Dis*. 1988;137(2): 380–392.
13. Madani A, Zanen J, de Maertelaer V, Gevenois PA. Pulmonary emphysema: objective quantification at multi-detector row CT – comparison with macroscopic and microscopic morphometry. *Radiology*. 2006; 238(3):1036–1043.
14. Müller NL, Staples CA, Miller RR, Abboud RT. "Density mask". An objective method to quantitate emphysema using computed tomography. *Chest*. 1988;94:782–787.
15. Quanjer PH, Tammeling GJ, Cotes JE, Pedersen OF, Peslin R, Yernault JC. Lung volumes and forced ventilatory flows. Report Working Party Standardization of Lung Function Tests, European Community for Steel and Coal. Official Statement of the European Respiratory Society. *Eur Respir J Suppl*. 1993;16:5–40.
16. Thurlbeck WM. Measurement of pulmonary emphysema. *Am Rev Respir Dis*. 1967;95(5):752–764.
17. Knudson RJ, Clark DF, Kennedy TC, Knudson DE. Effect of aging alone on mechanical properties of the normal adult human lung. *J Appl Physiol Respir Environ Exerc Physiol*. 1977;43(6):1054–1062.
18. Karimi R, Tornling G, Forsslund H, et al. Lung density on high resolution computer tomography (HRCT) reflects degree of inflammation in smokers. *Respir Res*. 2014;15(1):23.
19. Robert HB, Robert AW, Kirk G, Drummond MB, Mitzner W. Lung density changes with growth and inflation. *Chest*. 2015;148(4): 995–1002.
20. Triphan SMF, Breuer FA, Gensler D, Kauczor H-U, Jakob PM. Oxygen enhanced lung MRI by simultaneous measurement of T1 and T2* during free breathing using ultrashort TE. *J Magn Reson Imaging*. 2015; 41(6):1708–1714.
21. Anderson DE, D'Agostino JM, Bruno AG, Demissie S, Kiel DP, Bouxsein ML. Variations of CT-based trunk muscle attenuation by age, sex, and specific muscle. *J Gerontol A Biol Sci Med Sci*. 2013;68(3): 317–323.
22. Aaltonen HL, Jakobsson JK, Diaz S, et al. Deposition of inhaled nanoparticles is reduced in subjects with COPD and correlates with the extent of emphysema: proof of concept for a novel diagnostic technique. *Clin Physiol Funct Imaging*. Epub 2018 Apr 10.

Printed by Media-Tryck, Lund 2019 NORDIC SWAN ECOLABEL 3041 0903

Measuring distal airspace dimensions with nanoparticles

H Laura Aaltonen is a radiologist, working at Skåne University Hospital, Lund, Sweden. This thesis investigates a new nanoparticle inhalation –based method termed Airspace Dimension Assessment (AiDA) to evaluate distal airspace morphology. Chronic obstructive pulmonary disease originates in the distal airspaces, which are hard to evaluate non-invasively. Inhaled nanoparticles are able to reach this region and deposit almost exclusively by diffusion. We expect the deposition behavior to tell emphysema patients, with enlarged airspaces, apart from healthy persons.

The first two papers provide a proof-of-concept for the method, and the last two include investigation and validation in a larger cohort. Throughout the papers, a comparison to anthropometric, lung function and medical imaging-derived variables is conducted. The findings indicate that AiDA is a promising diagnostic biomarker candidate for emphysema.

LUND UNIVERSITY

FACULTY OF MEDICINE

Diagnostic Radiology
Department of Translational Medicine

Lund University, Faculty of Medicine
Doctoral Dissertation Series 2019:49
ISBN 978-91-7619-778-3
ISSN 1652-8220